Studies on the Annual, Interannual and Climatic Variabilities of Indian Ocean Warm Pool

Thesis submitted to

Cochin University of Science and Technology

In partial fulfilment for the award of

DOCTOR OF PHILOSOPHY

in

OCEANOGRAPHY

Under the Faculty of Marine Sciences

By

Saji P. K.

(Reg. No. 3725)

Department of Physical Oceanography

Cochin University of Science and Technology

Kochi

November 2015

Declaration

*I hereby declare that the thesis entitled "**Studies on the Annual, Interannual and Climatic Variabilities of Indian Ocean Warm Pool**" is an authentic record of research work carried out by me under the supervision and guidance of Prof. (Dr.) A. N. Balchand, Department of Physical Oceanography, Cochin University of Science and Technology, towards the partial fulfilment of the requirements for the award of Ph.D. degree under the Faculty of Marine Sciences and no part thereof has been presented for the award of any other degree in any University/Institute.*

Saji P. K.

Registration Number: 3725
Department of Physical Oceanography
Cochin University of Science and Technology
Kochi – 682016
India

Certificate

*This is to certify that this thesis entitled "**Studies on the Annual, Interannual and Climatic Variabilities of Indian Ocean Warm Pool**" is an authentic record of research work carried out by Mr. Saji P. K., under my supervision and guidance at the Department of Physical Oceanography, Cochin University of Science and Technology, towards the partial fulfilment of the requirements for the award of Ph. D. degree under the Faculty of Marine Sciences and no part thereof has been presented for the award of any other degree in any University/Institute.*

Prof. (Dr.) A. N. Balchand

Supervising Guide
Department of Physical Oceanography
Cochin University of Science and Technology
Kochi – 682016
India

Certificate

*This is to certify that this thesis entitled "**Studies on the Annual, Interannual and Climatic Variabilities of Indian Ocean Warm Pool**" is an authentic record of research work carried out by Mr. Saji P. K., under my supervision and guidance at the Department of Physical Oceanography, Cochin University of Science and Technology, incorporating all relevant corrections and modifications suggested by the audience during the pre-synopsis seminar and recommended by the Doctoral Committee.*

Prof. (Dr.) A. N. Balchand

Supervising Guide
Department of Physical Oceanography
Cochin University of Science and Technology
Kochi – 682016
India

Acknowledgements

First and foremost, I thank God for giving me a life and providing mental and physical strength to carry out this research work.

This thesis has become a reality only because of the kind attitude of my guide Dr. A. N. Balchand towards me as a student and also as a colleague. He gave me full support and confidence even at times when the thesis progress was lagging. I was greatly impressed by his attitude as a human being and also as my guide. My sincere and heartfelt thanks to you Sir for your invaluable guidance and unflattering support.

I am deeply grateful to two persons, Dr. M. R. Rameshkumar (Scientist, National Institute of Oceanography, Goa) and Dr. P. Rajeev (Professor (retd.), Department of Law, Cochin University of Science and Technology) for their persistent encouragement during the period of the thesis work. The discussions with Dr. Rameshkumar were very productive and helped me in building the thesis and also in publishing research papers. Dr. Rajeev, as a well-wisher, family friend and guardian, gave me adequate mental support throughout the period.

I am thankful to the faculties and staff of the department for their sincere support. Dr. R. Sajeev, as a colleague and Head of the Department during his tenure, provided good support for progress of the thesis. My sincere thanks to Phiroz Shah, research scholar, Department of Physical Oceanography for his active participation in the discussions related to this thesis and Oceanography in general. I thank all the office staff of the department for their timely

administrative support. I also thank Registrar, Cochin University of Science and Technology (CUSAT) for providing me the infrastructure and computing facilities for carrying out the Ph. D. work.

This study makes use of a large quantity of global ocean and atmospheric data sets that were downloaded from the websites of the respective data providers. I thank the data providers Asia-Pacific Data Research Center (APDRC), NOAA (National Oceanic and Atmospheric Administration), OAFlux (Objectively Analyzed air-sea Fluxes), Hadley Centre Sea Ice and Sea Surface Temperature data set (HadISST) and others for providing the datasets. Analysis of data was done using software such as Ferret, Generic Mapping Tools, and Fortran.

I extend my sincere thanks to Dr. N. Chandramohanakumar, Professor, Department of Chemical Oceanography, for his support. I also extend my sincere gratitude to all my teachers.

I am deeply indebted to my mother, brothers and family for their love and support extended to me throughout the life. My parents were inspirational to me in my studies and extra-curricular activities. I am unlucky that my father is no more to witness this most esteemed academic achievement by his son. Most importantly, I would like to thank my wife Manjusha for her support, encouragement, quite patience and unwavering love. Children are the bridge to heaven. Of all nature's gifts to the human race, nothing is sweeter than children. Thank you dear Harikrishnan and Parvathi for your love.

Finally, I thank each and every person who had directly or indirectly helped me to complete the thesis.

to … my family and teachers …

Contents

List of Figures

List of Tables

.

Chapter 1

Introduction

Oceans are of vital importance to the existence of man on this planet. The water cycle that brings freshwater to all living organisms has its origin in the ocean. It is well known that the climate of Earth is made habitable due to the large thermal capacity of the ocean water. Oceans limit the intensity of the global warming through the intake of a large portion of atmospheric carbon dioxide. Hence it is very important to understand the processes in the oceans and its behavior to the future of mankind.

The behavior of a natural system is explained in terms of its state variables. For the ocean, the state variables of climatic importance are temperature, salinity, velocity, sea level, sea ice, chlorophyll etc. Among this, temperature of the ocean is more important as it can affect other parameters and is climatically sensitive. Temperature of the ocean varies in space and time. Higher temperatures (~30^{o}C or more) are observed at the tropics and reduce towards poles. Temperature decreases vertically from its surface value at each geographical location. This spatial distribution of temperature undergoes changes from season to season and also year to year. The temperature at the ocean surface, termed as Sea Surface Temperature (SST), is even more important because it is where the temperature values are modified as a result of interaction with atmosphere. SST in turn influences a variety of atmospheric processes such as convection and conduction and also modulates atmospheric circulation and tropical cyclones.

1.1 Sea Surface Temperature (SST)

SST is broadly defined as the temperature of the sea water at surface. The word ‘surface’ is but not clearly defined and can vary from few millimeters to few meters. It is a parameter that can be easily measured and is therefore the best known oceanic parameter. SST has a wide range of applications: eg.,

monitoring climate change, defining boundary condition to models, marine fishing and studies related to air-sea interaction processes, monsoon and climate anomalies.

In the past, SST had been measured mostly from ships. Later, invention of platforms such as buoys and satellites greatly enhanced this database on oceans. SST observed from buoys and ships represent the temperature of 1 to 10 meters of the surface ocean and are often called as 'Bulk' SST. However, SST measured from satellites make use of the thermal radiation emitted from the top few centimeters of the sea surface and is called as 'Skin' SST. Usually the skin SST is found less than the bulk SST. The lesser skin SST is a result of direct heat loss with the atmosphere through conduction, evaporation and radiation. For many applications, both SSTs are being used [*Schluessel et al.*, 1987; *Fairall et al*., 1996b; *Wick et al*., 1996; *Zeng and Beljaars*, 2005; *Brunke et al*., 2008].

In response to atmospheric forcing and the internal dynamics of the ocean, SST varies spatially and temporally in a wide range of scales. Spatially, surface temperature of the oceans varies from about -1.9^{o}C at poles to about 30^{o}C in the tropics [*Shea et al.*, 1992; *Reynolds and Smith*, 1995]. The temperature at a location decides the weather and climate of that area and hence the possibility of life forms. Due to extreme cold temperature, polar areas are void of human life. Life is also not possible on the other extreme where atmospheric temperature exceeds 45^{o}C. Human causalities due to extreme temperatures are now reported every year. The situation can be even worse in the coming years if the global warming trend continues [*IPCC*, 2014].

SST influences a variety of other geophysical variables. Changes in SST bring about changes in sea level, wind, atmospheric convection, evaporation

from the ocean and can intense weather systems such as cyclones. Circulation of the atmosphere depends on the pressure variation created by SST and land temperatures. Recent studies indicate that the summer monsoon of India, a critical factor for the economy of this country, depends on the intensity and gradient of SST in Indian Ocean [*Roxy et al.*, 2015]. The trade wind, the back bone of ocean circulation, depends on the meridional gradient in SST.

1.2 Warm Pool

It was observed that the high SSTs in the tropical latitudes have an important role on the climate [*Gadgil et al.*, 1984; *Graham and Barnett*, 1987]. Strong atmospheric convection, an important process for weather activity through the transport of water vapor into the atmosphere, is found over warm oceanic areas. It has been observed that high convection do occur in oceanic areas where SST exceeds certain threshold value. Hence the warm ocean surface waters are often called as 'Warm Pools'.

Wyrtki (1989) had defined warm pool as waters with SST greater than 28^{o}C. This lower limit of temperature was used in most subsequent studies but occasionally other values were also used in specific applications. For example, *McPhaden and Picaut* (1990) used 29^{o}C as the lower limit to demarcate warm pool of Pacific. *Chacko et al*. (2012) used 30^{o}C in their study on the mini warm pool of Arabian Sea. Hence, the choice of the lower temperature cut off is not a universal one and is subjective. In this study, we followed the criteria followed by *Wyrtki* (1989) for the study of warm pool of Indian Ocean.

1.3 Global Warm Pools

Warm pools are well identified from SST data. Climatological maps of global SST show the presence of warm pools in all the tropical oceanic areas.

Figure 1.1 shows status of the distribution of the warm pools in the oceans during the month of April as obtained by *Vinayachandran et al*. (2007).

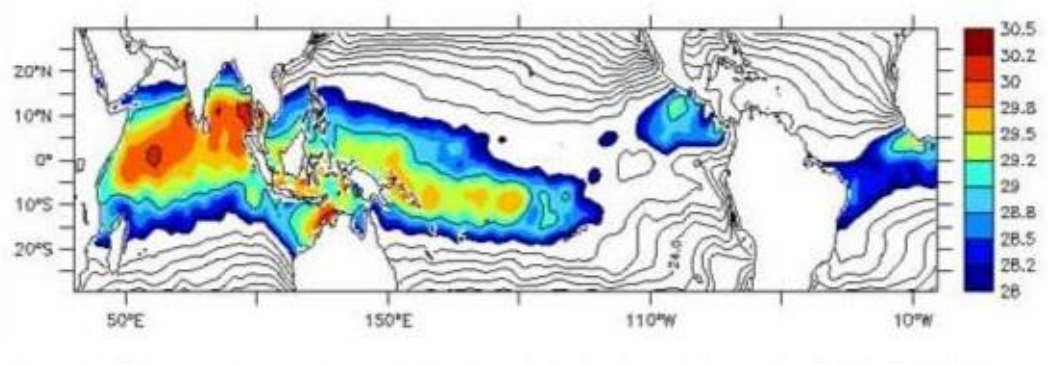

Figure 1.1 Climatological monthly mean SST during April
(after Vinayachandran et al., 2007)

Warm pools are named according to their place of formation and are called accordingly as Pacific Ocean Warm Pool (POWP), Indian Ocean Warm Pool (IOWP) and Atlantic Warm Pool (AWP). The distribution of the high SSTs of the Indian and Pacific Oceans could appear as a single water body. Hence the warm pools of both these oceans are studied as Indo-Pacific Warm Pool (IPWP) [eg., *Liu et al*., 2005; *Wang and Mehta*, 2008].

Among the warm pools of the global oceans, Pacific Ocean Warm Pool has received intensive attention over several decades due to its key role in the climatic anomalies associated with El Nino Southern Oscillation (ENSO). The warm pool of Indian Ocean is now attracting more attention due to its important role on the Indian climate, especially monsoon and cyclonic activities.

1.4 Significance of Warm Pool

Warm pool plays an important role in maintaining the climate of the planet through strong air-sea interactions. Dedicated field programs such as

TOGA-COARE have been conducted to study the warm pool dynamics. The warm pool size, temperature, displacement and heat content are some of the major parameters of a warm pool. Anomalies in these can have impacts on the weather and climate locally or even globally [*Allan et al*., 1996; *Trenberth*, 1997].

Warm pool has a direct role in atmospheric convection. The high SST creates a low sea level pressure which leads to the convergence of air mass. Large upward motion occurs in these areas which carries water vapor to higher levels in the atmosphere. This creates cloud systems in the atmosphere and thus becomes part of the water cycle. The latent heat released during the condensation process is an important source of energy for atmospheric circulation and convection at low latitudes maintains the Walker circulation in the atmosphere. Changes in the location and intensity of convection can alter the intensity of Walker circulation and in turn, ocean circulation.

Warm pools are also important in studies related to tropical cyclones. A cyclone is a rapidly-rotating storm characterized by a low-pressure center, strong winds and a spiral arrangement of thunderstorm clouds that produce heavy rain. SST above 26^{o}C is one of the favorable conditions to the formation of cyclones. The role of global warming on cyclogenesis is now an important area of study [*Webster et al.,* 2005; *Landsea et al.*, 2006; *Emanuel et al.*, 2008; *Robert et al.,* 2012]. Studies indicate that global warming can have a role in the frequency and intensity of tropical cyclones.

Warm pool is also found to have a role on Indian summer monsoon activity. The monsoon vortex, a prime factor for the onset of the Indian summer monsoon forms over the warm pool of Arabian Sea [*Krishnamurti et al*., 1981; *Rao and Sivakumar*, 1999; *Vinayachandran et al*., 2007]. Recently *Roxy et al*. (2015) have demonstrated that the role of spatial gradients in

ocean surface temperature could lead to a deficit in monsoon rainfall.

1.5 Objectives of the Study

The recurrent warming of oceans is an important process in maintaining the climate of earth. Ocean temperature is an important climatic indicator among others such as atmospheric humidity, tropospheric temperature, sea level, ocean heat content, temperature over land, sea ice etc. The oceans absorb large amounts of heat and Carbon dioxide, thereby reducing the impact of global warming. The important point here is the carrying capacity of the oceans and its future behavioral patterns to the present warming trend.

Warm pools represent upper ocean temperatures and act as an index for climate change. Its temporal and spatial variations can have crucial impacts on climate change. This study focuses on the warming of the Indian Ocean with an emphasis on the warm pool (IOWP) with the following objectives:

1. A detailed study on the annual characteristics of IOWP
2. Understand ENSO-induced variability on IOWP
3. Deduce the long term trend SST and IOWP in response to global warming and
4. Model SST using 1-Dimensional Mixed Layer Model.

1.6 Scheme of the thesis

Introduction is covered in Chapter 1. Chapter 2 details the review of literature for the present study. As the topic is climatically important, there has been ardent interest on warm pools of the global oceans over the past few decades. This thesis accounts for significant works on the warm pool of Pacific

Ocean too. Research on Indian Ocean warm pool had begun later in 1990s. A detailed review of the literature available on IOWP is provided.

Chapter 3 discusses the data sets used and the methods adopted in this study. Basin-scale multi-year data sets on SST, air-sea heat fluxes, wind and other geophysical variables from the tropical Indian Ocean sector were utilized. The datasets comes from different sources such as observation, satellite-derived and model re-analyzed.

A detailed study on the annual warm pool climatology is presented in Chapter 4. Various characteristics of the warm pool including spatial and temporal evolution and displacements have been discussed. A heat budget analysis was performed to understand the role of surface heat fluxes on the observed annual warm pool variability.

Chapter 5 discusses the inter-annual variabilities of warm pool caused by ENSO events. The anomalous behaviour of warm pool and SST during ENSO years was studied. The role of heat fluxes on SST was also examined. The climatic importance of the warm pool was addressed in Chapter 6. Long term trend in SST and warm pool was studied for the past 100 years using all available long term data sets.

Chapter 7 is devoted to modeling of SST to understand the combined role of wind stress and heat flux. A one-dimensional mixed layer model was used for this purpose. The response of SST to various atmospheric forcing was studied. Chapter 8 presents an overall summary of the thesis followed by the list of references.

Chapter 2

Literature Review

2.1 Introduction

The warm waters of the ocean and their variability have been an active area of research over the past decades, especially due to their role in the earth's climate. However, the concept of warm pool by defining temperature limits to ocean waters has come only by 1980's. Having detailed about the difficulties in fixing a lower limit, *Wyrtki* (1989) introduced a practical definition to the warm pool of the Pacific. According to him, warm pool is warm waters with temperatures above 28^{o}C.

However there are other characteristics also that are associated with warm pools. It has a lower salinity [*Sophie et al.*, 2009] and hence less density. The same criterion is also used to obtain the vertical scale of the warm pool. Hence the spatial extent of the warm pool is obtained as the area and volume of water enclosed by the 28^{o}C isotherm both in the horizontal and vertical directions. It was then followed by several investigators to understand the dynamics of the Pacific warm pool [*McPhaden and Picaut,* 1990; *Lukas and Lindstrom,* 1991; *Webster and Lukas,* 1992; *Picaut and Delcroix,* 1995; *Chen et al.,* 2004; *Mignot et al*., 2007; *Sophie et al.,* 2009].

2.2 Annual Characteristics of IOWP

Studies on the warm pool of Indian Ocean (IOWP) began in early 1990s. A description of the warm pool of the Indian Ocean was given by *Vinayachandran and Shetye* (1991). Using climatological data they have identified the annual variation in the warm pools of Indian and Pacific oceans (Figure 2.1). IOWP attains the maximum (23×10^{6} km^{2}) area during the months of April and May. As the monsoon advances, the warm pool shrinks with reduction in its amplitude, thus attaining a minimum area (8×10^{6} km^{2}) by the end of the summer monsoon (August-September). Hence the annual

variability of the warm pool area is about 15×10^6 km^2. They have also noted the differences in the evolution of Indian and Pacific warm pools. Unlike Pacific, Indian Ocean is influenced to a great extent by the seasonally reversing winds and the associated oceanographic processes. This makes the evolution of the warm pool and the overall SST different from other oceans.

The annual feature of the warm pool was further investigated later by *Zhang et al*. (2009) (Figure 2.2). Since the warming was found stronger and nearly steady at the east, they named it as Eastern Indian Ocean Warm Pool (EIWP). Their result on the annual variability of IOWP was similar to that observed by *Vinayachandran and Shetye* (1991) though the data set used was different. Maximum area of warm pool was found to occur in spring season and minimum during summer (August).

This information points to the validity of the naming as 'summer'. They further studied the seasonal variability in the boundary of IOWP marked by the 28^oC isotherm. The southern boundary of IOWP extends maximum southward during April-May and minimum during August. The western edge similarly moved maximum towards west during April-May and maximum eastward in August. However the warm pool surface area reported by them was much less than that of *Vinayachandran and Shetye* (1991). The absence of warm pool at the western Indian Ocean during summer is due to the advection of cold water by intense upwelling [*Zhong et al.*, 2005].

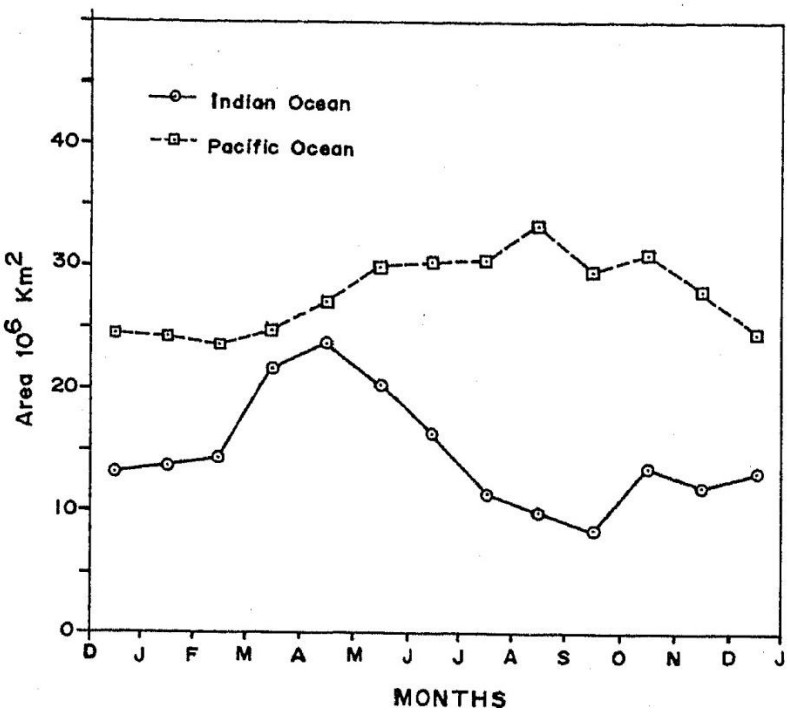

Figure 2.1 Annual variation in the area of Indian and Pacific warm pools (after Vinayachandran and Shetye, 1991)

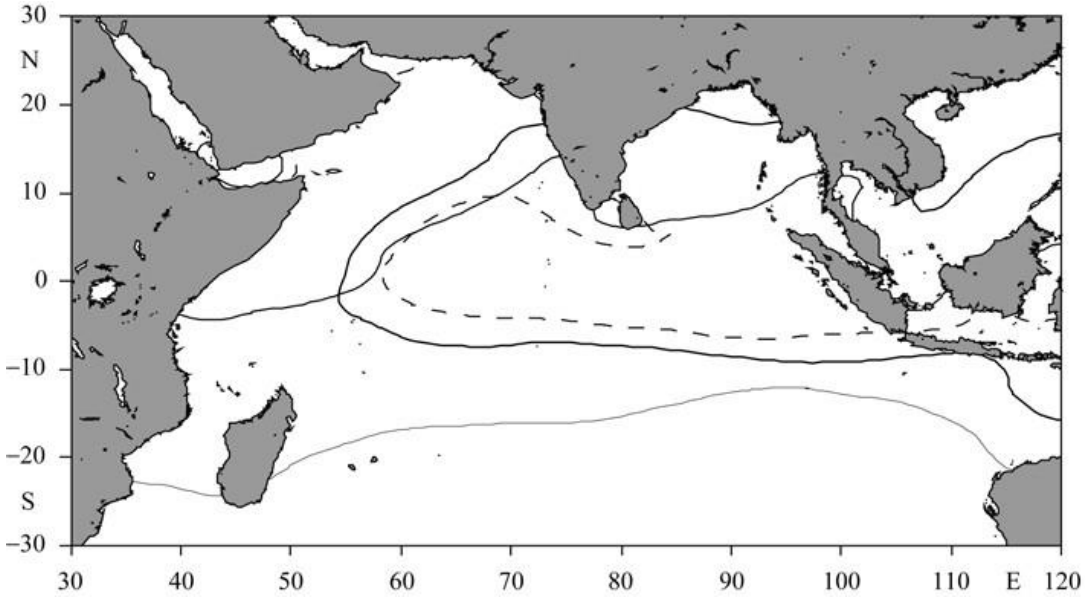

Figure 2.2 Area covered by warm pool as annual mean (thick line), in February (thin line) and in August (dashed line) [after Zhang et al., 2009]

Recently *Kim et al.* (2012) studied the distinct characteristics of warm pools of the Indian and Pacific Oceans. They have found that Pacific Warm Pool (PWP) responds more to the heat fluxes as compared to IOWP. This is due to the contribution from the oceanic processes on IOWP variability. To have a better clarity on this aspect, it would be better to classify the oceanic areas based on their dynamics controlled by heat fluxes and ocean processes. They have also identified a change in the timing of the warm pool intensity in the two oceans. The peak of IOWP occurs in April-May whereas PWP stands weak during this time. Similarly, as IOWP becomes weakest in August, PWP becomes stronger. This shows that PWP maximum follows the summer heating whereas other process in Indian Ocean modifies the warm pool characteristics during summer. Their results on seasonal IOWP variability were in agreement with those reported by previous authors [eg., *Vinayachandran and Shetye*, 1991].

2.3 ENSO-induced inter-annual variability

Though seasonality is the dominant variability in the ocean and is repeated each year, there are variations in the oceans from year to year. These are called inter-annual variabilities or anomalies. Such anomalies can become intensive in some years and can cause anomalies in the climate either locally or even globally. In such situations these anomalies are given special importance and are studied with special interest.

Inter-annual anomalies of this sort were identified in the each ocean. El Nino Southern Oscillation (ENSO) is such an inter-annual anomaly in the Pacific Ocean that affects the climate around the world. ENSO is a change in the ocean atmosphere system due to unusual warming. The warming phase is called as El Nino and the cold phase as La Nina.

During normal conditions (Figure 2.3), trade wind blows westward across the equatorial Pacific Ocean and piles up the warm water at the west. Hence, SST becomes higher at the west leading to the formation of a warm pool that is centered at the west, called as West Pacific Warm Pool (WPWP). Due to the high SST, deep atmospheric convection occurs at the west. The zonal SST gradient thus maintains the Walker circulation in the atmosphere with ascending motion at the west and descending motion at the east. During certain years, the warm pool displaces towards east due to a weakening of trade winds and the situation is referred to as El Nino (Figure 2.4). As the warm pool migrates, the convective activity also displaces towards east causing large-scale anomalies in the ocean-atmosphere system.

Number of attempts had been made to understand the dynamics of El Nino and its implications on climate [*Rasmusson and Carpenter*, 1982; *Rasmusson and Wallace*, 1983; *Gill and Rasmusson*, 1983; *Wyrtki*, 1985; *Ardanuy et al*., 1987; *Lukas and Webster,* 1989; *Gopinathan and Sastry*, 1990; *McPhaden and Picaut*, 1990; *Yan et al.*, 1992; *Ho et al.*, 1995; *Picaut et al.*, 1996; *Delcroix,* 1998; *Delcroix et al.*, 2000; *Meinen and McPhaden*, 2000; *Sun*, 2003; *Zhang et al*., 2004; *Zhang et al*., 2007; *Qi et al*., 2008; *Cai et al*., 2012; *Stuecker et al*., 2013; *Cai et al*., 2014; *Wittenberg et al*., 2014; *Cai et al*., 2015]. The occurrence of El Nino in the Pacific has global teleconnections and modifies the climate around the planet. There are a few studies that looked into the role of El Nino in Indian Ocean. It has been observed that majority of inter-annual variations in Indian Ocean has been attributed to El Nino [*Zhang et al.*, 2009].

Klein et al. (1999) found that the Indian Ocean tends to become warmer (cooler) during the El Nino (La Nina) event. This enhanced warming was found to be due to an increased net heating. It was also reported that the entire tropical Indian Ocean respond to El Nino events.

Xie et al. (2002) investigated the role of oceanic Rossby waves on ENSO-induced variability of IOWP. *Zhang et al.* (2009) confirmed the inter-annual variation of IOWP area to El Nino events. Warm pool expansion at its boundaries was studied based on the anomalous displacements in the edge of the warm pool. IOWP had anomalous expansion to the west and south during the 50 year period (Figure 2.5).

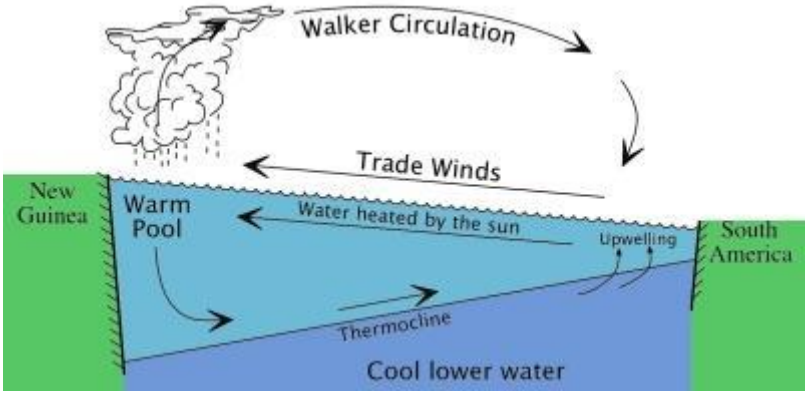

Figure 2.3 Schematic of normal conditions in Pacific

[source: www.seos-project.eu]

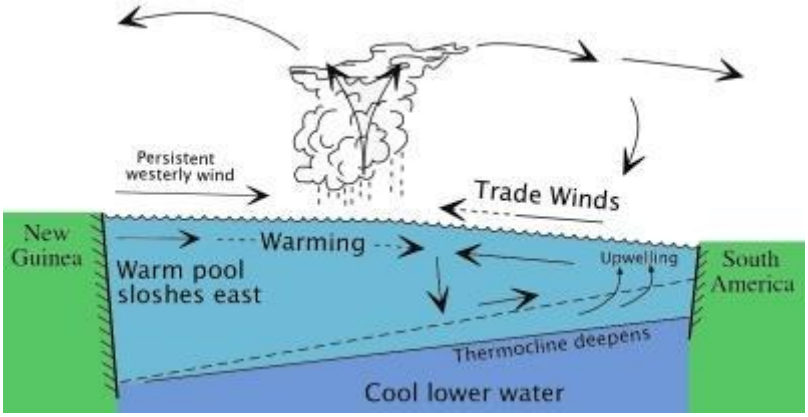

Figure 2.4 Schematic showing El Nino conditions in Pacific
[source: www.seos-project.eu]

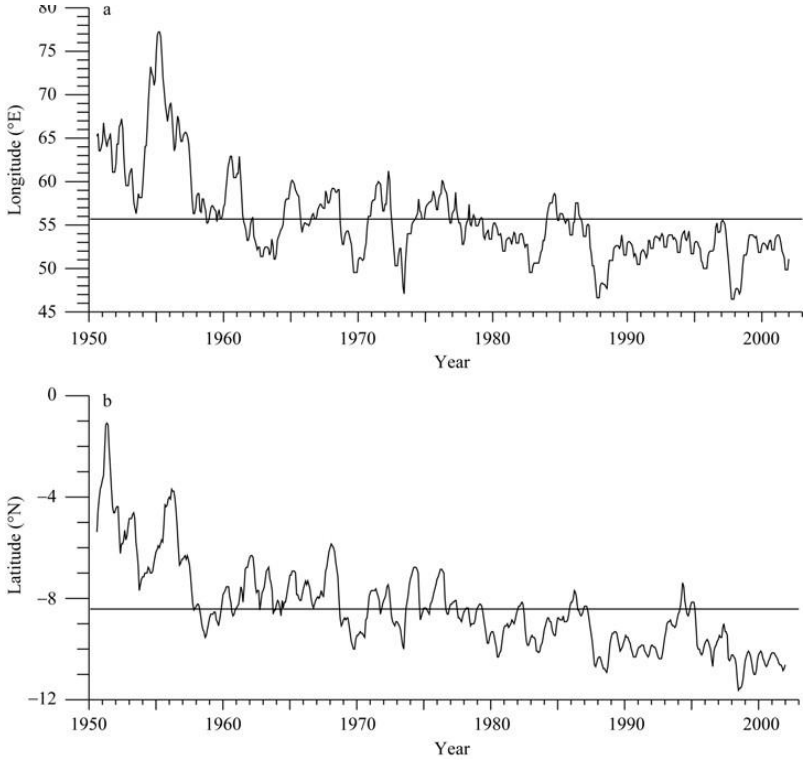

Figure 2.5 Inter-annual changes in the (a) western and (b) southern edges of IOWP [from *Zhang et al.*, 2009]

Suryachandra et al. (2012) also observed fluctuations in IOWP associated with ENSO years. *Kim et al*. (2012) compared the inter-annual variations of IOWP and WPWP in detail. They have observed that magnitudes of inter-annual anomalies were comparable for both Pacific and Indian Oceans but seasonal amplitudes were higher in the Indian Ocean. Zonal displacements were generally higher than that of meridional. An important feature is the time lag between ENSO and the warming in Indian Ocean. They have found that Indian Ocean SST lags behind ENSO by 3 to 4 months.

Other studies [*Annamalai et al*., 2005; *Yang et al*., 2007; *Xie et al*., 2009; *Du et al*., 2009] also reported the anomalous behavior of Indian Ocean during El Nino years. *Du et al*. (2009) identified the cause for prolonged

warming of the Indian Ocean. They found that the increased shortwave radiation was responsible for the initial phase of warming whereas a reduced latent heat at a later stage extended the warming for few more months. *Cai et al*. (2014) have recently studied the impact of global warming on ENSO. Using climate models, they suggested an increase in the extreme ENSO events such as those of 1982-83 and 1997-98 in the future if global warming continues at the present rate. *Cai et al*. (2015) studied the impact of global warming on La Nina. They found that the frequency of extreme La Nina events also will increase in the future.

2.4 IOD-induced inter-annual variability

Saji et al. (1999) identified an inter-annual oscillation in Indian Ocean and named the process as Indian Ocean Dipole (IOD). IOD is a coupled ocean-atmosphere phenomena occurring in the tropical Indian Ocean. Along with ENSO, IOD also has a significant contribution to the inter-annual variabilities in Indian Ocean. As in other such climatic events, IOD also has positive and negative phases (Figure 2.6). The phase and intensity of IOD were expressed with an Index called as Dipole Mode Index (DMI). DMI is estimated from the SST anomalies in the tropical western (10^{o}N to 10^{o}S and 50 to 70^{o}E) and eastern (equator to 10^{o}S, 90 to 100^{o}E) Indian Ocean. The major recent IOD events are that during 1961, 1967, 1972, 1982, 1994 and 1997. Positive phase of IOD is characterized by anomalous cooling in the eastern Indian Ocean and a concurrent warming at the west whereas the negative phase is associated with anomalous warming at the east and a cooling at west.

IOD has been the key topic of study for the past decade in the context of climate change [*Saji et al.,* 1999; *Webster et al*., 1999; *Murtugudde et al*., 2000; *Saji and Yamagata.*, 2003; *Zhang et al*., 2009]. During positive IOD, zonal SST distribution induces atmospheric convection at the west

bringing heavy rain to Africa and drought conditions at the east. *Ajayamohan and Rao* (2008) had observed an increasing trend of IOD events as a consequence of global warming.

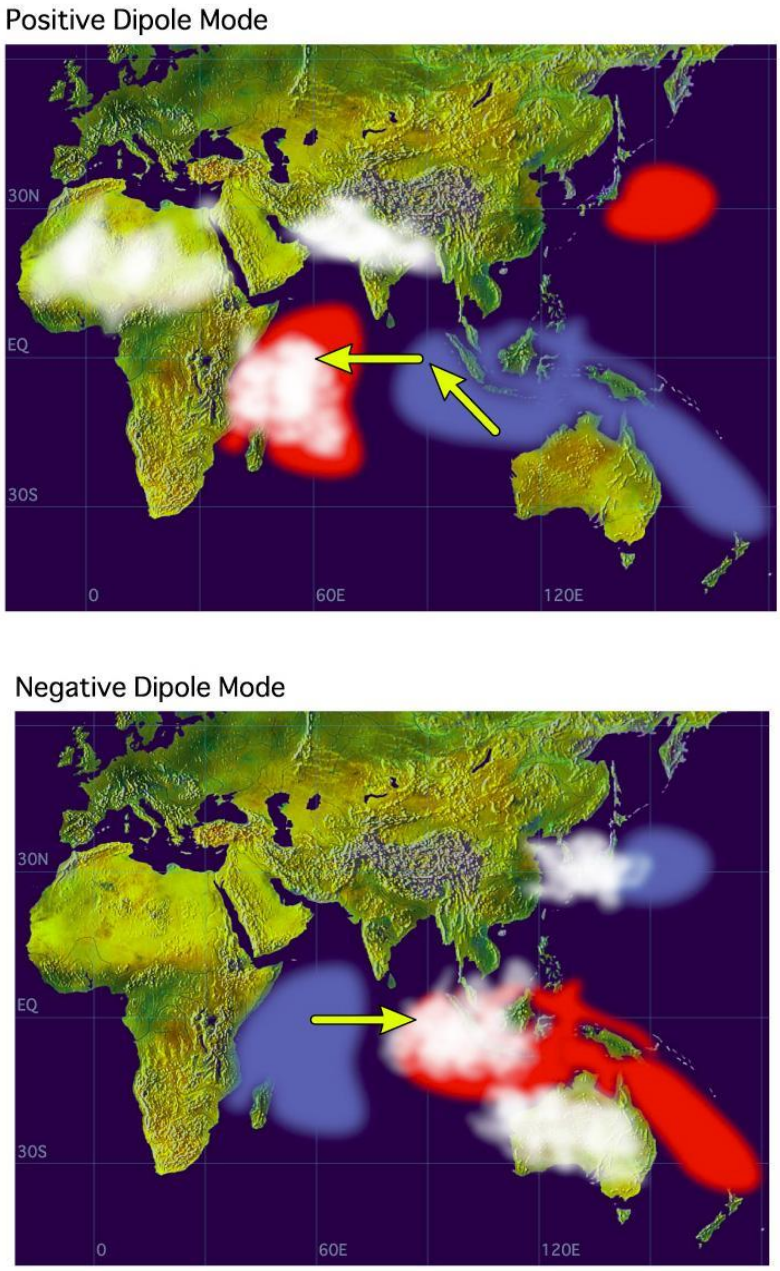

Figure 2.6 Schematic showing the positive (upper) and Negative (lower) phases of IOD [source: www.jamstec.go.jp]

Zhang et al. (2009) studied the impact of warm pool of Indian Ocean by IOD events. They have found good correlation between DMI and IOWP southern edge and a negative correlation with western edge. This result shows that the warm pool expansion occurs only at southern boundary during IOD years. A further study is desired to have a better understanding on the role of IOD events on the evolution of Indian Ocean SST and the warm pool.

2.5 Long term trend of IOWP

The annual and inter-annual variabilities are episodic events and the system normally comes back to its normal state. However, in the period of global warming, long term trends are expected in many geophysical parameters. The observed long term trend in ocean temperature clearly indicates the response of the ocean to global warming. Along with SST, warm pools also have long term trends in their area and intensity. Long term warming of the ocean has further consequence on the climate as it can modify the hydrological cycle, carbon storage, tropical cyclones etc.

Warming trends in the global oceans have been identified in many recent studies. *Levitus et al.* (2000) observed warming trends in the upper 3000m of the world oceans during a period of five decades. They found an increase in the heat content by about 2×10^{23} J during this period that was responsible for the warming. The timing of the warming trend did not occur at the same time in the oceans. Warming of Atlantic and Pacific Oceans began in 1950's but that in Indian Ocean was delayed by almost a decade. The reason for this is not known. *Willis et al.* (2004) carried out an improved estimate of heat content by combining both in-situ and satellite data. *Levitus et al*. (2005), however, obtained a reduced estimate of 1.45×10^{23} J as the heat content of the same water.

Effect of global warming on warm pools was also attempted by few researchers. *Webster et al.* (2006) observed an expanding trend of surface area of tropical warm pools during the past 150 years. The acceleration in the rate of warming since 1970s indicates the role of human activities.

Using historical data from the upper 1000m, *Alory et al*. (2007) identified a linear trend in Indian Ocean temperature. They found a cooling trend for subsurface waters which disagrees with the estimate of *Levitus et al*. (2000). Using NOAA ERSST data, *Wang and Mehta* (2008) studied the long term trend in Indo Pacific warm pool SST during the period 1948 to 2005. They have observed a warming trend of 0.1^{o}C per decade for warm pool SST. It was also found that the rate of warming is higher for the Indian Ocean.

Zhang et al. (2009) studied the trends in the IOWP displacement during the past 50 years. The western warm pool edge showed a westward trend indicating the expansion of the warm pool towards west. The westward displacement was found weaker since 1980s. Southern edge had a southward displacement during this period indicating the expansion towards south.

Suryachandra et al. (2012) studied warming tendency in Indian Ocean using ERSST data. They have observed a warming trend throughout the tropical Indian Ocean with a maximum at central equatorial area. Warming trend could not be explained by air-sea heat fluxes alone which suggest the role of other processes such as ocean advection on the observed warming. They proposed a feedback mechanism for the warming trend. Though these studies confirm the warming trend during the past several decades, there are uncertainties in many aspects such as

- How the local warming trend can be accounted by large-scale global warming?
- If global warming causes oceanic warming through trapping of

long wave radiation, why net heat fluxes do not correlate with the warming trend?

- If the ocean warming is not forced by heat fluxes, then why should blame human activities for the present climate change?

2.6 Warm Pool Dynamics

The primary factors that control SST are the air-sea heat fluxes. An increase in the net heat flux to the ocean should result in an increased SST and vice versa. The heat added to the surface water is then mixed down by turbulent eddies. Increased mixing leads to a decrease in SST. Apart from these local processes, three-dimensional advection can modify the local SST. The relative roles of these factors can vary from place to place and from time to time. *Huang and Robinson* (1995) estimated the role of each factor in the Bay of Biscay and found that the major contribution of SST variability comes from turbulent mixing (38%) and advection (32%). Dynamics of high SST (warm pool) may however stand different from that of low SST due to a non-linear relationship between SST and atmospheric convection. Hence it is suggested that warm pool SSTs are controlled by feedback processes than by local forcing.

Ocean and atmosphere exchanges heat, water vapor and momentum. Transfer of heat fluxes occurs through radiative and turbulent fluxes. Ocean receives heat through solar radiation. The absorbed heat is lost back to atmosphere and space through long wave radiation and latent and sensible heat fluxes. The heat budget, estimated as the sum of heat flux terms, determines the net heat input to the ocean and hence the temperature. On a global scale, there is a balance in the heat gain and loss which reflects that the mean temperature of the planet is in a steady state. However, on regional scale, the balance need not be achieved which results in spatial differences in

temperature. Net heat flux is positive at tropics and negative at higher latitudes which cause meridional gradients in SST and drives atmospheric circulation.

Newell (1979) showed that evaporative heat flux limits SST below 32^{o}C. Modeling attempt by *Shetye* (1986) showed that SST in Arabian Sea is controlled by oceanic advection during summer and air-sea heat fluxes during other seasons. *Vinayachandran and Shetye* (1991) later confirmed the roles of advection and heat fluxes on regional SST in the Indo-Pacific warm pool areas. Advection was found to dominate the equatorial areas whereas heat fluxes in other regions of the warm pool.

Ramanathan and Collins (1991) showed the importance of cirrus clouds on SST. They proposed that these clouds reduce incident radiation and limit SST from further increase and called the cirrus clouds as 'thermostat'. But *Wallace* (1992) questioned the role of clouds in the maintenance of warm pool SST.

Later studies [*Fu et al*., 1992; *Hartmann and Michelsen*, 1993; *Del and Kovari*, 2002] proved that the feedback between clouds and SST is not purely local, but also depends on the spatial gradients in SST. *Hartmann et al*. (1992) and *Del and Kovari* (2002) were in favor of clouds. *Clement et al*. (2005), in an attempt to model the warm pool in Indian Ocean, found that cloud feedback together with ocean dynamics can produce the observed SST distribution.

Schneider et al. (1996) found heat flux as the controlling factor for the warming at the eastern Indian Ocean. *Sadhuram et al*. (1999) studied the warm pool of Bay of Bengal during post monsoon season. They found the presence of a low pressure which creates stronger wind and hence low SST at the head Bay. A mini warm pool was also reported off Srilanka where the local heat flux was found to dominate the warm pool dynamics. The atmosphere

over Bay of Bengal was unstable and hence supports a basin-wide convection. Model studies by *Kumar et al*. (2005) had produced good results. Surface heat fluxes tend to dominate SST in the north Indian Ocean and advection in equatorial regions. However their model results were not valid at southern Indian Ocean.

Clement et al. (2005) analyzed the role of individual factors on warm pool SST distribution through numerical modeling. Their model could not simulate realistic SST pattern with heat fluxes alone. They suggested that under purely local balance, the most prominent SST would be the highest one. This is not what actually is observed in the oceans where the prominent SST is that which is lower than the highest. This indicates the role of other factors to the observed SST distribution that moderate SST in warm pool areas. Introducing ocean dynamics through Ekman drift had improved the results but with a low temperature. The failure of the combined effect of air-sea heat fluxes and ocean dynamics on SST distribution led them to include effect of clouds and the results were encouraging. *Zhang et al*. (2009) also found the role of heat fluxes, winds, current and other environmental factors on the warm pool dynamics.

Interestingly, salinity was also found to play an important role on warm pool. Precipitation often exceeds evaporation in warm pool areas. The net freshwater input makes the warm pool low saline. Hence warm pools are also called as 'fresh pools' [*Sophie et al*., 2009]. Indo-Pacific warm pool receives about 1-2m fresh water annually [*Chen et al.*, 2004; *Huang and Mehta*, 2004]. This buoyancy flux increases the stability of warm pool and hence the dynamics and thermodynamics [*Lindstrom et al*., 1987; *Godfrey and Lindstrom*, 1989; *Lukas and Lindstrom*, 1991; *Huang and Mehta*, 2004].

Boyer et al. (2005) found a freshening trend in warm pools. Pacific Ocean exhibits a basin-wide freshening except for the subtropical areas. Interestingly, in Atlantic Ocean, freshening trend was found at higher latitudes and an increasing salinity trend within the tropics and subtropics. Increase in salinity was also found in Indian Ocean. Hence the decrease in salinity within warm pools appears not to be a universal feature and may be decided by regional factors.

The stabilizing effect of low salinity is evident in Bay of Bengal where precipitation exceeds evaporation [*Shenoi et al*., 2004]. Increased stratification due to excess rainfall and weak winds causes a reduction in mixed layer depth. The shallow mixed layer traps the heat and causes higher SST.

The spatial anomalies of IOWP found to have an influence on the climate conditions in the eastern Africa [*Williams and Funk*, 2011]. The anomalous westward extension of the warm pool alters the geographic position of deep atmospheric convection and shifts the Walker circulation towards west. This often leads to an enhanced drought conditions in the eastern Africa. *Sanilkumar et al*. (2004) found the role of salinity in the spatial distribution of warm pool. The warm pool in Arabian Sea is influenced by the intrusion of low salinity waters from Bay of Bengal. However, the vertical extent of the warm pool is controlled by the intensity of heating and thickness. *Liu et al*. (2013) have suggested the dominant positive role of longwave radiation on the warm pool variability of Atlantic Ocean.

It is now evident that warm pools of the oceans play a very important role in modulating local weather and also long term climate. Particularly, for the situation in Indian Ocean, detailed study will be helpful to elucidate new information on this oceanic feature and thus understand the underlying

factors that bring about changes in the characteristics of warm pool, year to year. Subsequent chapters of the thesis address the various aspects of the Indian Ocean Warm Pool.

Chapter 3

Data and Methods

The thesis makes use of a variety of ocean-atmosphere data sets to investigate the warming in Indian Ocean. As the study is on large-scale processes, spatially gridded, basin scale data sets were used. The primary for this study is the Sea Surface Temperature (SST). Other data sets such as heat fluxes and wind speed were used as supplementary data to understand the cause of variability in SST.

Oceanographic data come from direct observations from ships and buoys and also from remote observation from satellites. The direct measurements are considered as true data but have the limitation of less coverage in both time and space. Satellite data on the other hand has more spatial coverage and is synoptic in time. Their accuracy is limited but widely used for large scale processes in both ocean and atmosphere. There are other kinds of data that combines data from different sources such as models, satellite and observations and make best estimates by performing statistical analysis. The thesis makes use of all kinds of these data sets.

3.1 Sea Surface Temperature

SST was one of the first oceanographic parameter to be measured in the history of oceanography. In the beginning, SST was measured by using thermometers which still continues as an efficient method. Later, SST data was obtained automatically by measuring the temperature of the water in the intake port of large ships on a continuous basis. Unmanned buoys, both fixed and drifting, later enhanced the data coverage. The introduction of satellites in 1970s had revolutionized the ocean observation. It provided global synoptic data that helped the understanding of the ocean to a great extent.

ERSST

NOAA NCDC (National Oceanic and Atmospheric Administration National Climate Data Center) provides analyzed SST data called as ERSST

(Extended Reconstructed SST) data for the period from 1854 to present [*Reynolds et al*., 2002; *Smith and Reynolds,* 2004]. The data is monthly mean and with a global coverage. The data is generated by performing statistical interpolation on the ICOADS (International Comprehensive Ocean Atmosphere Data Set) data. Later versions of the data include SST data from satellites in addition to in-situ observations. ERSST data is suitable for long-term studies of global oceans.

HadISST

Hadley Centre Sea Ice and Sea Surface Temperature (HadISST) data is a unique combination of monthly globally-complete fields of SST and sea ice concentration on 1 degree latitude-longitude grid from 1870 to date [*Rayner et al*., 2003]. The SST data were taken from the Met Office Marine Data Bank (MDB), which from 1982 onwards also includes data received through the Global Telecommunications System (GTS). Data coverage was enhanced by estimating monthly median SSTs for 1871-1995 from the Comprehensive Ocean-Atmosphere Data Set (COADS) where there were no MDB data. HadISST temperatures are reconstructed using a two-stage reduced-space optimal interpolation procedure, followed by superposition of quality-improved gridded observations onto the reconstructions to restore local detail.

OAFlux

OAFlux (Objectively Analyzed air-sea Fluxes) project aims to provide consistent, multi-decade, global analysis of air-sea heat, freshwater (evaporation), and momentum fluxes for studies related to global energy budget, water cycle, atmosphere and ocean circulation, and climate [*Yu and Weller*, 2007]. The OAFlux project is so called because it applies objective analysis approach that takes into account data errors in the development of enhanced global flux fields. The objective analysis involves the process of

synthesizing SST measurements and estimates from various sources. This reduces error and produces an estimate that has the minimum error variance. The OAFlux makes use of surface meteorological parameters and then computes the global fluxes by using the state-of-the-art bulk flux parameterizations. The OAFlux project aims to provide daily and 1°×1° resolution data on air-sea fluxes and SST for the global ocean basins that are free from ice. To obtain the best possible global daily estimates, surface meteorological fields derived from satellite remote sensing and reanalysis outputs produced from NCEP and ECMWF models were employed. However OAFlux synthesis does not assimilate ship meteorological reports.

SST input data to OAFlux comes from NOAA Optimum Interpolation (OI) 0.25-degree daily SST analysis produced by *Reynolds et al.* (2007). The analysis has two products: one uses Advanced Very High Resolution Radiometer (AVHRR) infrared (IR) satellite SST data and the other combines AVHRR infrared with AMSR-E microwave SST data. Both products use in situ data from ships and buoys and include a large-scale adjustment of satellite biases with respect to the in situ data. OAFlux SST data covers a period of 1958 to 2009.

3.2 Heat Flux

OAFlux

OAFlux project at the Woods Hole Oceanographic Institution (WHOI) provides estimates of air-sea flux data on latent and sensible heat fluxes, ocean evaporation, and flux-related surface meteorological variables on daily and 1-degree resolution. Latent and sensible heat flux estimates are commonly computed from the parameterization of the fluxes as a function of surface meteorological observables, such as wind speed, sea-air humidity and temperature gradients [*Liu et al.*, 1979]. These flux-related variables were from three major sources: marine surface weather reports from Voluntary

Observing Ships (VOS), satellite remote sensing, and NWP reanalysis and operational analysis outputs. Correspondingly, the heat flux products are grouped into three categories: ship-based products, satellite-based products, and NWP reanalysis products. The OAFlux project improves the estimates of latent and sensible heat fluxes through utilizing the best possible surface meteorological variables and the best possible bulk algorithm [*Fairall et al.*, 1996a].

ISCCP

Radiation data (shortwave and longwave) was obtained from ISCCP (International Satellite Cloud Climatology Project) [*Schiffer and Rossow,* 1985]. ISCCP was established in 1982 as part of the World Climate Research Programme (WCRP) to collect and analyze satellite radiance measurements to infer global distribution of clouds, their properties, and their diurnal, seasonal, and inter-annual variations. The radiation data covers the period 1983 to 2009.

3.3 Ocean Subsurface Temperature

World Ocean Atlas

World Ocean Atlas (WOA) is a climatological database provided by National Oceanographic Data Center (NODC) on temperature, salinity, oxygen, phosphate, nitrate, and silicate at standard depth levels [*Levitus and Boyer*, 1994]. Historical data collected from various sources were subjected to objective analysis to interpolate data at each grid in the ocean. The first version of this database was created in 1994 and updated thereafter to produce new versions in 1998, 2005, 2009 and 2013. The subsurface temperature data from WOA was used to study the annual characteristics of warm pool.

SODA

The Simple Ocean Data Assimilation (SODA), analysis is an ocean

reanalysis data set consisting of gridded variables for the global ocean, as well as several derived fields. The objective of the project was to provide an improved estimate of ocean state from those based solely on observations or numerical simulations. There are several versions of SODA [*Carton et al*., 2000; *Carton et al*., 2005; *Carton and Giese*, 2008], depending on the experiment setup. The ocean model is based on Parallel Ocean Program physics with an average 0.25°×0.4°×40-level resolution. Observations include virtually all available hydrographic profile data, as well as ocean station data, moored temperature and salinity time series, surface temperature and salinity observations of various types, and nighttime infrared satellite SST data. The output is in monthly-averaged form, mapped onto a uniform 0.5°×0.5°×40-level grid. The reanalysis provides three types of variables, those well constrained by observations, those partly constrained by dynamical relationships to variables frequently observed, and those poorly constrained such as horizontal velocity divergence.

RAMA

Research Moored Array for African-Asian-Australian Monsoon Analysis and Prediction (RAMA) is the moored buoy component of the Indian Ocean Observing System (IndOOS) which is based on a constellation of Earth observing satellites complemented by a variety of in-situ measurement arrays [*McPhaden et al.*, 2009]. RAMA buoy system is a component of the Global Tropical Moored Buoy Array program which is a multi-national effort to provide data in real-time for climate research and forecasting. Other components are TAO/TRITON array in the Pacific, PIRATA in the Atlantic. Physical and meteorological data collected within RAMA come primarily from ATLAS 9 Autonomous Temperature Line Acquisition System), TRITON (Triangle Trans Ocean Buoy Network) and equivalent moorings. Additional measurements are made from ADCP moorings and deep-sea moorings.

3.4 Wind

QuikSCAT Climatology

Satellites with sensors operating at microwave frequencies are used to observe ocean surface winds under nearly all-weather conditions. Both active (radar) and passive (radiometer) microwave sensors have been shown capable of retrieving the ocean surface wind speed, with active microwave instruments used to retrieve the wind direction. QuikSCAT wind data, processed by NOAA/NESDIS, are retrieved from NASA/JPL's SeaWinds Scatterometer. The empirical retrieval model currently used is referred to as QSCAT1, which relates normalized radar cross-section with wind speed and direction.

OAFlux

Wind data from OAFlux was also used. The input data sources of satellite wind speeds come from SSMI (Special Sensor Microwave Imager), AMSR-E (Advanced Microwave Scanning Radiometer – Earth Observing System) and QuikSCAT scatterometer. SSMI has been operating since July 1987 on board Defense Meteorological Satellite Program (DMSP) spacecraft. The data are available at a temporal resolution of 12 hour and at a swath resolution of 25 km. AMSR-E was developed by the National Space Development Agency of Japan (NASDA) and was launched on the NASA's Aqua satellite on May 4, 2002 in a sun synchronous near-polar low orbit at an altitude of 705 km and period of 99 min. The NASA QuikSCAT was launched into a sun-synchronous near polar orbit on June 19, 1999, at an altitude of approximately 800 km and period of 101 min. The main instrument on the QuikSCAT satellite is SeaWinds, which is an active radar scatterometer. This scatterometer operates by transmitting microwave pulses at a frequency of 13.4 GHz (Ku-band) to the ocean surface and measuring the echoed radar pulses bounced back to the satellite. Wind speed and direction at 10 m above

the surface of the water are then derived from the backscatter energy.

3.5 Outgoing Long wave Radiation (OLR)

OLR data acts as a proxy to atmospheric convection. Low OLR values indicate high convective activity. Climatological OLR data from NOAA was used to study atmospheric convection associated with warm pool [*Liebmann and Smith*, 1996]. The data was collected from a combination of several satellites.

3.6 *Oceanic Nino-3.4 Index (ONI)*

NOAA's Climate Prediction Center has determined the average monthly sea surface temperature for a particular swath of the tropical Pacific Ocean by averaging measurements collected there over the past 30 years. Scientists refer to that swath as the Niño 3.4 region. The observed difference from the average temperature in that region-whether warmer or cooler-is used to indicate the current phase of ENSO.

The Oceanic Niño Index (ONI) has become the de-facto standard that NOAA uses for identifying El Niño (warm) and La Niña (cool) events in the tropical Pacific. It is the running 3-month mean SST anomaly for the Niño 3.4 region (5^{o}N-5^{o}S, 120^{o}-170^{o}W). Events are defined as 5 consecutive overlapping 3-month periods at or above the +0.5 anomaly for warm (El Niño) events and at or below the -0.5 anomaly for cold (La Niña) events. The threshold is further broken down into Weak (with a 0.5 to 0.9 SST anomaly), Moderate (1.0 to 1.4), Strong (1.5 to 1.9) and Very Strong (≥ 2.0) events. Table 1 shows the summary of data set used.

3.7 Software Tools

Generic Mapping Tools (GMT)

GMT is an open-source software with command-line tools for manipulating geographic and Cartesian data sets such as filtering, trend

fitting, gridding and projecting. It produces PostScript illustrations ranging from simple x–y plots via contour maps to artificially illuminated surfaces and 3D perspective views. GMT was used to plot ascii data sets.

Table 1. Summary of data sets.

Type of Data	Source	Period	Spatial Resolution
SST	NOAA NCDC (ERSST)	1854-2013	2^{o} x 2^{o}
	Marine Data Bank (HadISST)	1870-2012	1^{o} x 1^{o}
	OAFlux	1958-2012	1^{o} x 1^{o}
Shortwave Radiation	ISCCP	1984-2009	1^{o} x 1^{o}
Longwave Radiation	ISCCP	1984-2009	1^{o} x 1^{o}
Latent Heat	OAFlux	1984-2009	1^{o} x 1^{o}
Sensible Heat	OAFlux	1984-2009	1^{o} x 1^{o}
Ocean Subsurface Temperature	SODA	1997	0.5^{o} x 0.5^{o}
	WOA Climatology	Annual	1^{o} x 1^{o}
	RAMA	2008	Profile data
Wind	QuikSCAT Climatology	Annual	25km
	OAFlux	2008	Time series
OLR	NOAA OLR Climatology	Annual	2.5^{o} x 2.5^{o}
ONI (ENSO Index)	NOAA	1854-2014	Time series

Ferret

Ferret is an interactive computer visualization and analysis environment designed to meet the needs of oceanographers and meteorologists who analyze large and complex gridded data sets. The features that make Ferret distinctive among other packages are Mathematica-like flexibility, geophysical formatting, memory management for very large calculations, and symmetrical processing in 4 dimensions

[http://www.ferret.noaa.gov/Ferret/]. In this study, the data in the netcdf format was analyzed using Ferret.

Fortran

Fortran is a general-purpose computer programming language that is suited to numeric computation and scientific computing. Fortran has wide applications in numerical weather prediction, finite element analysis, computational fluid dynamics, computational physics and computational chemistry. The ASCII data in this study were extensively analyzed using Fortran to generate new data outputs.

Chapter 4

IOWP Annual Climatology

SST and warm pools undergo annual variation owing to annual variation in solar radiation, wind and ocean processes. The resultant seasons, according to temperature variation, are often the summer and winter. During summer, solar radiation is maximum and in winter, it is minimum. Seasons are further classified into subdivisions and also on a regional basis. And, especially in Indian Ocean, monsoon is a dominant annual feature. Hence, the seasons around India are classified in terms of monsoon, as southwest monsoon and northeast monsoon. The objective of this chapter is to quantify the variations of IOWP within the annual period, with due emphasis on summer/winter seasons.

4.1 Evolution of IOWP

Ocean warms and cools on an annual time scale due to heat exchange through shortwave solar radiation, long wave back radiation, latent heat and sensible heat. Due to the excess heat input, tropical water is warmer, reaching temperatures over 30^{o}C. Hence, warm pools are formed on tropical waters drive atmospheric circulation. If solar radiation without clouds is the only factor for warming the oceans, then the isotherms and hence warm pool would align purely east-west. However due to various other factors, there can be large difference in the zonal distribution of ocean temperature and hence warm pools.

Monthly World Ocean Atlas (WOA) temperature climatology data [*Levitus and Boyer,* 1994] was used for this study. Maps of SST above 28^{o}C were prepared on a monthly basis to understand the annual variations in the horizontal extent of IOWP (Figure 4.1). IOWP attains the annual maximum horizontal area during the period April- May. This period of the year is called as pre-monsoon season. It is to be noted that the maximum warming did not

occur at the peak of the summer but at the beginning. During this time, IOWP had the maximum meridional extent of 20^{o}S to 20^{o}N. Highest warming occurred at the central and eastern part of the warm pool having temperatures above 30^{o}C. Large differences in the distribution of warm pool were found between Arabian Sea and Bay of Bengal. While the warm pool covered the entire Bay during this time, warming was weaker towards the northern Arabian Sea.

As the monsoon season begins in June, warming of the oceans stands greatly reduced by the presence of monsoon clouds, increased turbulent mixing and vertical movement. There is an overall decrease in the temperature and the area of IOWP. It is to be noted that the warm pool attained its minimum intensity in the month of August which falls within the 'summer' season. Monsoon weakening of IOWP is more pronounced at the western Indian Ocean and in Arabian Sea. The strong coastal upwelling makes the surface temperature low and appears to displace warm pool towards east. Along with an eastward shift, IOWP also experienced northward displacement during summer which together made the warm pool to have the lowest intensity. Meridional displacement was higher at the western side than at the east.

The vertical distribution of temperature was analyzed to confirm the role of coastal upwelling for the absence of warm pool waters at the western Indian Ocean (Figure 4.2). A zonal temperature section at 10^{o}N was prepared for the months of May and August that represents the peaks of the warm pool. During May, the temperature distribution was generally independent of depth and the isotherms were nearly horizontal. This shows the absence of oceanic vertical movement. During August, large variation in the zonal distribution of isotherms was noticed. Isotherms at the west bend towards surface. This usually happens when vertical movement is strong that brings

subsurface colder water to surface and referred to as coastal upwelling. Hence, it can be confirmed that the absence of warm pool at the western Indian Ocean is due to oceanic advection and not due to a reduction in the heat fluxes.

During November to January solar radiation falls normally in southern hemisphere and makes a corresponding change in the appearance of IOWP. The core of the warm pool now migrates towards south. Here again large displacements were found at the western Indian Ocean. The warm pool at the eastern Indian Ocean had minimal meridional displacement and was also the warmest region of IOWP throughout the year. A higher warming occurred at the western and eastern regions unlike that during the pre-monsoon where the warming was maximum at the central Indian Ocean. Warm pool was almost absent in both Arabian Sea and Bay of Bengal during this time.

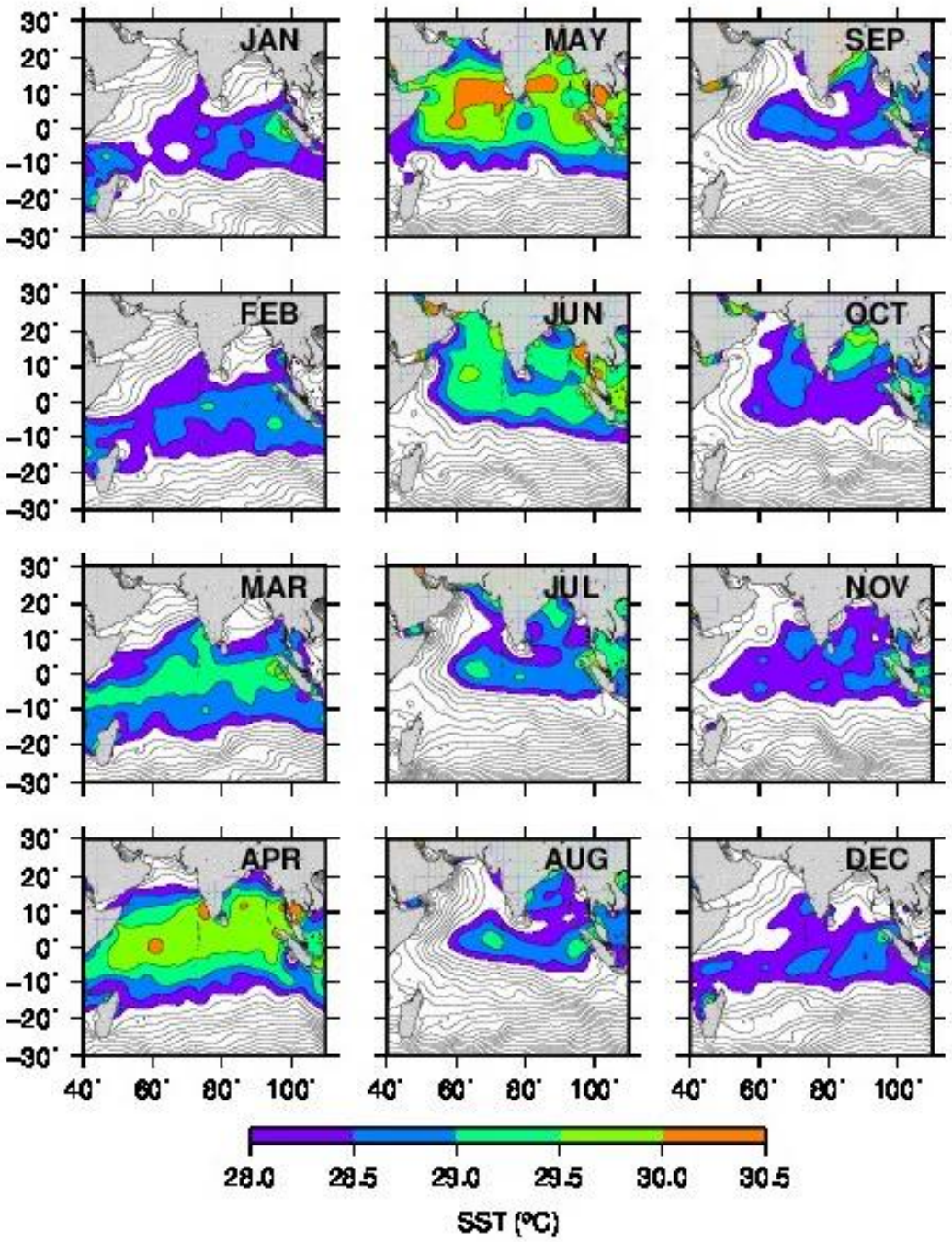

Figure 4.1 Annual variation of IOWP using Levitus Climatological data. SST above 28°C is colored. Contour interval is 0.5°C

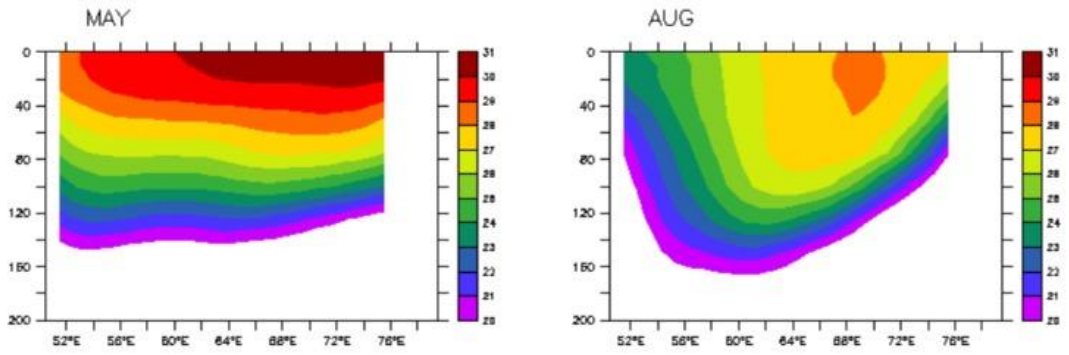

Figure 4.2 Horizontal section of temperature at 10°N in the Arabian Sea during May and August showing the changes in the vertical distribution of warm pool induced by vertical movements associated with upwelling.

4.2 IOWP Indices

Warm pool characteristics are often represented in terms indices that represent surface area, mean temperature and volume of the warm pool. Warm Pool Area Index (WPAI) is the horizontal area covered by the warm pool waters. It was estimated by multiplying the number of grids of SST above 28°C with the area of a grid in km^2. For a 1x1 degree grid, such as in Levitus data, the area of a grid is 110x110 km^2. Since the warm pools are limited to the tropics, the variations in the grid size as a function of latitude can be neglected.

Warm Pool Temperature Index (WPTI) is another index that represents the mean temperature of the warm pool. It was estimated by averaging the temperature from all warm pool grids. Volume of the warm pool is expressed in terms of Warm Pool Volume Index (WPVI) that was obtained by computing the volume occupied by the warm pool waters. In this study, the annual variations of these warm pool indices are addressed. Figure 4.3 shows the annual variation of the three indices of IOWP. The result of this analysis will provide additional information on the quantity of IOWP variability. WPAI undergoes the annual cycle with the maximum area ($26x10^6$ km^2) during pre-

monsoon season (March to May) (Figure 4.3a).

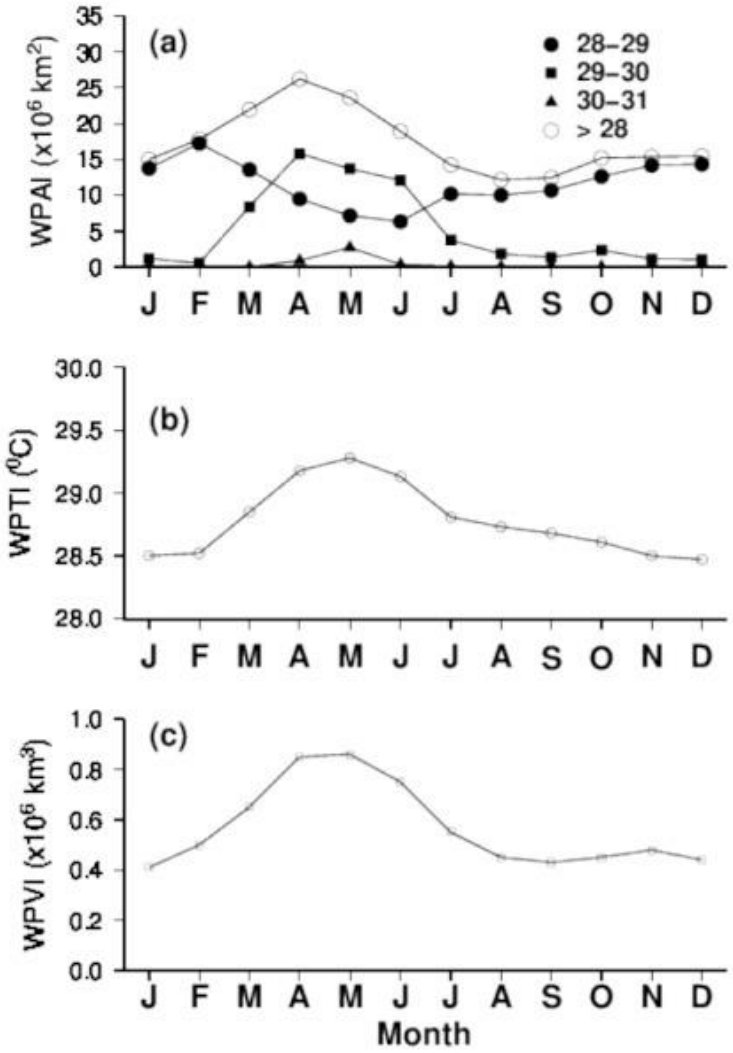

Figure 4.3 Annual variation of warm pool indices of (a) area (WPAI), (b) temperature (WPTI) and (c) volume (WPVI). WPAI was obtained by estimating the surface area covered by the warm pool whereas WPTI represents the mean temperature of the warm pool. WPVI is estimated by integrating the area covered by warm pool in the vertical.

This value is slightly higher than that reported by *Vinayachandran and Shetye* (1991). The difference might be due to the small difference in the geographical limit of study area especially at the eastern side. WPAI decreased as the monsoon season sets up. Warm pool shrinks to a minimum area of

$12x10^6$ km^2 in the month of August. After the summer monsoon, WPAI showed a mild increase. It is noted that the warm pool did not respond equally to the summers of each hemisphere. Southern summer could not produce a similar warm pool at the south as that done by the northern summer.

The area covered by 1 degree temperature differences (28-29, 29-30 and 30-31^oC) showed different distribution pattern. The area covered by 28-29^oC showed maximum during winter and minimum during summer. The other two temperature bands had maximum intensity during summer and nearly insignificant during other periods. Hence, the total variation of warm pool is mainly contributed by the 28-29^oC except during summer where the 29-30^oC also had a significant contribution. As expected, there is a negative relationship between the two; as the area of the 28-29^oC band increases, that of 29-30^oC reduces and vice versa. This would imply that as the ocean warms, larger changes to temperatures occur at higher temperatures and changes that occur to lower temperatures are comparatively lesser.

Warm pool temperature, represented by WPTI also had a similar distribution as that of WPAI (Figure 4.3b). It is obvious that as the water gets heated, the temperature and the area of the warm pool increased. WPTI was high during the pre-monsoon season. As monsoon onsets, mean temperature of warm pool also decreased. It is noted that though warm pool area had a mild increase during winter, a corresponding increase was not found in WPTI. The volume index, WPVI also had a similar variation as that of the other two indices (Figure 4.3c).

4.3 IOWP Vertical Extent

An understanding of the vertical extent of the warm pool would be helpful in estimating the heat content of the upper waters. The vertical limit of IOWP was obtained by identifying the depth of 28^{o}C isotherm (D28) in the vertical. Figure 4.4 shows the geographical distribution of D28 for the months January, April, August and September. The D28 is plotted over SST contour maps to make comparison between both.

The close relationship between the distribution of SST and D28 is not surprising. However, a minor mismatch in the locations of their maxim is but surprising. The higher values of D28 can occur due to higher mixing induced by stronger winds and buoyancy. If winds are weak, turbulent mixing will reduce and would make lower D28 if buoyancy is also weak. During January, SST is higher at the eastern and western Indian Ocean. During this time, D28 is also found higher at these locations. During April, as the warm pool intensifies, a corresponding deepening of the warm pool is also occurs. The maximum warm pool depth was 70m during this time. However, there was a marked difference in the position of maxima in SST and high D28. The maximum SST was found at the equatorial area whereas the maximum of D28 was north of SST maxima. The higher D28 away from SST maximum indicates the role of other processes on warm pool vertical dynamics rather than diffusion. During August, a D28 maximum was found at the western and eastern end of the warm pool. During October, D28 maximum was found over the warm pool core areas.

4.4 Meridional Displacement of IOWP

The annual variation in the meridional displacement of warm pool was studied by locating the warm pool edge at its southern and western boundaries (Figure 4.5). The time-latitude plot of SST was made at western

(60°E) and eastern (90°E) Indian Ocean. The southern edge of IOWP had undergone annual variation of more than 10 degrees of latitude. The western side of IOWP had larger merdional displacement than that at east. The maximum southward extend of IOWP occurs during the pre-monsoon season at both ends. The difference in the IOWP distribution at north is due to the difference in warm pool characteristics of Arabian Sea and Bay of Bengal. *Zhang et al*. (2009) also obtained similar observations even though they used a different data set.

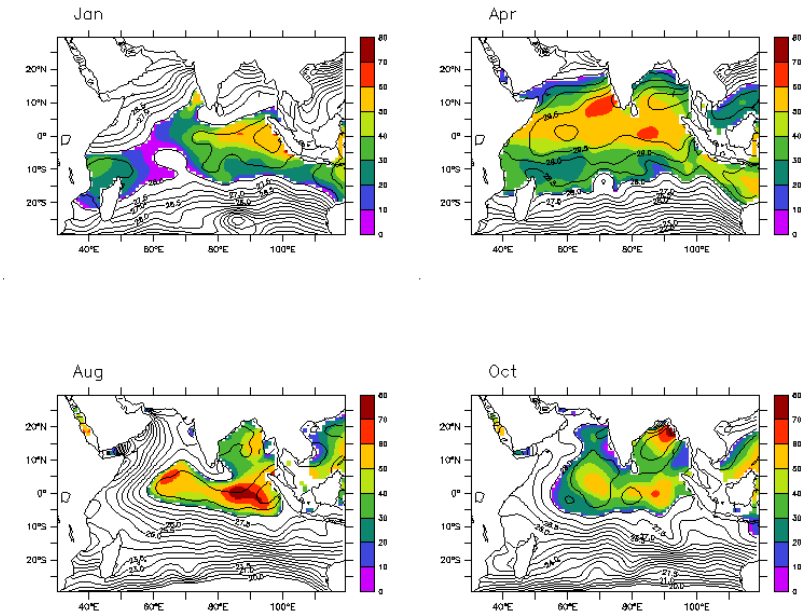

Figure 4.4 Depth of 28°C isotherm (D28) and SST. D28 values (in meters) are colored and plotted over SST contours. Contour interval is 0.5°C

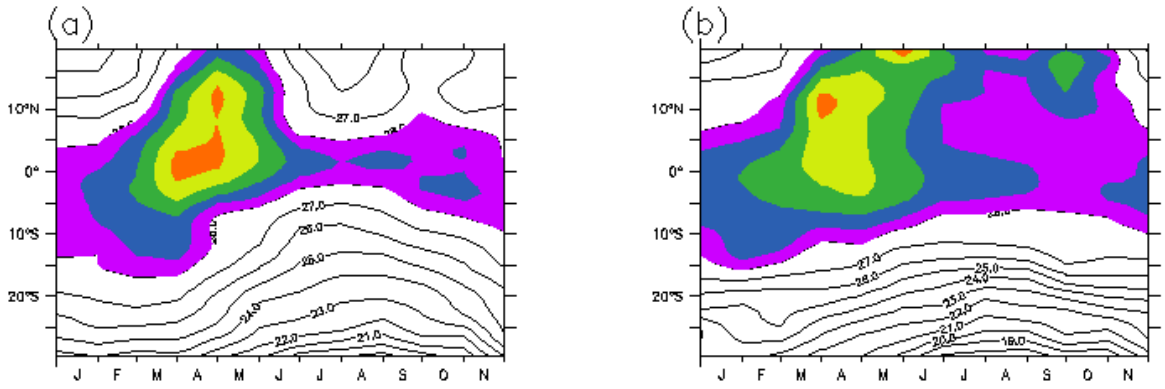

Figure 4.5 Meridional displacement of IOWP at (a) western (60°E) and eastern (90°E) Indian Ocean. Warm pool SST (above 28°C) is colored

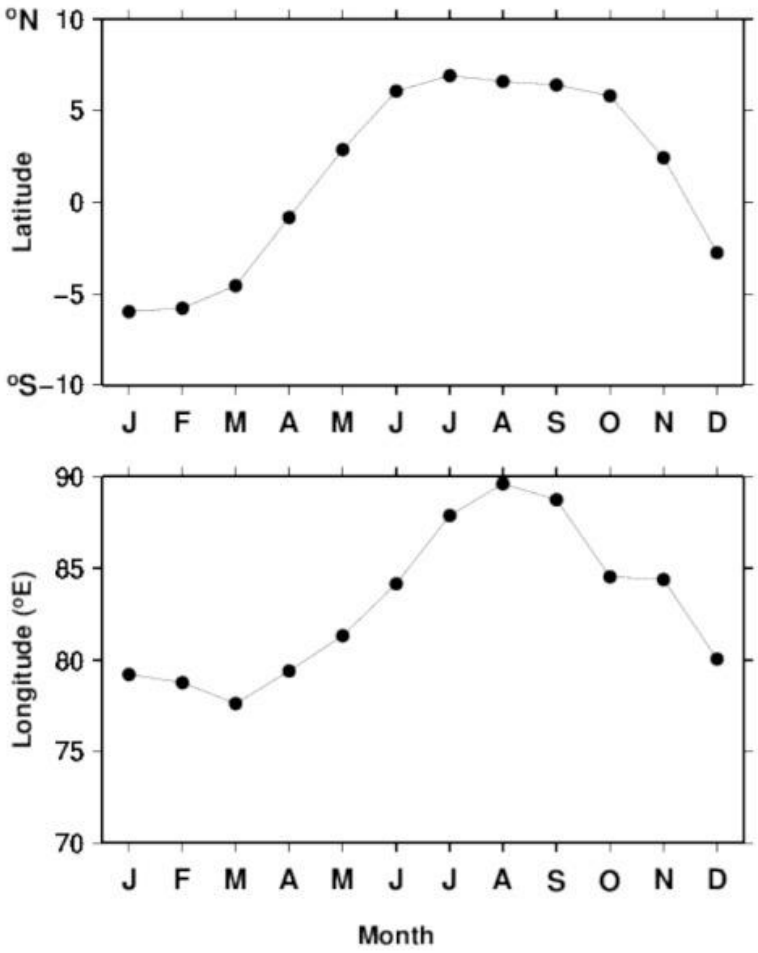

Figure 4.6 Annual variation of mean latitude and longitude of warm pool

The zonal and meridional displacement of the entire warm pool was

studied by estimating the changes in mean latitude and longitude position of IOWP. The monthly variation of the mean position of the warm pool is shown in Figure 4.6. The mean latitude of the warm pool followed the respective hemispheric summer. During the northern summer, the mean latitude was in the northern hemisphere, and was at south during southern summer, but with a large hemispheric asymmetry. The mean position varied from 5^{o}S to 7^{o}N. Time duration of IOWP was more for the northern hemisphere. The mean longitude also had an east-west oscillation. Warm pool shrinks towards east during summer season. The mean longitude moved up to 90^{o}E during the weak period and had a maximum westward limit of 77^{o}E during the time of its maximum intensity in spring season.

4.5 Frequency Distribution of Temperature

The frequency distribution of warm pool temperature is helpful to understand the nature of variability of warm pool. A characteristic feature of warm pool is that the highest contribution comes from temperature that is few degrees less than the highest [*Clement et al*., 2005]. They have reported a negatively skewed distribution for SST. Their model experiments confirmed the presence of cirrus clouds on the observed frequency distribution of warm pool temperatures. The dominance of a particular temperature band also shows the homogeneity of temperature within the warm pool.

Figure 4.7 shows the monthly variation of the percentage of area covered by each one degree interval temperature bands. The analysis was performed for SST above 20^{o}C. During northern winter (Dec-Jan-Feb), maximum area was covered by the 28-29^{o}C temperature band. Higher temperatures had only little contribution during this time. During the pre-monsoon period (Mar-May), the 29-30^{o}C temperature band dominated the area. The 30-31^{o}C band also had a significant contribution at this time. During the monsoon period (June to September), highest area contribution came

from the 28-29^{o}C band.

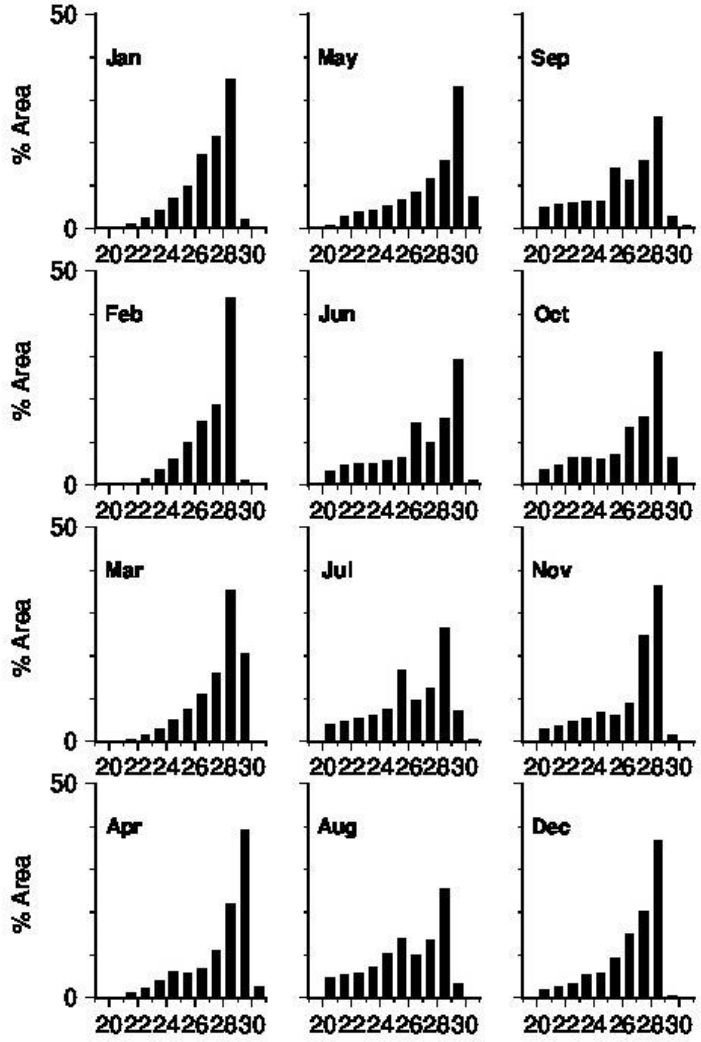

Figure 4.7 The annual frequency distribution of temperature

4.6 IOWP and Wind Distribution

Warm pool is an area with low sea level pressure that leads to the convergence of surface winds [*Rasmusson and Carpenter*, 1982]. The relation between warm pool and wind distribution is shown in Figure 4.8. Wind vectors were plotted over SST contour for the months of January and July.

QuikSCAT climatological wind data was used.

The seasonal reversal of wind is evident from the figure mainly in the north Indian Ocean. Winds south of 10^{o}S was mostly unaffected by the seasonality. During January, wind was north-easterly and converged towards the core of the warm pool at the eastern equatorial area. Wind from northern Pacific also converged here. Wind speed was greatly reduced over warm pool areas.

Wind speed during this time was weaker than during July. The low wind speed distribution aligned similar to that of warm pool. This shows that wind speed is lesser over the warm pool area. Low wind speed had positive feedback on the warm pool development by reducing diffusion of heat vertically in the ocean. During July, wind in the north Indian Ocean reverses and becomes south westerly. Warm pools weaken during this time and have the core in the central and eastern areas. Convergence of wind is again evident over the warm pool waters during this time. Due to the higher temperatures of south Asian land masses, wind tends to converge over the land than over ocean, bringing monsoon to India. Wind speed was again lesser over the warm pool area.

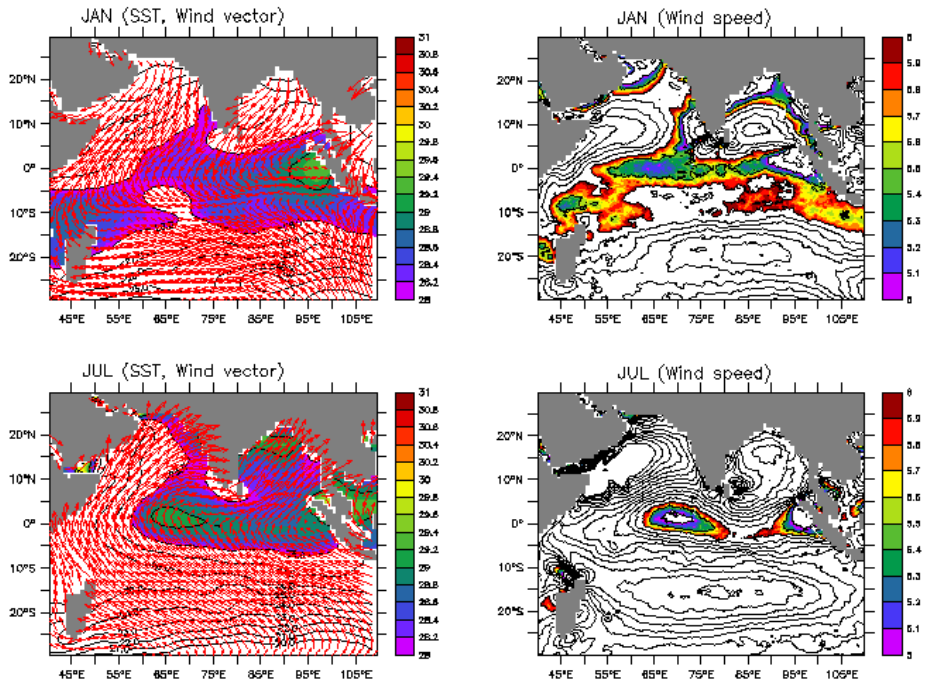

Figure 4.8 Warm pool and surface wind distribution during January and July. In the left panel, wind vector is plotted over SST contours. Warm pool is colored. In the right panel, wind speed is plotted as contours and low wind speed areas (less than 6m/s) are colored

The area covered by the low wind now reduced. This indicates that the wind speed is higher throughout the Indian Ocean. Hence, the result shows that warm pool acts as areas of convergence of wind and the wind becomes weaker too.

4.7 IOWP and Atmospheric Convection

As the warm pools are low pressure centers, deep atmospheric convection are associated with warm pools. Atmospheric convection is an important mechanism that transports heat and water vapor deep into the atmosphere. Atmospheric convection is indirectly represented in terms of

Outgoing Longwave Radiation (OLR). Convective areas are represented by low OLR values (less than 240 W/m^2). The low OLR is due to the presence of deep convective clouds that prevent the long wave radiation from escaping to space. Hence, the satellites will record a lesser OLR in convective areas. Figure 4.9 shows the warm pool and OLR for the months of January and July. From the figure, it is evident that OLR values are less than 240 W/m^2 over warm pool areas. The orientation of warm pool SST and OLR had a close resemblance. At the eastern areas where SST is highest, still lower OLR values were found.

During July, warm pool appears as a tongue from east to west and the OLR also had a similar appearance. Hence the warm pools are associated with high vertical transport of moisture and hence an important area for air-sea interaction studies. A non-linear relationship exists between SST and atmospheric convection at high SSTs. It was found that atmospheric convection increases with SST until SST become 29^oC. Further increase in SST, however, was found to decrease the convection [*Gadgil et al*., 1984; *Graham and Barnet*, 1987].

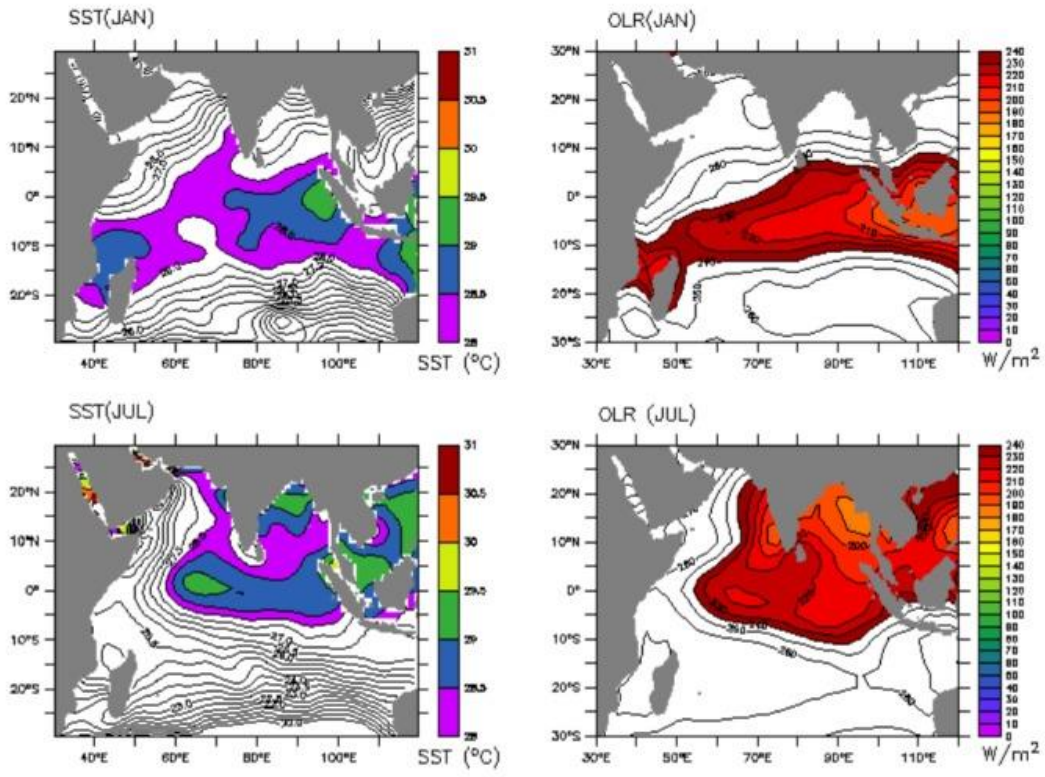

Figure 4.9 Warm pool and Outgoing Longwave Radiation (OLR) during January and July

4.8 Annual Heat Budget

The solar radiation warms the oceans on a seasonal scale. The Earth's axis of rotation and the annual revolution around the sun together creates the annual variations in the incoming solar radiation. The warm ocean loses heat through other processes such as evaporation, conduction and radiation. The net heat received as the algebraic sum of heat input and output decides the temperature of the oceans. However temperature can also be influenced by other processes in the ocean such as advection, diffusion and mixing. The calculation of individual heat fluxes and their total is termed as heat budget.

$$Q_{NET} = Q_S - (Q_B + Q_E + Q_H)$$

where Q_{NET} is the net heat input/output, Q_S is the shortwave radiation, Q_B is the backward emitted radiation from the ocean, Q_E the evaporative (latent)

heat and Q_H is the sensible heat lost due to conduction with atmosphere. The turbulent heat fluxes (latent and sensible) were estimated by using bulk flux algorithms with surface meteorological variables.

Several attempts were made to estimate the heat budget of Indian Ocean [*Hastenrath and Lamb*, 1979; *Esbensen and Kushnir*, 1981; *Hsiung*, 1985; *Oberhuber*, 1988; *da Silva et al*., 1994; Fasullo and Webster, 1999; *Josey et al*., 1999; *Yu et al.*, 2007]. Majority of heat stored from solar heating is lost back to atmosphere and space through evaporation and radiation. Heat loss due to conduction is a small quantity as compared to others. Part of the heat is also transported to other areas by Ekman currents. This transport of heat by currents is responsible for reducing the temperature gradient between the tropics and higher latitudes. Excess heat added will make the SST to increase and otherwise will cool.

Yu et al. (2007) estimated the heat balance using different data sets. The correlation between SST and Q_{NET} was higher south of 10^oS. This suggests that heat fluxes play an important role in the evolution of SST in those areas. Poor relationships were found at western Arabian Sea and at eastern equatorial Indian Ocean. The lack of correlation in the western Arabian Sea is due to the vertical movement from upwelling [*Schott and McCreary*, 2001]. In upwelling areas, cooler waters are brought to the surface and make the SST low. A higher heat input is often found in upwelling areas because of low cloud cover and reduced latent heat loss. Hence the correlation between SST and heat flux can be negative. The low correlation observed at the southern central region is found to be due to the presence of a thermocline ridge [*Wyrtki*, 1971].

To understand the role of heat fluxes on the annual variation of SST, heat fluxes were compared with SST for each month representing summer

(August), winter (January) and pre-monsoon (May) season (Figure 4.10). Heat flux data from OAFlux was used for this study. Climatological mean of heat flux was estimated by averaging the 26-year monthly data for each month. Similar procedure was applied for SST also.

SST showed distinct patterns during each season. During winter, SST was lowest in magnitude and was oriented from west to east as a band. During this season, highest shortwave radiation was received at southern latitudes (south of 20^{o}S) much away from the peak SST. This shows a weak role of solar radiation on SST. Longwave radiation had higher values at extreme north of Arabian Sea and Bay of Bengal that caused a higher cooling in SST. In the equatorial areas longwave radiation had smaller values indicating lesser heat loss. This positively correlates with the higher SST there. Latent heat flux also had lesser values in the equatorial areas, again supporting the warming. The net heat flux, computed from all the heat flux terms, shows net heat input to the ocean at south of about 5^{o}N. Overall, the highest SST did not match with the highest net heat gain. However, it was observed that in the areas of warm pool, net heat is positive but in low magnitudes.

Hence, it can be concluded that the SST at southern tropical Indian Ocean (south of 20^{o}S) must be influenced by some other mechanisms, probably within the ocean, that reduce the SST. The reason for this could be due to the influence from other processes such as vertical movement, remotely forced waves and others on SST [*Zhong et al*., 2005].

During May, the pre-monsoon season, SST reaches its maximum. Warm pool covers the entire north Indian Ocean, north of 10^{o}S. Warm pool core was found at the southern Arabian Sea. Solar radiation was maximum at the northern Arabian Sea where SST was found lesser. A gradual decrease in the intensity of solar radiation was found towards south. The patterns of SST and

Qs were not aligned, indicating a weaker relationship. Longwave radiation was nearly uniform and did not show any positive relationship with the SST. Higher evaporation from strong winds caused a high latent heat loss at southern latitudes. Lowest evaporative heat loss did not match with the high SST. The net heat flux was positive north of 20^{o}N and was in general supporting the warming at the northern Indian Ocean.

During monsoon season, represented by August, warm pool was restricted to a small area at the eastern equatorial Indian Ocean. Shortwave radiation greatly reduced during this time by the monsoon clouds. Higher heat input was found at the western Indian Ocean where SST was much less. Longwave radiation has a weaker loss at the northern Arabian Sea and Bay of Bengal, possibly due to the presence of clouds. Shortwave radiation was also had a low value in this area, supporting the presence of clouds. Latent heat flux was weak at the western Indian Ocean and could be due to the cold upwelled water. Highest latent heat loss was found again at the southern latitudes.

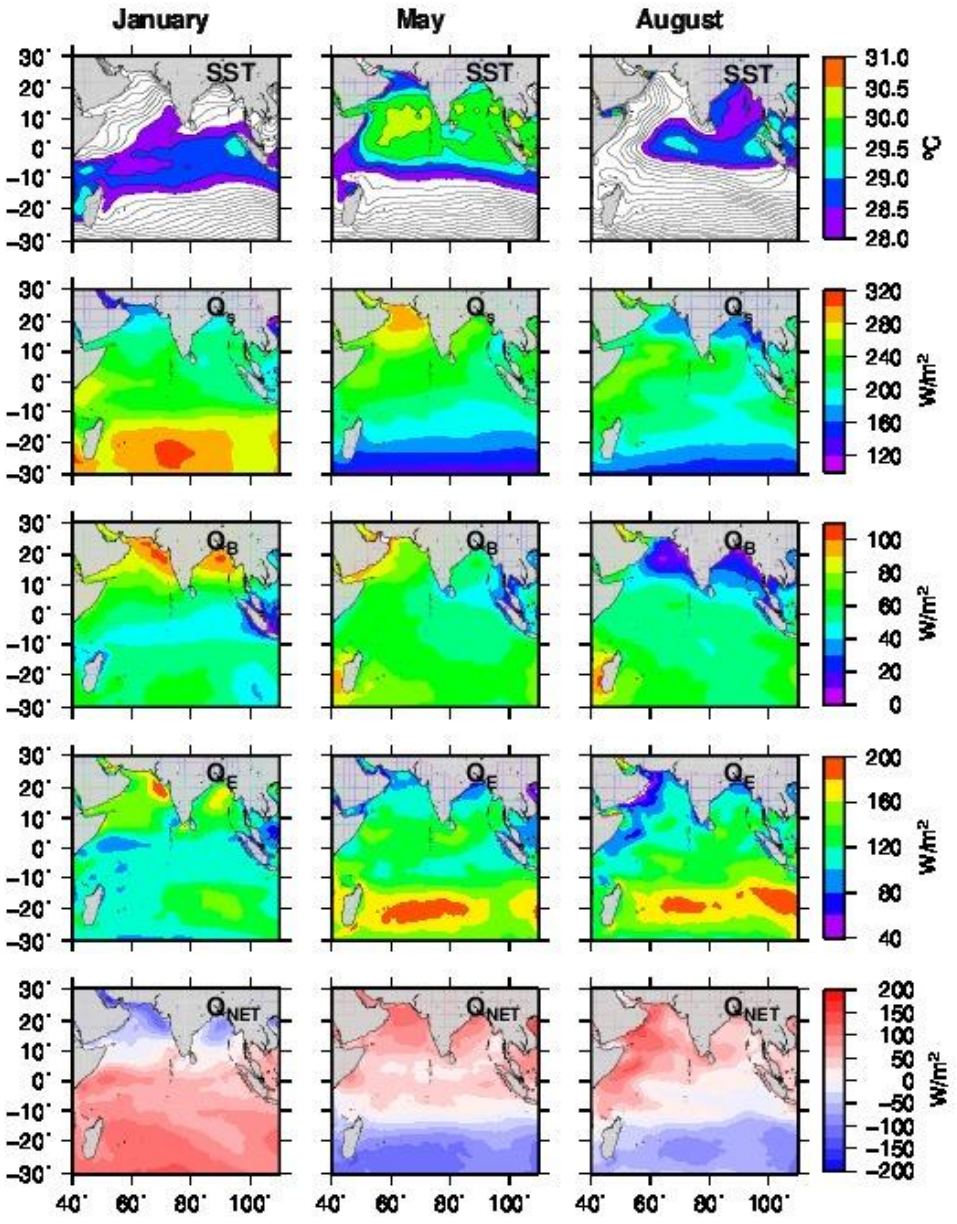

Figure 4.10 Seasonal variation of SST, shortwave radiation (Q_S), Longwave back radiation (Q_B), latent heat (Q_E) and net heat Flux (Q_{NET}) during January (left panel), May (middle panel), and August (right panel)

The net heat flux shows a heat gain at the western and northern Indian Ocean and negative at south of equator. Though high SST did not coincide with the high heat gain, net heat flux was found at least positive over the warm pool areas. In conclusion, a perfect correlation between net heat flux and SST is lacking but the warm pool had occurred in areas where net heat flux was moderate and not the lowest. So in areas with high net heat input, the heat absorbed by the ocean might have been transported or mixed to make the SST low or the thermocline oscillation induced by planetary waves may have a dominating role.

4.9 Conclusions

IOWP undergoes variations on annual cycle in accordance with the annual forcing from Sun. Warm pool attains maximum intensity during the pre-monsoon season (April-May) and not at the peak of the summer. The weakening of warm pool during summer owes to the presence of clouds and vertical movement in the ocean. In fact, the warm pool reaches the minimum at the middle of the summer. Warm pool indices (area and mean temperature) also had annual variability. From the depth of 28^{o}C isotherm it was observed that warm pool extends up to a depth of 100m. The deepest part of the warm pool did not coincide with a high SST.

Meridional displacement of warm pool was characterized by southward migration during pre-monsoon and northward during monsoon season. Frequency distribution of temperature showed the dominance of each temperature band during the respective seasons. Warm pool is identified as an area where wind converges. Convergence of wind is followed with ascending motions in the atmosphere that leads to clouds and rain. Convergence of wind was found towards the core of warm pool. Converging wind becomes weaker which can impose a positive feedback on SST for

further warming.

Heat budget analysis was performed to understand the role of heat fluxes on SST. There was only a weak relationship between the two especially at their core areas. High net heat input did not coincide with the high SST. This confirms the role of other processes on modulating SST.

Chapter 5

ENSO-Induced Inter-annual Variations in IOWP

5.1 Introduction

Oceanographic properties vary on time scales ranging from seconds to hundreds of years. The energy of such variations is not uniform among the scales but centered at few specific scales. The dominant period of variability is the annual cycle with a period of 12 months. The diurnal variation of solar radiation as a result of Earth's rotation is also a major contributor to variabilities especially at coastal areas where tides dominate. As the time changes from year to year, changes in the seasonality can occur. This change that occurs from year to year is called as inter-annual variability.

Inter-annual variabilities are found in each ocean. They may magnify at selected regions of the oceans and sometimes are even capable of altering the global climate. The dominant modes of inter-annual variabilities in the oceans are El Nino Southern Oscillation (ENSO), Indian Ocean Dipole (IOD), Pacific Decadal Oscillation (PDO), Quasi-Biennial Oscillation (QBO), North Atlantic Oscillation (NAO) etc. This part of the study investigates the role of ENSO on the inter-annual variabilities in Indian Ocean with an emphasis on Indian Ocean Warm Pool.

ENSO is observed as an oscillation in the distribution and magnitude of SST in the equatorial Pacific Ocean and the associated changes in the ocean-atmosphere system such as sea level pressure, rainfall, atmospheric convection, oceanic thermocline, coastal upwelling etc. (Figure 5.1).

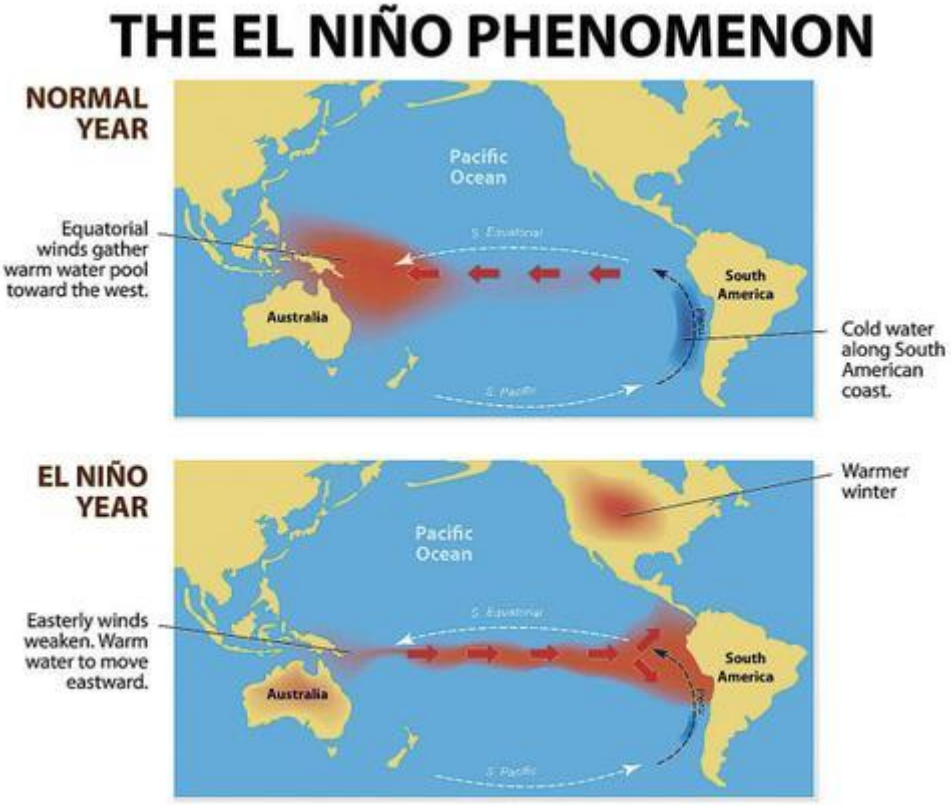

Figure 5.1. Schematic showing the equatorial Pacific Ocean during normal (upper) and El Nino (lower) years [source: https://scienceisland.org/]

Since ENSO is a result of changes in SST, its oscillation is classified into 'warm' and 'cold' phases. The warm phase of the oscillation is called as 'El Nino' and the cold phase as 'La Nina'. In normal years, western Pacific is warmest and an active area of atmospheric deep convection. This maintains the east-west Walker circulation. However, during an El Nino, the weakening of trade wind leads to a displacement of the warm water from the west to central and eastern Pacific. This modifies the zone of atmospheric convection and alters the Walker circulation. The whole process disrupts the normal weather conditions in Pacific and also at places far from Pacific.

ENSO induced anomalies begin to form by the middle of the year and enhance to a maximum by the end of the year (December) and weaken further. The periodicity of occurrence of ENSO is 2 to 7 years. The strongest El Nino so far is that of 1997-98. It is interesting to note that there is no strong El Nino event occurred during the past decade. La Nina is the cooling phase of ENSO. Unlike El Nino, La Nina does not have negative impacts on the climate and was given lesser importance. The periods of occurrence of El Nino and LaNina since 1950 are shown in Table 2.

ENSO intensity is quantified in terms of an Index. There are two types of indices in use, called as Southern Oscillation Index (SOI) and Oceanic Nino Index (ONI). SOI is an estimate based on the atmospheric pressure anomaly over the central (Thahiti) and western (Darwin, Australia) Pacific Ocean. ONI on the other hand is based on SST anomaly over the equatorial Pacific. ONI has been obtained from different regions. Among these, the Nino-3.4 index, estimated from the area 5S to 5N; 170W to 120W, is the commonly used one and is also used in this thesis.

Cadet and Diehl (1984) identified ENSO impacts on most of the meteorological parameters such as SST, wind, sea level pressure, air temperature, and cloud. Spectral analysis revealed the presence of oscillations at semi-annual and annual time periods. More importantly, peak energy was also found at a period of about 40 months. This could represent the ENSO variability as the mean periodicity of ENSO is about 3 years.

El Nino	La Nina
1957-58	1955-56
1965-66	1970-71
1972-73	1973-74
1982-83	1975-76
1986-87	1988-89
1991-92	1998-99
1997-98	2007-08
2002-03	
2009-10	

Table 2. Years of occurrence of El Nino and La Nina during 1950-2010

[source: http://ggweather.com]

Karnauskas and Busalacchi (2009) studied the inter-annual variability of eastern Pacific Ocean caused by ENSO. They observed that the primary mechanism governing ENSO-induced inter-annual variability of SST in the warm pool is the surface shortwave radiation. Increased SST anomaly at the tropics due to ENSO leads to an increase in the convection at the equator and a subsidence off equator. The subsidence of air makes the atmosphere free of clouds and leads to the increased shortwave radiation and hence the formation of warm pool. This theory did not look good due to the previously established fact that warm pools are active areas of convection rather than subsidence.

Studies showed that ENSO contributes to more than 25% of inter-

annual variabilities of SST in Indian Ocean [*Klein et al.*, 1999; *Zhong et al*., 2005]. There has been a number of studies that looked into the inter-annual variabilities in Indian Ocean due to ENSO events [*Rasmusson and Carpenter*, 1982; *Nicholls*, 1984; *Meehl*, 1987; *Kiladis and Diaz*, 1989; *Hastenrath et al.*, 1993; *Klein et al.*, 1999; *Lau and Nath*, 2000, 2003; *Alexander et al.*, 2002; *Huang and Kinter*, 2002; *Hendon*, 2003; *Krishnamurthy and Kirtman*, 2003; *Wang et al.*, 2003]. The general consensus of these studies is that Indian Ocean experiences a basin-wide warming during El Nino years. Since the geophysical variables in the ocean and atmosphere are highly coupled, changes in the SST can induce changes in other variables and hence the entire ocean-atmosphere system.

Based on their "atmospheric bridge" concept, *Klein et al.* (1999) found that ENSO impact in Indian Ocean is not immediate but lags behind the developments in the Pacific by about a season (3 to 4 months). They found the magnitude of SST anomaly of about 0.2-0.3^{o}C with extremes up to 0.5^{o}C. The anomalous warming is not uniform within the tropical Indian Ocean but has strong regional variations. *Yu and Rienecker* (1999, 2000) studied the evolution of ENSO-warming in Indian Ocean. They observed that the warming begins in the western equatorial Indian Ocean as a first response to the El Nino by the middle of the year. Warming then extends to other regions as El Nino develops in the Pacific. The basin-wide warming is achieved by about April of the next year. The cause of the anomalous warming, its regional dependency and evolution was found to be due to the variabilities in wind and heat fluxes, mostly by solar radiation [*Klein et al.*, 1999; *Yu and Rienecker*, 1999; *Venzke et al*., 2000; *Lau and Nath,* 2003; *Shinoda et al*., 2004].

Recently, *Kumar et al*. (2015) have studied the SST variabilities in Arabian Sea and Bay of Bengal. They observed warm (cold) SST anomalies during El Nino (La Nina) events. The magnitude of SST anomaly was, however,

higher in the Arabian Sea. The variabilities in the local heat fluxes could not account for the observed SST anomalies. In fact, they have observed an inverse relationship between SST and heat fluxes. Hence, further study is needed to find the mechanism for SST variabilities during El Nino events. This chapter is planned to study the inter-annual variability of the Indian Ocean with an emphasis on IOWP due to ENSO activities.

5.2 Energy Spectra

Power spectrum analysis is performed on SST and heat flux data. It is a mathematical tool to identify the dominant variabilities in a data. Fast Fourier Transform (FFT) is performed on the monthly data to extract the dominant components of oscillations from the raw data. The analysis requires long period data to obtain stable estimates of energy peaks. The data was split into ensembles of size 120 months. The ensemble length determines the maximum retrievable period of oscillation. Sampling interval (here one month) of the data, on the other hand, determines the lowest period of oscillation that can be extracted.

Power spectra analysis was previously done by *Cadet* (1985) on meteorological parameters in Indian Ocean. He found significant peak in the power spectrum at a period of 40 month. This response can be either local or remote. Locally, the only possibility is through the Indonesian flow where the Indian and Pacific Oceans exchanges water. If this is dominant, then the eastern Indian Ocean would have responded first to ENSO events. But studies showed that the whole north Indian Ocean responds equally to ENSO without much spatial lag. Hence, the local influence can be discarded. *Klein et al*. (1999) emphasized the role of remote forcing of ENSO on Indian Ocean. They proposed ‘atmospheric bridge’ concept as the mechanism for the ENSO-induced variabilities in Indian Ocean.

Energy spectra were obtained for SST, wind speed, and heat fluxes (shortwave radiation, longwave radiation, latent heat flux and sensible heat) from OAFlux (Figure 5.2a). These data sets had different observational period. SST spans a period of 55 years whereas all other data had a period of only 25 years. Hence different ensemble lengths were used while performing the analysis. Time series of each data was obtained after spatially averaging over the tropical Indian Ocean before performing spectral analysis.

All data showed energy peaks at annual (T=12 months) and semi-annual (T=6 months) periods [Figure 5.2a]. These peaks had similar magnitudes and dominate within the selected periodicity range of 1 to 120 months. The higher magnitude of energy at annual period indicates the strong seasonal variations in each parameter. A wide peak with a period of about 30-40 month was seen in the SST data. The amplitude of this peak was much lower than that of annual and semi-annual. This observation is in agreement with that of *Cadet* (1985).

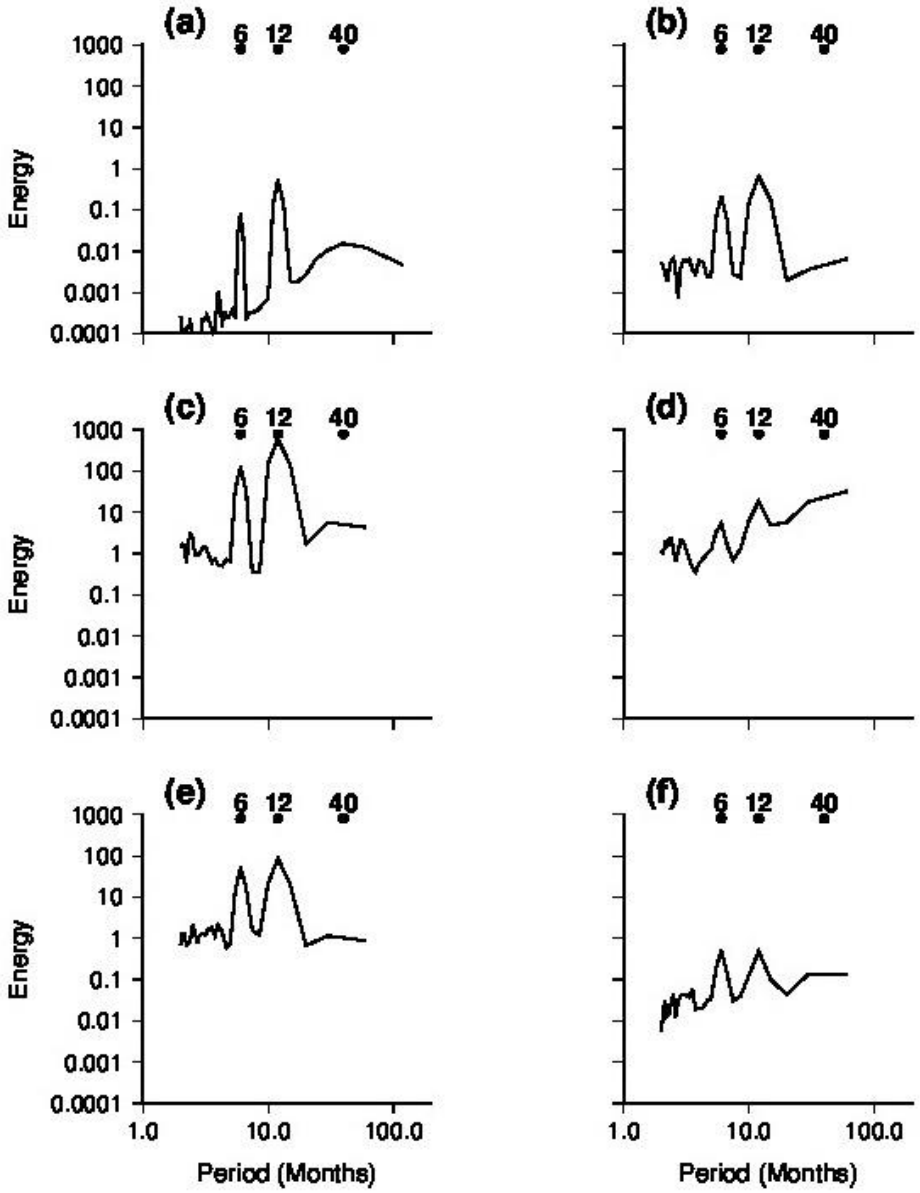

Figure 5.2a Spectral energy of (a) SST, (b) wind speed, (c) shortwave radiation, (d) longwave radiation (e) latent heat flux and (f) sensible heat flux

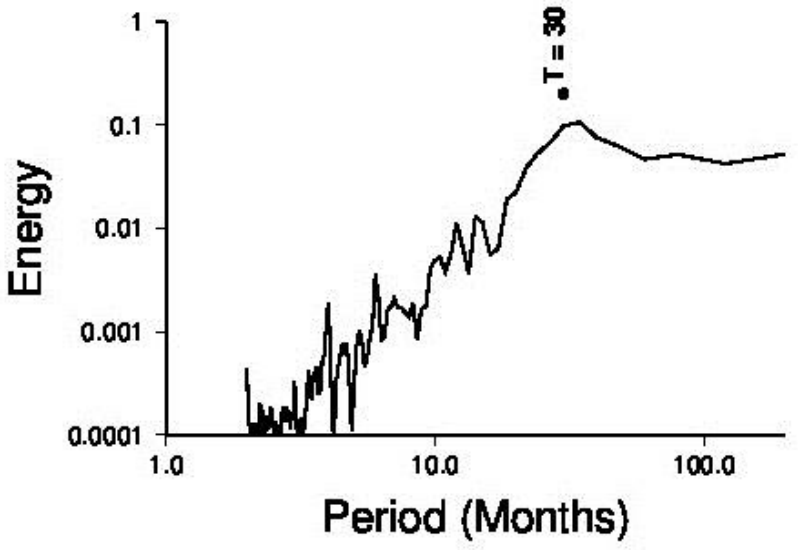

Figure 5.2b Energy spectra for Nino-3.4 Index

A spectral analysis was also performed on Nino-3.4 index to obtain the oscillations present in ENSO (Figure 5.2b). Peak energy was found at about 30 months. This would reflect that the average periodicity of ENSO events varies from 2 to 7 years. Hence, the variability of SST at 30-40 month period can be considered to be due to ENSO.

However, the energy peak at 40 month was not found in heat flux data. This could possibly be due to the shorter period (25 years) of the data. Heat flux data with sufficiently longer duration would be required to confirm the role of heat fluxes on SST variability at El Nino periods.

5.3 Variance of Annual and Inter-annual Anomalies

Inter-annual variation of a property is a deviation from the mean annual cycle. Hence, inter-annual anomalies are obtained by subtracting the annual cycle from the yearly data. The objective of this analysis is to identify areas of strong annual and inter-annual variability in SST and to look into any correspondence between the two.

Few studies were carried out on the magnitude of SST variability on seasonal and inter-annual time scales. *Zhong et al*. (2005) obtained standard deviation of inter-annual SST for the global oceans. Inter-annual variability of SST was higher (1.5^{o}C) in the Pacific Ocean as compared to that (0.5^{o}C) in the Indian Ocean. However, seasonal variability was higher for Indian Ocean than that in the Pacific. This is an effect of the strong seasonal reversal of winds and its impact in the SST than that of heat fluxes. *Kim et al*. (2012) also obtained the magnitude of SST in Indian and Pacific Oceans on annual and inter-annual time scales. They also obtained similar results as that of *Zhong et al.* (2005).

In this study, estimates on range and standard deviation of SST were obtained for the mean annual and inter-annual timescales. The range and standard deviation was estimated at each grid point for the annual cycle. To get inter-annual estimate, range and standard deviation were estimated from annual mean data. The analysis was performed on SST and heat flux data. SST data from different sources (HadISST, NOAA ERSST and OAFlux) have been used to have an inter-comparison among the data sets. HadISST and ERSST data had a time period of more than 100 years whereas OAFlux SST data span only about 50 years. There is also a difference in the spatial resolution of these data sets. HadISST and OAFlux SST had a resolution of one degree, whereas that of ERSST is 2 degrees.

Figure 5.3 shows the range of SST for annual and inter-annual time scales for all the three data sets. SST had similar distribution and similar magnitude in all the data sets. However, some differences were noticed for the inter-annual variations. For the annual period, SST varied from about 1 to 6^{o}C. Minimum annual variation in SST was found in the eastern equatorial Indian Ocean and was nearly symmetric to the equator. Larger annual variation was noticed over southern latitudes and at northwestern Arabian Sea having magnitudes above 6^{o}C. The higher magnitude of SST at south should correspond to the large annual variation in heat fluxes, mostly from solar radiation. The high in the western Indian Ocean could be contributed mainly by the upwelling induced low SST due to summer-time.

Magnitude of inter-annual range of SST was also found to have a similar distribution among the datasets with minor deviations. The magnitude of inter-annual SST variation was similar to that of annual.

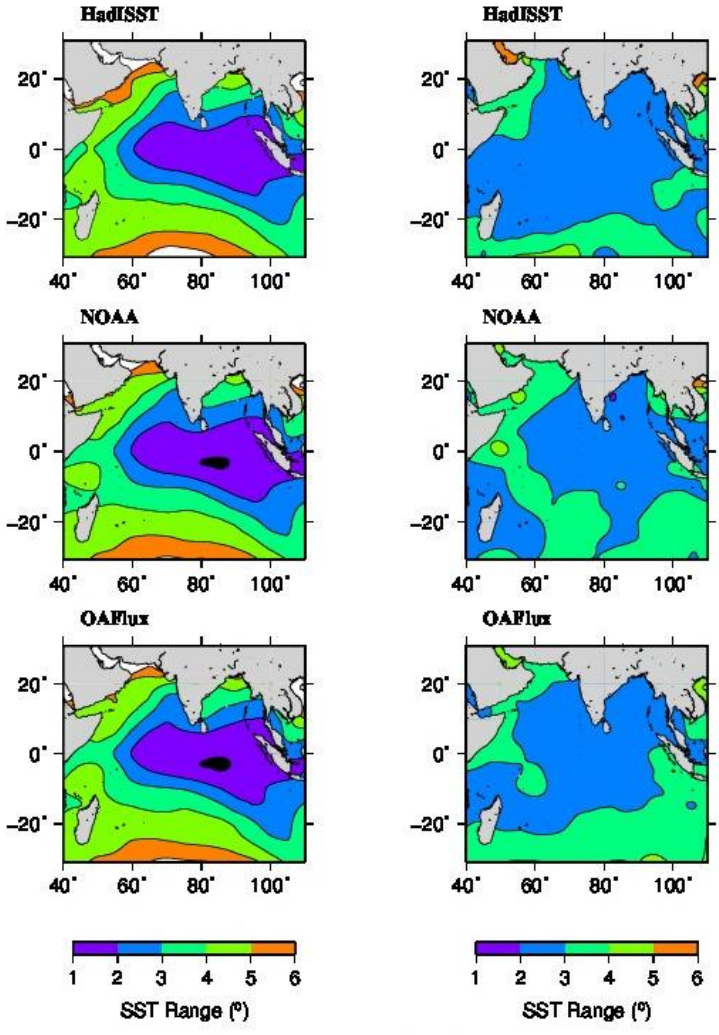

Figure 5.3 Range of SST on annual (left) and inter-annual (right) time scales using different SST data products.

The distribution of inter-annual range had a similar appearance as that of the annual which indicates a regional similarity in the variability of SST at both these scales. The minimum SST range was noticed at the equatorial areas as in the case of the annual one. Hence, the equatorial area seems undergo smaller annual and inter-annual variations in SST. Higher inter-annual SST was found at southern and western Arabian Sea that also had some similarity with the annual feature.

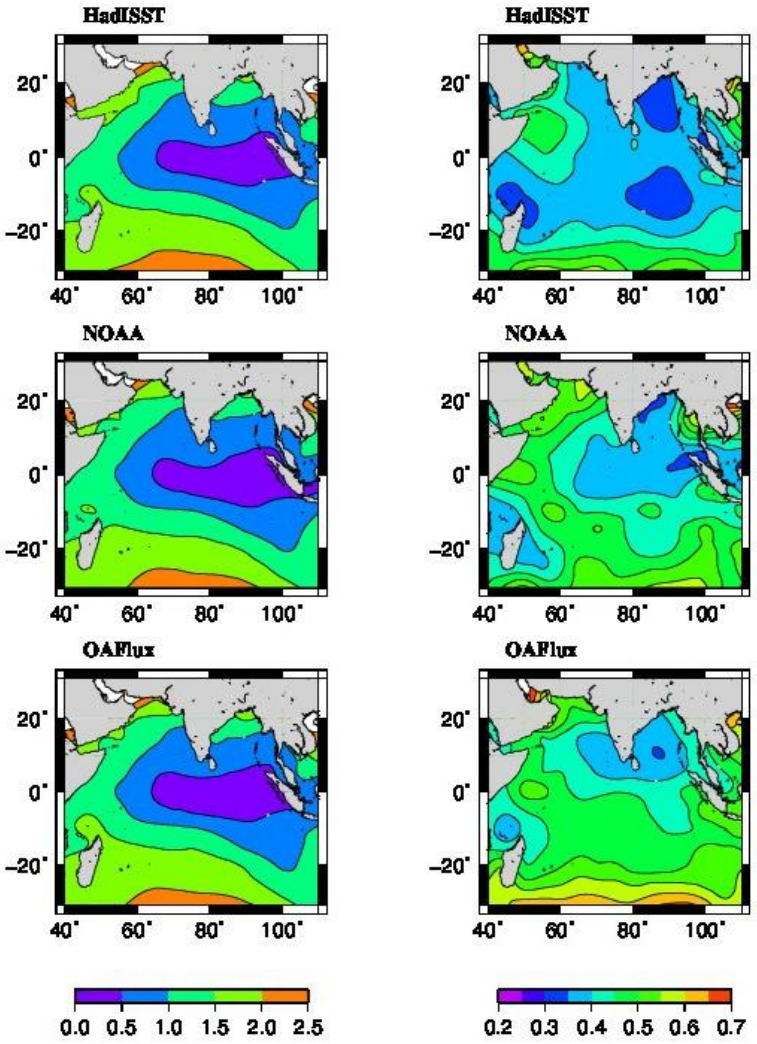

Figure 5.4 Standard deviation of SST on annual (left) and inter-annual (right) time scales using different SST data products.

Standard deviation of SST is shown in Figure 5.4. Standard deviation of SST was more comparable for the annual period. The amplitude of standard deviation was higher for the annual (up to 2.5^{o}C) than the inter-annual (0.7^{o}C). As in the case of SST range, standard deviation also had low magnitudes at eastern equatorial Indian Ocean and higher values at the south and western

Arabian Sea. Inter-annual variation was lesser at the central equatorial Indian Ocean.

5.4 Comparison of El Nino events

Figure 5.5 shows the time series of Nino-3.4 index. In the upper panel (Figure 5.5a), the index for the last 100 years is shown. In the lower panel, the index was extracted for the 1997-98 periods to make more information on the evolution phase of ENSO. Nino-3.4 index varied roughly between -2.5 to +2.5. Positive ONI values indicate El Nino and negative for La Nina.

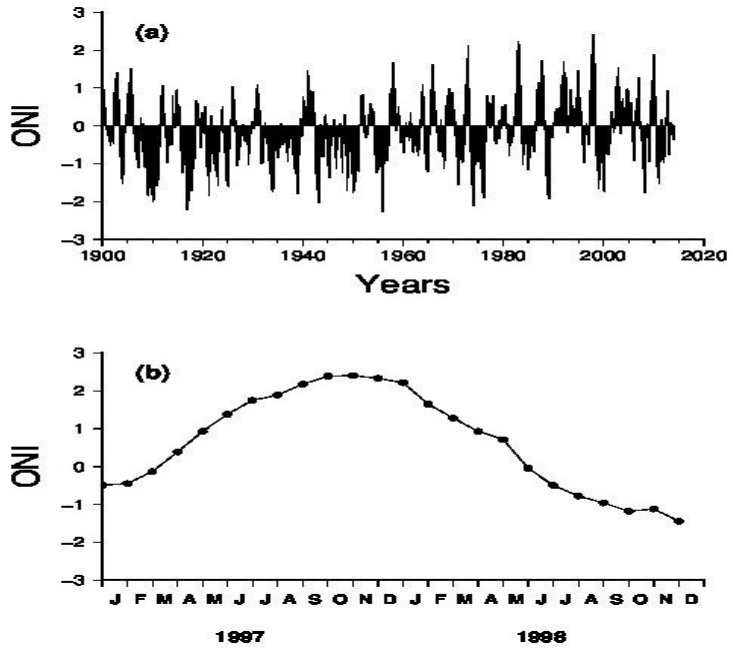

Figure 5.5 Oceanic Nino-3.4 index (ONI) (a) for the period 1900 to present and (b) during 1997-98 El Nino

It can be seen that the Nino index has large scale variability during the 100 year period. During the first half of the century (1900-1950), lesser magnitudes were found for the positive index values (El Nino) and higher for the negative index values (La Nina). Magnitude of La Nina was found much higher than the El Nino anomalies. This has reversed during the second half (1950-2000).

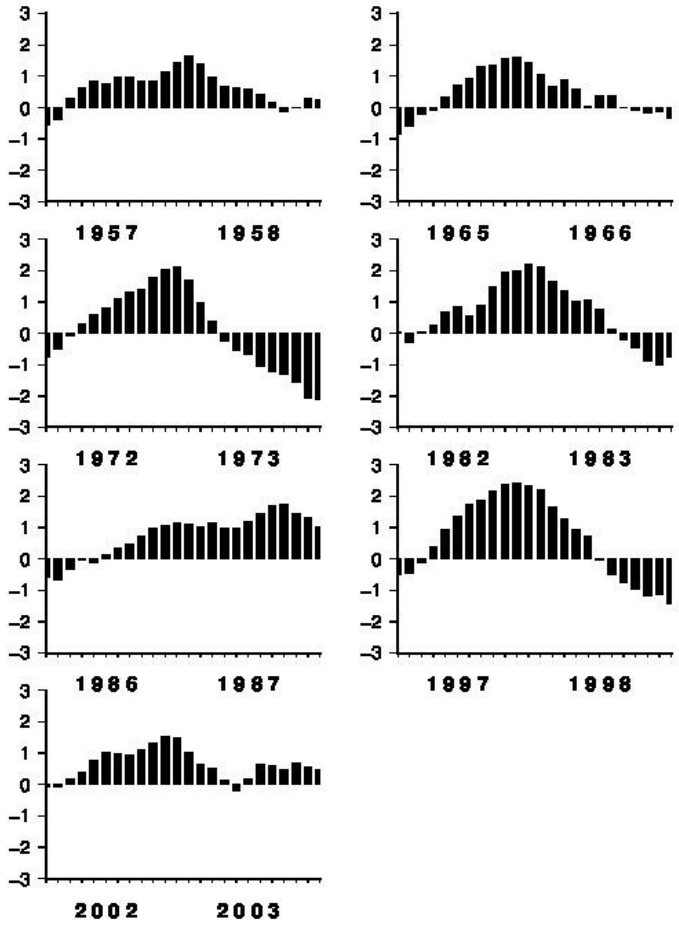

Figure 5.6 Comparison of Nino-3.4 Index of different El Nino events.

This could be an artifact of taking the anomaly that is based on the entire period. The magnitudes of positive SST anomalies during El Nino years were much higher than the negative anomaly during La Nina as compared to the normal years. However, anomalies were computed from the mean of the entire data.

Figure 5.5b shows the ONI index for the 1997-98 El Nino. Nino index changed sign from negative to positive in the month of March 1997 as the indication of the beginning of an El Nino. It continued to increase with time

and reached the maximum by November-December 1997.

Figure 5.6 shows comparison of Nino index since 1950 (1957-58, 1965-66, 1972-73, 1982-83, 1986-87, 1997-98 and 2002-03). Large differences were noticed in the intensity and amplitude of the El Nino events. Among them the strongest event was that during 1997-98. Except the 1986-87 El Nino, all other had uniformity for the month of peak intensity as December. In general the index becomes positive by the month of April-May. Duration of an El Nino event varied from 10 to 15 months.

It is interesting to note that each El Nino event reaches the maximum intensity during the month December of the year. Magnitude of Nino index often exceeds 2 during this time. Intensity of the El Nino then began to decrease almost at a similar rate of its developing stage. Index values crossed the zero mark by the month of June 1998. Hence, this El Nino event lasted for about a year.

5.5 Indian Ocean Mean SST and ENSO

The response of the tropical Indian Ocean to ENSO was studied by comparing the basin-wide mean SST with the Nino Index. SST data of HadISST was used for this analysis. From the spatial SST data, inter-annual anomaly was estimated at each location by subtracting the corresponding climatological value from monthly data. The SST anomaly was then computed and averaged for the tropical Indian Ocean for each month.

The time series of basin wide mean SST anomaly is plotted along with Nino-3.4 Index (Figure 5.7). The figure shows a close relationship between the mean Indian Ocean SST anomaly and ENSO. The relationship is not only found during the period of anomalous events such as ENSO but also exists for other periods as well. The correlation between them was found as 0.48. The lower magnitude correlation is due to the temporal lag between Indian and Pacific

Oceans as reported earlier [eg., *Klein et al*., 1999].

Since the Nino-3.4 index is a measure of SST anomaly in the Pacific Ocean, this analysis indicates that the SST in Indian and Pacific Oceans are in a close relationship with each other. From the closer observation the temporal lag can be found between the two parameters. SST anomaly in the Indian Ocean lags that of Nino Index by few months which is consistent with earlier studies [*Klein et al.*, 1999].

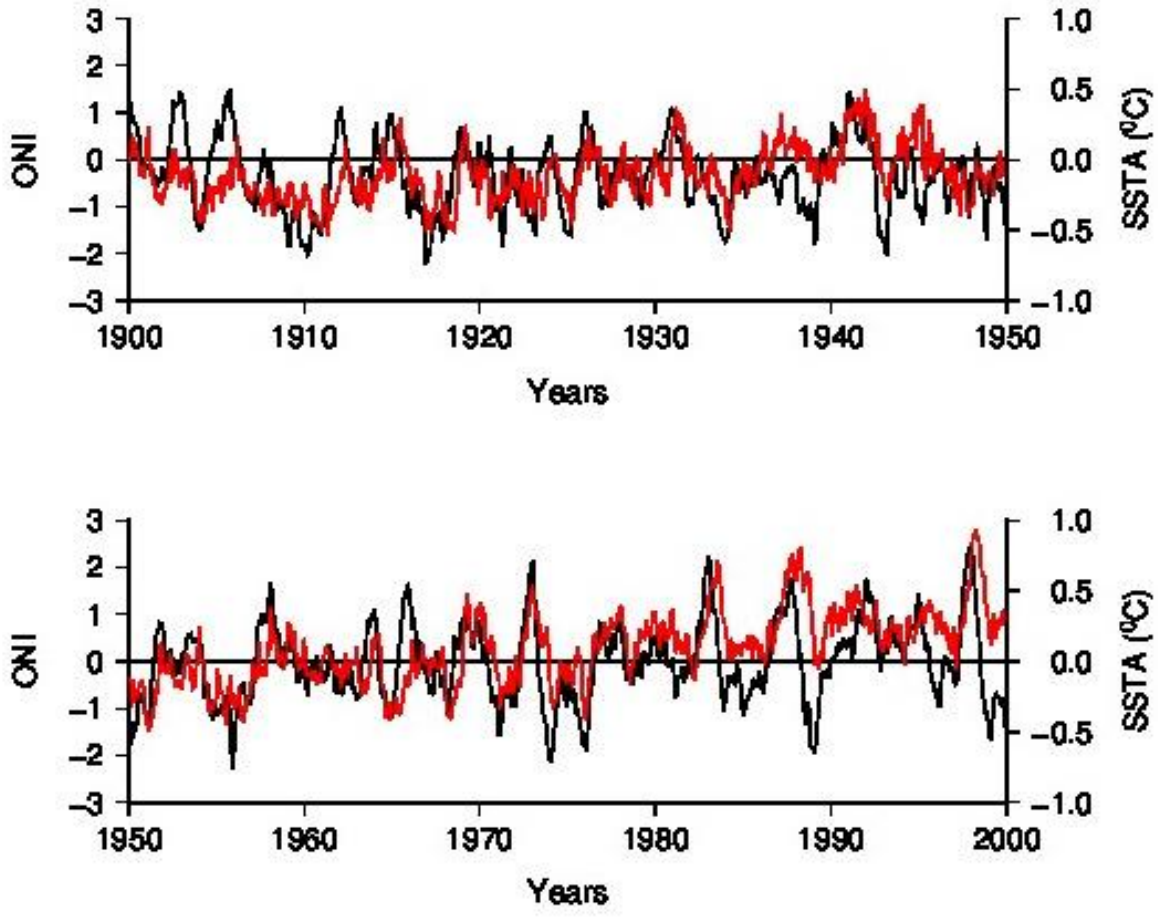

Figure 5.7 Time series of mean tropical SST anomaly from HadISST (red line) and Nino-3.4 Index (black line)

5.6 Evolution of warming during ENSO

Though the results obtained in the previous section show a clear dependency on the tropical Indian Ocean SST as a whole on the developments in the Pacific Ocean, there can be regional differences in the evolution of SST anomaly during an ENSO event. This section analyses the regional biases in the observed SST anomalies and their evolution in accordance with the evolution of ENSO event.

Previous studies found that the warming is not uniform throughout the Indian Ocean. *Yu and Rienecker* (1999) found the initial warming signal at the western Indian Ocean as the ENSO begins in the Pacific. As the ENSO develops further, the SST anomaly spreads to larger areas. Though ENSO peaks in December, the SST anomaly reached its peak by April of next year that again showed the 4-month phase lag.

The evolution of SST was examined for the El Nino events of 1972-73, 1982-83, 1987-88 and 1997-98 using monthly SST data from HadISST. From the monthly data, climatological mean was estimated at each grid point. The inter-annual anomaly was then computed by subtracting the climatological mean from the monthly data. The objectives of this study are:

1. General tendency of mean SST anomaly during El Nino years.
2. Evolution of SST anomaly for the 1997-98 El Nino.
3. Comparison of the evolution of SST anomalies during different El Nino years.

SST Anomaly during El Nino Years

Figure 5.8 shows the time series of mean SST anomaly over the Indian Ocean and the Nino Index for the El Nino events during the period 1970 to 2000. The El Nino years during this period were 1972-73, 1982-83, 1987-88

and 1997-98 and were shown as shaded area in the figure.

From the figure it is clear that the Indian Ocean SST responds positively with the SST in the Pacific. There is a close relationship between the SST in Indian and that in the Pacific during El Nino and non-El Nino years. During El Nino periods, SST anomalies had magnitudes above 1^{o}C. It can also be seen that the SST in Indian Ocean lags that of the El Nino (or Pacific SST) by few months. El Nino peaks by the month of December whereas SST in Indian Ocean attains a peak by April next year.

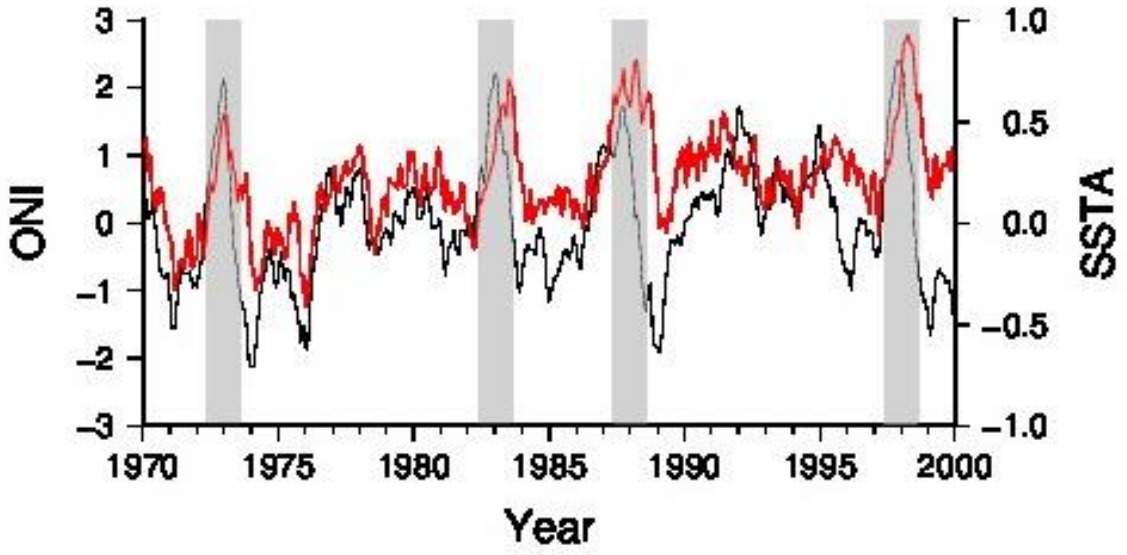

Figure 5.8 Time series of ONI (black line) and basin wide mean SST from HadISST (red line) during 1970 to 2000. El Nino events during this period are shown in grey color.

Spatial Evolution of SST anomaly during 1997-98 El Nino

Figures 5.9a-c shows the inter-annual anomaly of SST during the 1997-98 El Nino period. From Figure 5.5b, it can be seen that the Nino Index becomes positive from March-April onwards of 1997 showing the onset of the El Nino. However, ENSO signal begins to form by June with an anomaly above

$1^{o}K$ [or $1^{o}C$] at the western equatorial Indian Ocean. This anomaly amplifies in the coming months and spreads almost the entire tropical Indian Ocean by December 1997 except for a small region at the eastern equatorial area. The SST anomaly at the eastern part was negative which is associated with the Indian Ocean Dipole (IOD) event. Hence, the year 1997-98 was a combined year of El Nino and IOD.

El Nino peaks in November-December 1997, but the SST anomaly continued to develop further and reaches the maximum by April-May 1998, again keeping the phase shift. The El Nino induced positive SST anomaly returns to normal by October 1998 (Figure 5.9b). The signs of La Nina are seen soon after the demise of El Nino from July 1998 onwards with negative SST anomalies in the southern tropical Indian Ocean. It continues to develop but without much spatial expansion and reaches a maximum by January 1999 (Figure 5.9c).

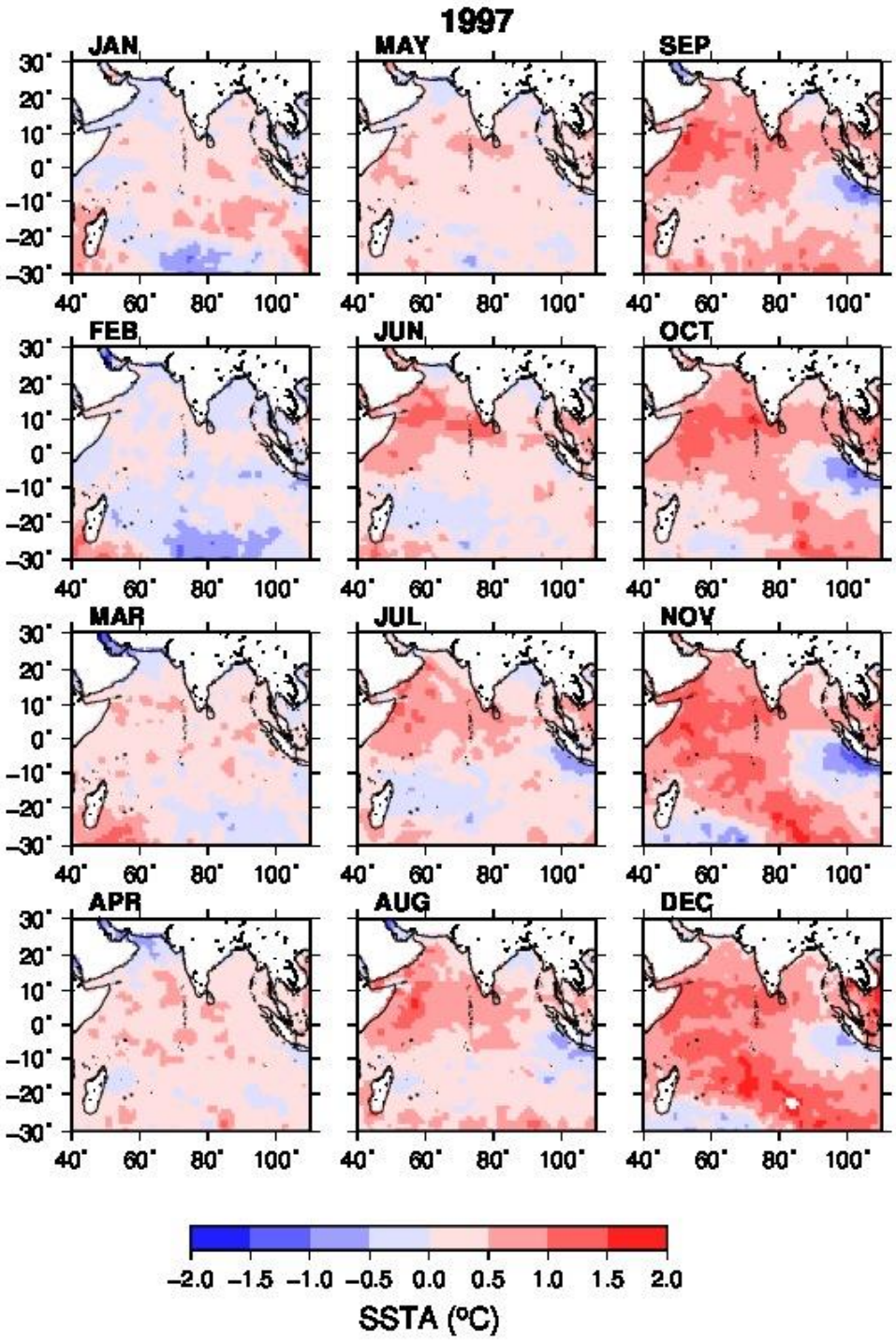

Figure 5.9a SST anomaly from HadISST during the year 1997

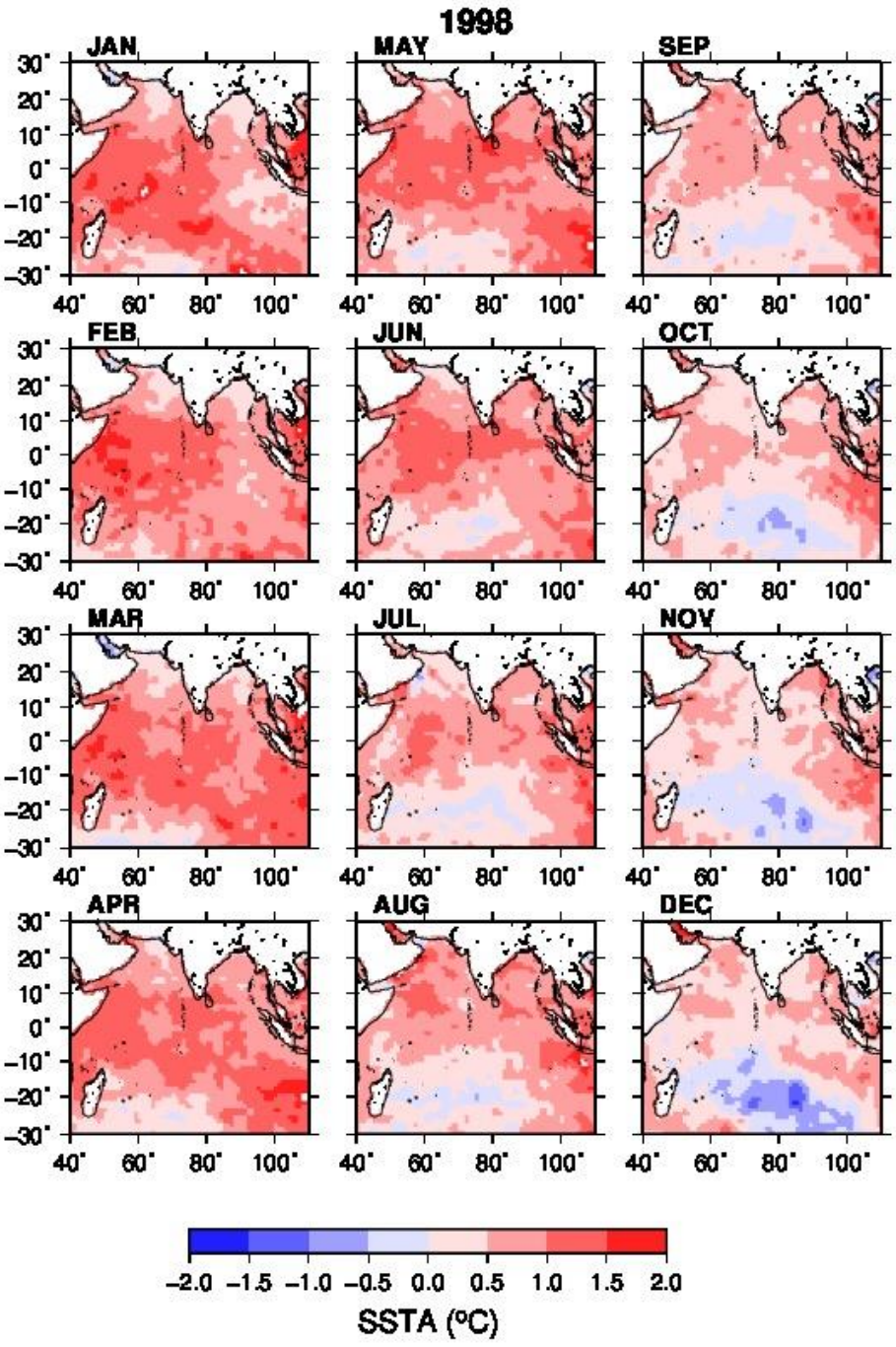

Figure 5.9b. SST anomaly during 1998

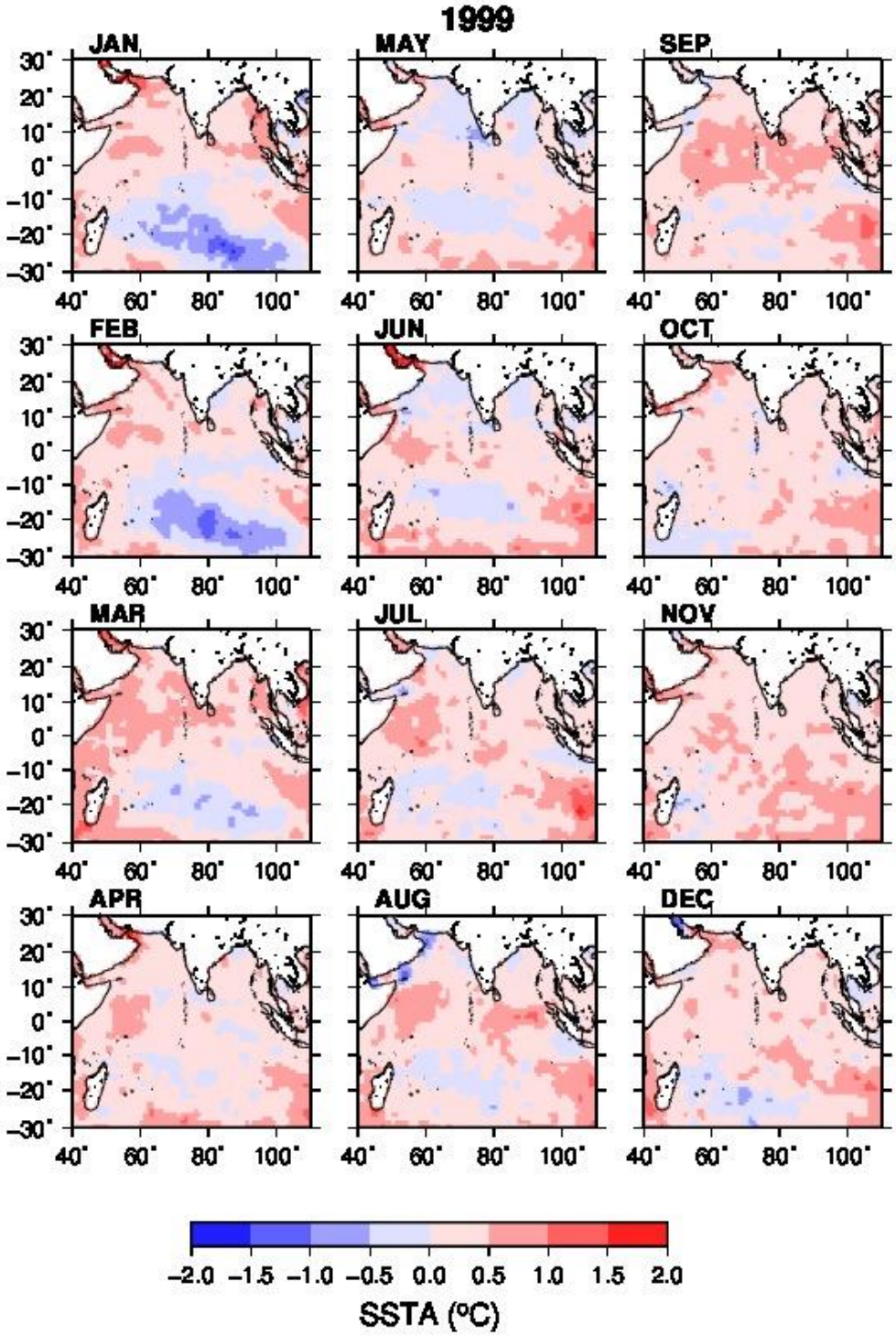

Figure 5.9c SST anomaly during 1999

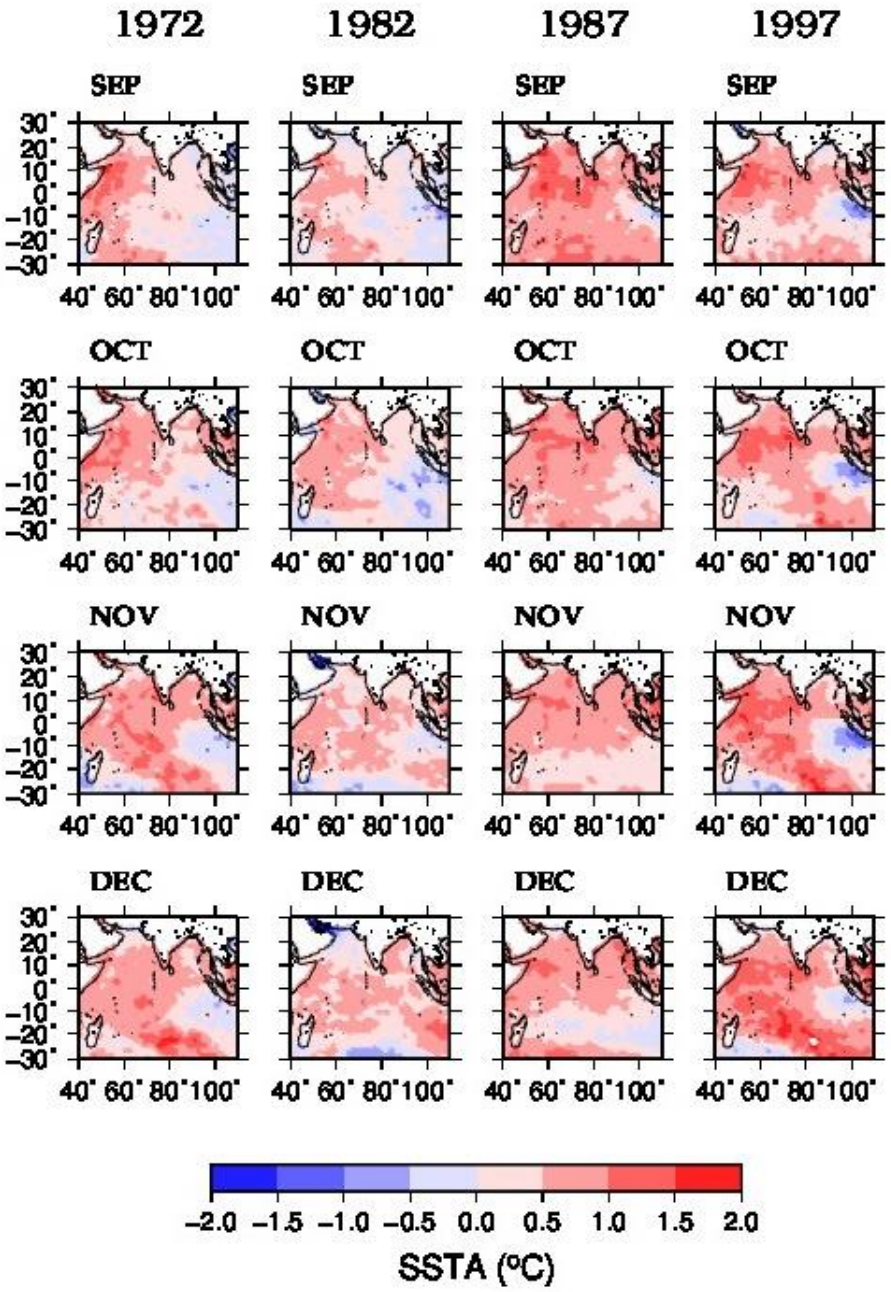

Figure 5.10 Evolution of SST anomalies during the developing stage (September to December) of El Nino of 1972-73, 1982-83, 1987-88, and 1997-98

Comparison of SST anomalies among El Nino Events

Figure 5.10 shows a comparison of SST anomalies among the four El Nino events. The anomaly during the developing period (September to December) was only shown. Warm basin wide SST anomalies were found during all the El Nino events. Both 1972-73 and 1997-98 El Nino had negative SST anomaly (cooling) at the eastern equatorial Indian Ocean that was induced by IOD event. Among the four events SST anomaly was found lowest for the 1982-83 El Nino. For the 1987-88 El Nino, the SST anomalies were negative in the southern areas unlike during other years.

5.7 IOWP variability during 1997-98 El Nino

It has been found that El Nino induces anomalous warming in the tropical Indian Ocean with anomalies above 1.5 degrees. The response of IOWP to ENSO is studied in this section. As SST increases, a corresponding increase in warm pool is also expected during El Nino periods. Here the warm pool mean temperature and area (number of warm pool grids) were estimated using HadISST data.

IOWP Mean Temperature

Figure 5.11 shows the time variation of ONI and anomalies in warm pool temperature. Warm pool temperature anomaly was estimated from the mean temperature of the warm pool (above 28^0C) for each year and subtracting the monthly values from climatological mean. Warm pool mean temperature anomaly attains the peak of about 1 degree by April-May of 1998 with a time lag of about 4 months with the peak of ONI. Positive SST anomaly was observed throughout the period (1997-1998) indicating the anomalous warming of the warm pool during the El Nino period.

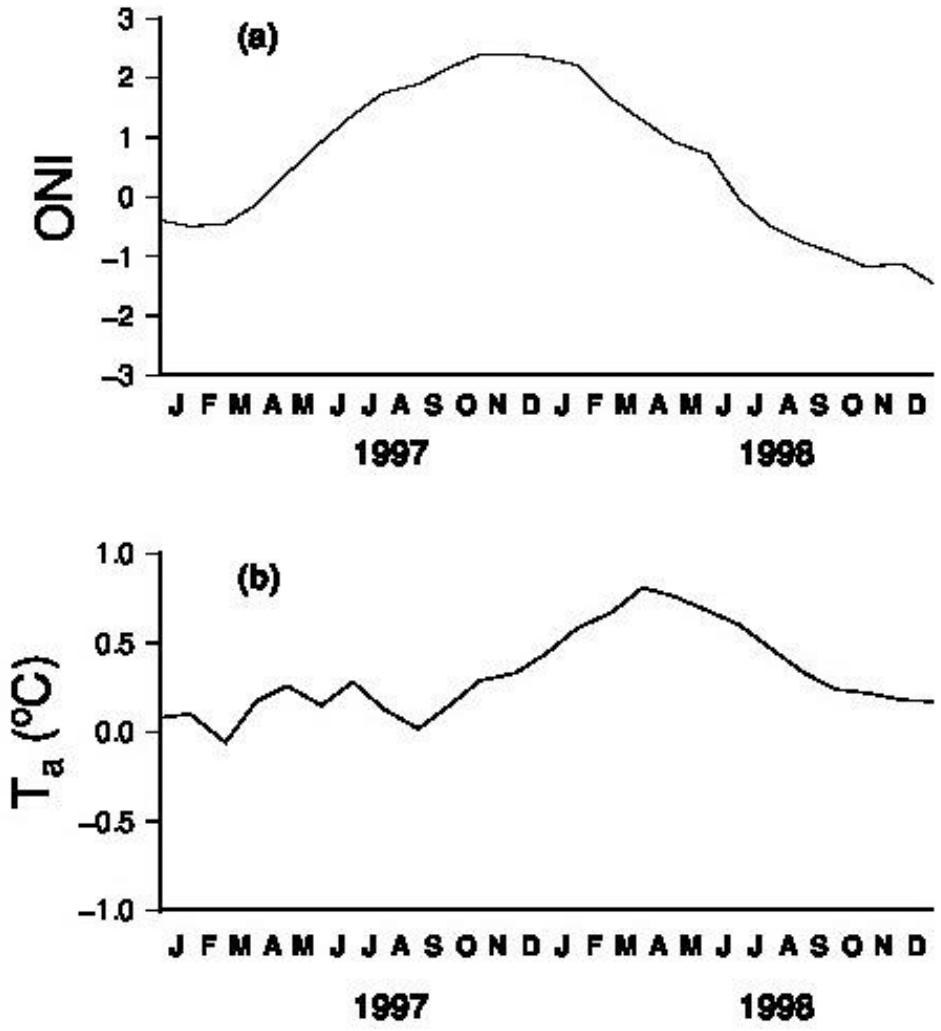

Figure 5.11 Time series of (a) Oceanic Nino Index and (b) mean IOWP temperature anomaly during 1997-98 El Nino

The warm pool area anomaly showed a different pattern from that of its temperature. The maximum anomaly for this was occurred by December 1997. Hence, it is observed that the impact of ENSO is reflected in the pre-monsoon warming of the year following El Nino. This might have an impact on the monsoon rainfall that follows the excess pre-monsoon warming.

IOWP Area

The enhancement of warm pool temperature and area during El Nino is

studied by comparing the spatial distribution SST during El Nino with that of climatology. The comparison was made for the months April and July. The SST anomaly in Indian Ocean attains the maximum during the pre-monsoon (April-May) season of the post El Nino. Figure 5.12 shows the distribution of SST during April 1998 and the climatological SST of April. HadISST was used for this study. The objective is to estimate the enhancement in the intensity and spatial extent of the warm pool during the El Nino event of 1997-98.

During April (Figure 5.12a), climatological mean warm pool was distributed almost zonally and restricting to the latitude band of 20°S to 20°N. The peak of the warm pool had a temperature range of 29.5 to 30°C and is aligned in an inclined fashion as compared to the lower SST values.

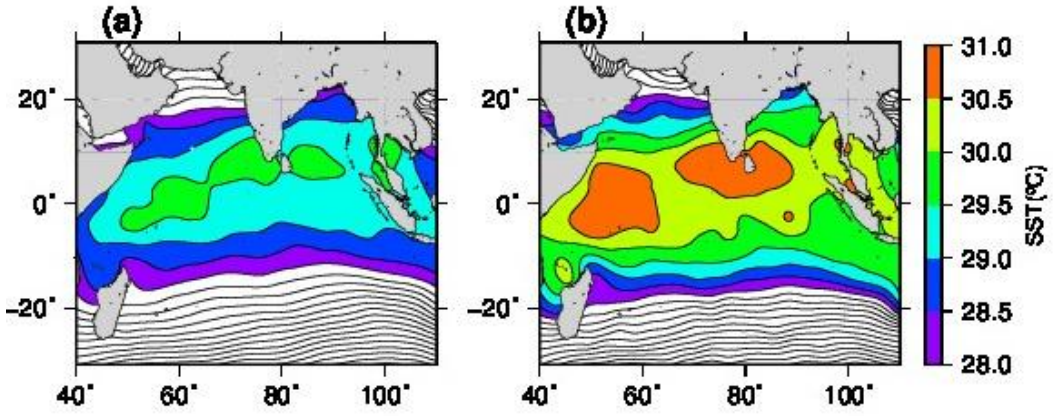

Figure 5.12 Comparison of spatial distribution of (a) climatological SST for April and (b) SST during April 1998. SST above 28°C is colored.

By April 1998, El Nino began to decay in the Pacific, but SST in Indian Ocean attains the peak with a phase lag of about 3 months (Figure 5.12b). The core temperature is now enhanced to 30.5-31.0°C that is about one degree more than the climatological mean. Warm pool core SST had similar spatial distribution in both cases. There is a significant enhancement in the area of

the warm pool during El Nino towards south and north. An increase in IOWP area of 17% was noticed in April 1998.

A similar analysis was performed for the month of July (Figure 5.13). Though it is still the summer season, SST in Indian Ocean reduced considerably due to the monsoon. Reduced shortwave solar radiation from increased cloud, higher latent heat from stronger winds and advection all makes the SST less. The climatological mean warm pool appears as a tongue from east to west. It covers the entire Bay of Bengal but only a small area in the southeastern in Arabian Sea. The core IOWP temperature was 28.5-19.0^{o}C. During July 1998, warm pool intensified similar to that in April 1998. IOWP expansion was mostly towards western Indian Ocean. Core SST of IOWP also had increased by about 1^{o}C. Increase in area of IOWP for this month is 32%, much higher as compared to April.

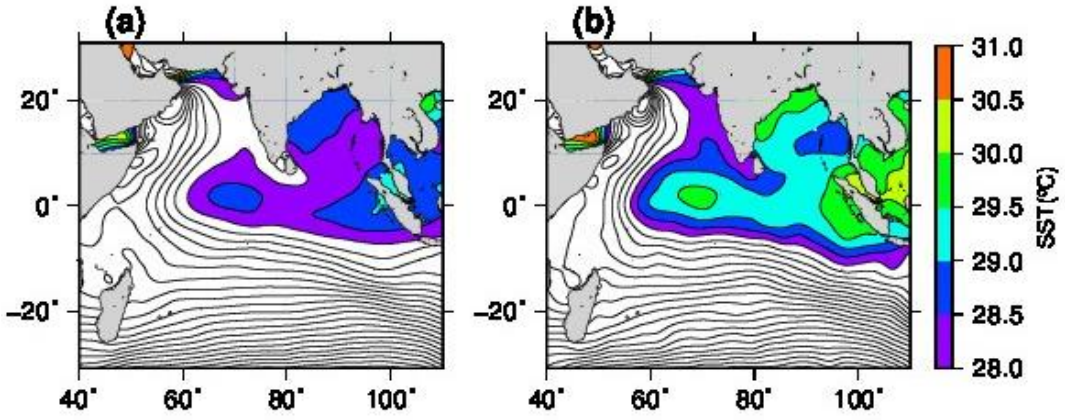

Figure 5.13 Comparison of spatial distribution of (a) climatological SST For July and (b) SST during July 1998. SST above 28^{o}C is colored.

5.8 ENSO warming: Forcing factors

A number of attempts were made to understand the cause warming of the north Indian Ocean during El Nino periods. *Klein et al*. (1999) suggested

the cause of ENSO induced warming to an increase in the shortwave radiation. They observed good relationship between ENSO and cloud in Indian Ocean. The reduced cloud during El Nino resulted in an increased shortwave radiation that raised the SST. They also found a reduction in the monsoon winds. However they found that the net heat flux was weak.

Zhong et al. (2005) also observed easterly anomaly in the zonal wind during the onset of El Nino. This causes upwelling at the east and a rise of thermocline and hence cooling in SST. Warming takes place in other areas due to a combination of reduced LHF and increased solar radiation. The El Nino induced anomaly begins to appear in June. Weaker winds were observed in the western Indian Ocean, especially in Arabian Sea that resulted in the reduced LHF. As El Nino develops, the zonal equatorial SST gradient increases in Indian Ocean. By March of the next year, easterly wind anomaly reduces that further leads to the return of Indian Ocean to the normal state.

Du et al. (2009) studied the factors for the long persistence of warming in Indian Ocean. They also supported the role of heat fluxes on the tropical Indian Ocean except at southern areas where Rossby waves play a major role. They also found an increase in the solar insolation that might result from a reduced cloud cover. They also found the roles of shortwave radiation and LHF as the factors in the warming but with a difference in their time of operation. The primary warming is found to be caused by the anomalous shortwave radiation, whereas the secondary warming is due to the reduced LHF as a result of the reduced wind speed. They found the warming of the north Indian Ocean due to the reduced latent heat loss from the reduced wind speed.

Zhang et al. (2009) studied the inter-annual variability of IOWP. They noted the significant response in the IOWP area to El Nino events. They found a consistent expansion of the warm pool during El Nino events. A different

opinion came from *Suryachandra et al*. (2012) who opposed the role of heat fluxes on the inter-annual warming. They found that net heat fluxes cannot explain the anomalous warming during El Nino years. *Kim et al*. (2012) got similar results of that obtained by *Klein et al*. (1999). Rao et al. (2015) have studied the inter-annual variability of Arabian Sea warm pool. They have identified both pre-conditioning mechanism and local heat fluxes for the anomalous warming during the pre-monsoon season.

Recently *Kumar et al*. (2015) studied the long term variations in Arabian Sea and Bay of Bengal. They found warm SST anomalies during El Nino and cold anomalies during La Nina. A regional difference in the amplitude of ENSO signal was found between Arabian Sea and Bay of Bengal that points the non-uniformity in the ENSO impact within the Indian Ocean. Their study showed a negative relationship between SST and heat fluxes. Hence, there are different opinions among the researchers on the role of heat fluxes on ENSO induced warming in the north Indian Ocean. The objective of this section is to do a further analysis on this issue and find out any relationship between them.

In this study, the anomalies of SST were compared with heat fluxes and wind speed for the El Nino of 1986-87 and 1997-98. The analysis was done for the developing phase (September to December). This analysis made use of SST, heat flux and wind data from OAFlux project. Heat flux data covers a period of 1984 to 2009, whereas SST and wind data are obtained for the period of 1958 to 2009. The major El Nino events during this period were 1986-87 and 1997-98. A comparison among the variables was made for these two El Nino episodes.

Ocean temperature data from SODA was used for estimating mixed layer depth (MLD) in the ocean. MLD is the surface mixed layer of the ocean and is estimated from density and temperature profiles. Here, the

temperature criterion was used with a temperature difference of 1.0^{o}C. MLD was estimated for the El Nino periods to make comparison with SST and heat fluxes.

Shortwave Radiation

Figures 5.14 and 5.15 show the distribution of anomalies of SST, heat fluxes (shortwave radiation, longwave radiation, latent heat and net heat flux) and wind speed for the 1997-98 El Nino. The positive SST anomaly began to form at the western Indian Ocean in June 1997. But the SWR anomaly did not show any marked positive anomaly there and was in fact negative (not shown). As the El Nino peaks by the end of the year 1997, strong negative SST anomaly forms at the east due to upwelling. Basin wide warming occurs in other places except at the southwestern Indian Ocean.

During this time, a dipole-like structure also was found for the SWR anomaly at the equatorial areas with positive anomaly at the east and negative anomaly at the west. The increased SWR anomaly at the east could be due to the reduction in cloud associated with the underlying cool sea surface. There is a negative SWR anomaly at the west during this time where the SST anomaly was positive. Hence the SWR anomaly had negative relationship with the SST. Therefore, SWR could not explain the ENSO induced warming in Indian Ocean as was previously thought.

Longwave Radiation

The magnitude of LWR anomaly was much less compared to other fluxes and hence may have lesser impact on SST anomaly. The spatial distribution of LWR anomaly was also much different from that of SST anomaly indicating weak relationship between them.

Latent Heat

Latent heat flux (LHF) had negative anomalies at the eastern equatorial

area. LHF is the amount of heat lost from the sea due to evaporation. Lower LHF anomaly corresponds to lesser heat loss which supports warming and vice versa. Low LHF anomaly was found at the eastern equatorial areas where SST anomaly was strongly negative. This again indicates a negative relationship between the two. Since the low SST in that area was upwelling induced, there cannot be a positive relationship between LHF and SST. The negative LHF anomaly there is due to the reduced SST. The relationship between SST and LHF is also weak even in non-upwelling open ocean areas. In regions where SST anomaly was highly positive, the LHF anomaly was not strongly negative but even found positive. Hence a direct relationship between SST and LHF is lacking.

Net Heat Flux

The net heat flux anomaly was computed as the algebraic sum of all the heat fluxes. Positive (negative) values indicate a net heat gain (loss). In the eastern equatorial areas, where SST anomaly was negative, net heat flux shows positive values. This is due to the positive anomalies of shortwave and LHF anomalies. In warm SST areas, net heat flux anomaly was negative. Hence, the heat fluxes had only a weak role in the SST distribution in the Ocean.

Wind Speed

The wind speed was stronger in a narrow band at the equator throughout the period of El Nino development. It was reported earlier that the easterlies strengthened during El Nino periods. Winds towards north and south of it were reduced and showed as negative anomaly. This stronger easterly wind might have caused the coastal upwelling off Sumatra. The distribution of positive SST anomalies in the south had a co-occurrence of negative wind anomaly.

This suggests a better relationship between them at least in areas where ocean advection is absent. The wind influences SST in different ways. A

higher wind causes higher turbulent (latent and sensible) heat losses and at the same time responsible for stronger mixing in the surface layer that further reduces SST. Hence, the weaker wind in the south caused lesser evaporative loss and a reduced mixing. To further understand the mixing strength, a comparison with mixed layer depth is necessary.

Mixed Layer Depth (MLD)

To understand the role of ocean mixing, mixed layer depth (MLD) was estimated using SODA data (Figure 5.16). MLD was estimated for the period September to December 1997 for a comparison with SST. Lower MLD values were noticed at southern area where the SST anomaly was positive. There was a similarity in the orientation of the low MLD values with that of the positive SST anomalies especially during November and December. From this qualitative study, it was found that the unusual warming of the tropical Indian Ocean at the western and southern areas could largely be contributed by the reduced mixed layer than by an enhanced surface heating. However, a quantitative study would require understanding the relative contributions of heat fluxes and mixed layer depth on SST.

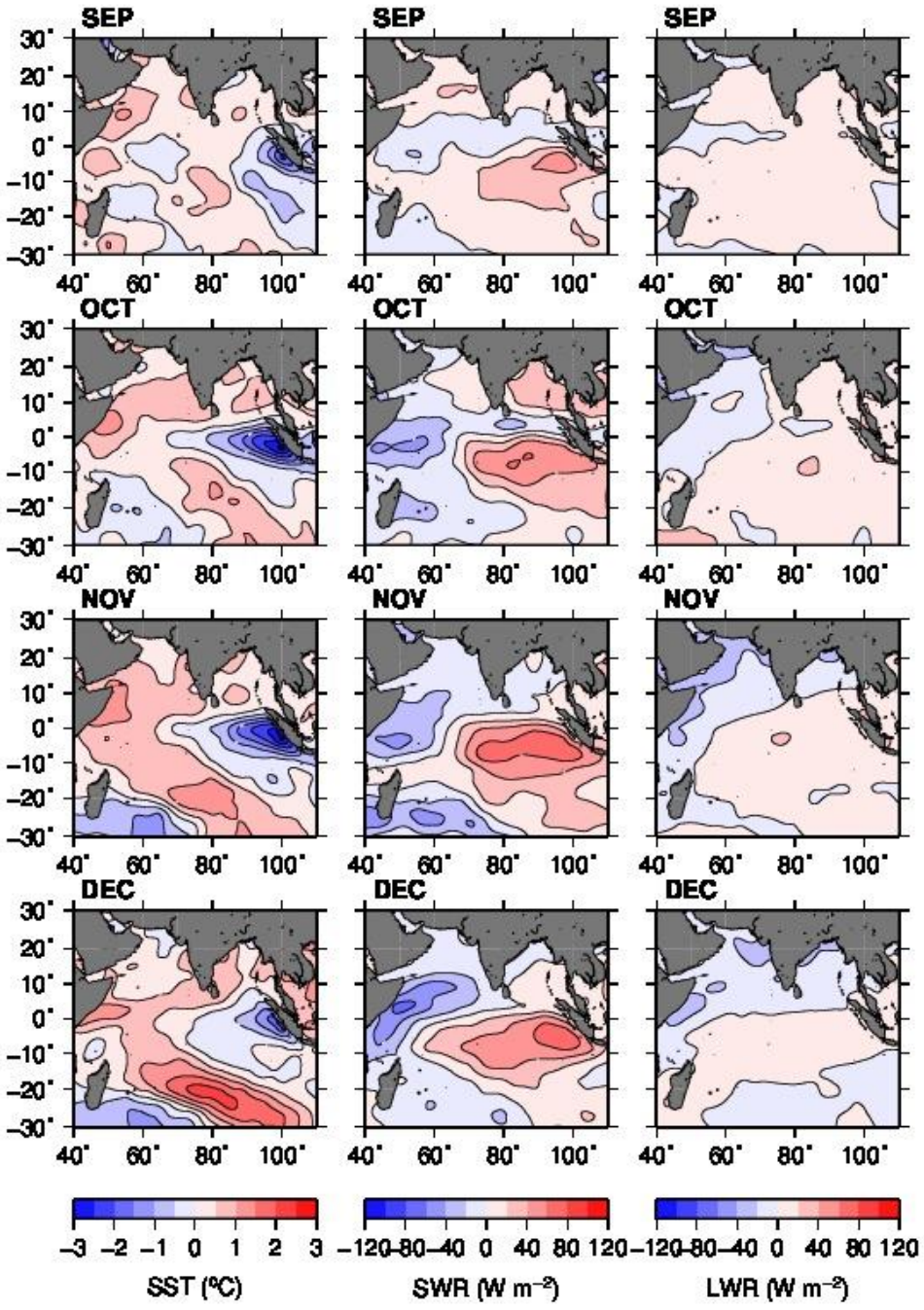

Figure 5.14 Anomalies of SST (left panel), shortwave radiation (middle panel) and long wave radiation (right panel) during September to December 1997

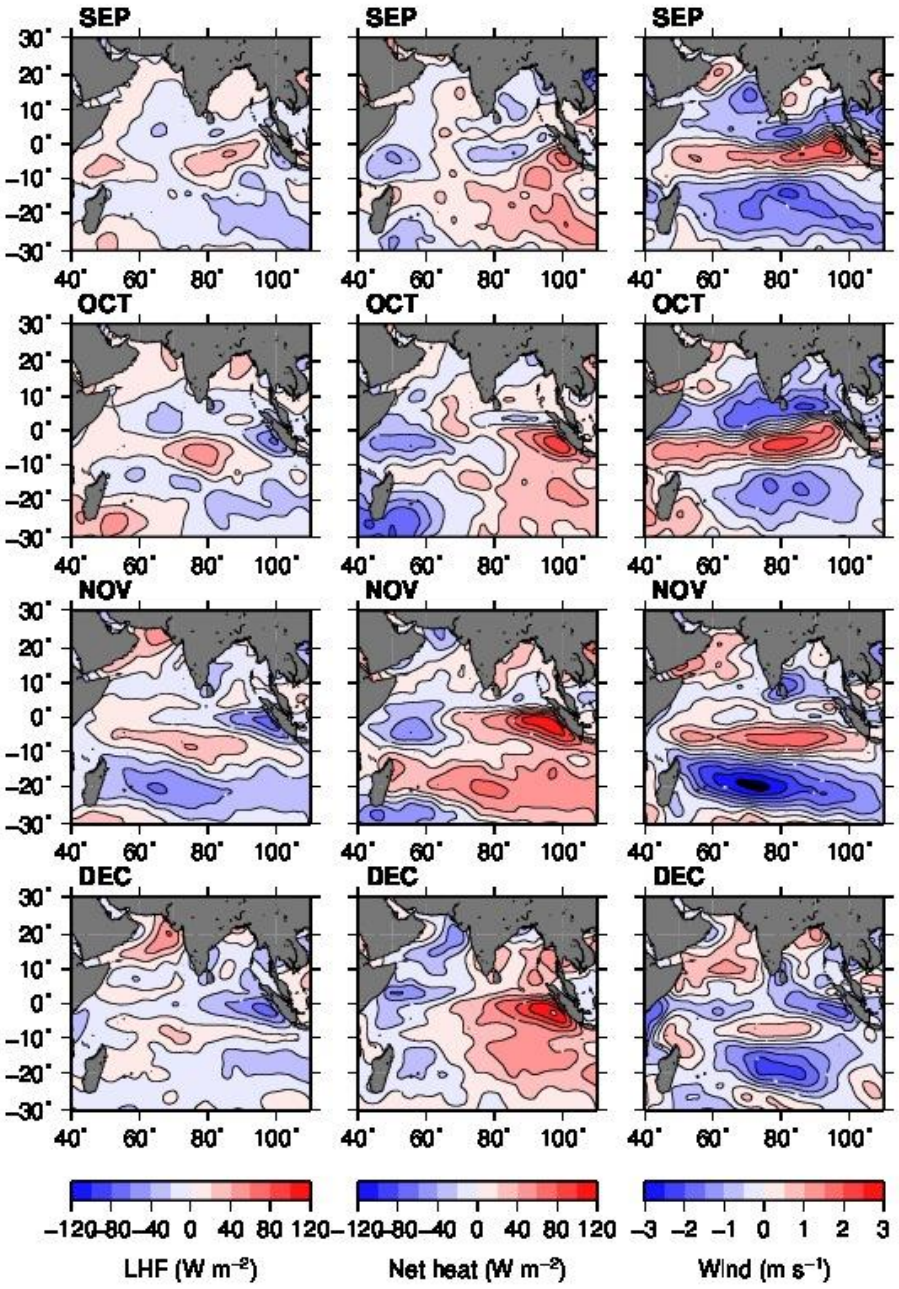

Figure 5.15 Anomalies of latent heat (left panel), net heat (middle panel) and wind speed (right panel) during September to December 1997

Depth of 25°C Isotherm

The depth of 25°C (D25) isotherm was estimated using temperature data obtained from SODA (Figure 5.17). D25 can have a good relationship with the MLD because as MLD increases, the depth of isotherms will also increase. Figure shows low D25 (less than 20m) values off Sumatra. This shallowing of D25 is due to the uplift of the thermocline due to coastal upwelling.

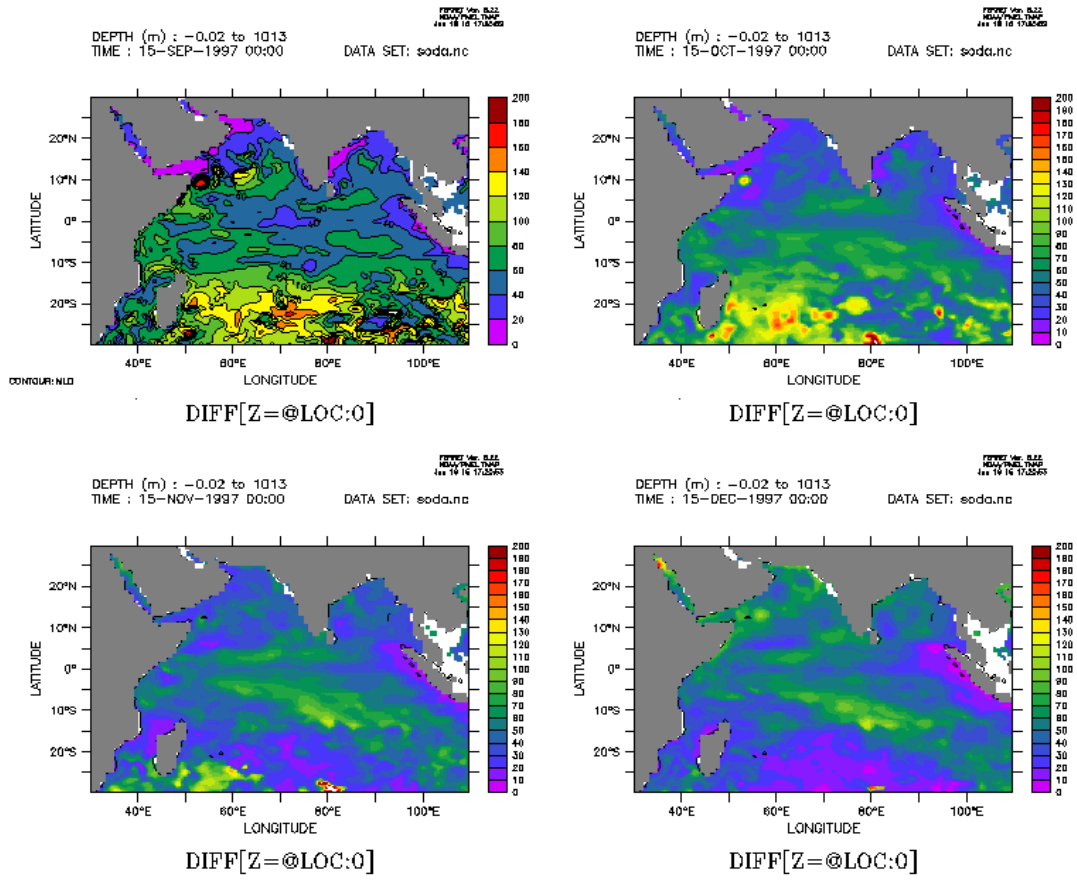

Figure 5.16 Ocean mixed layer depth estimated from SODA data. MLD was estimated based on temperature criteria

This was also evident in the MLD which had lower values in this area. In areas of warm SST anomalies, both MLD and D25 had lesser values. For example, high positive SST anomaly at the location 20°S, 80°E was coincided

with a low D25 and MLD. Hence this analysis further supports the role of oceanic mixing on SST.

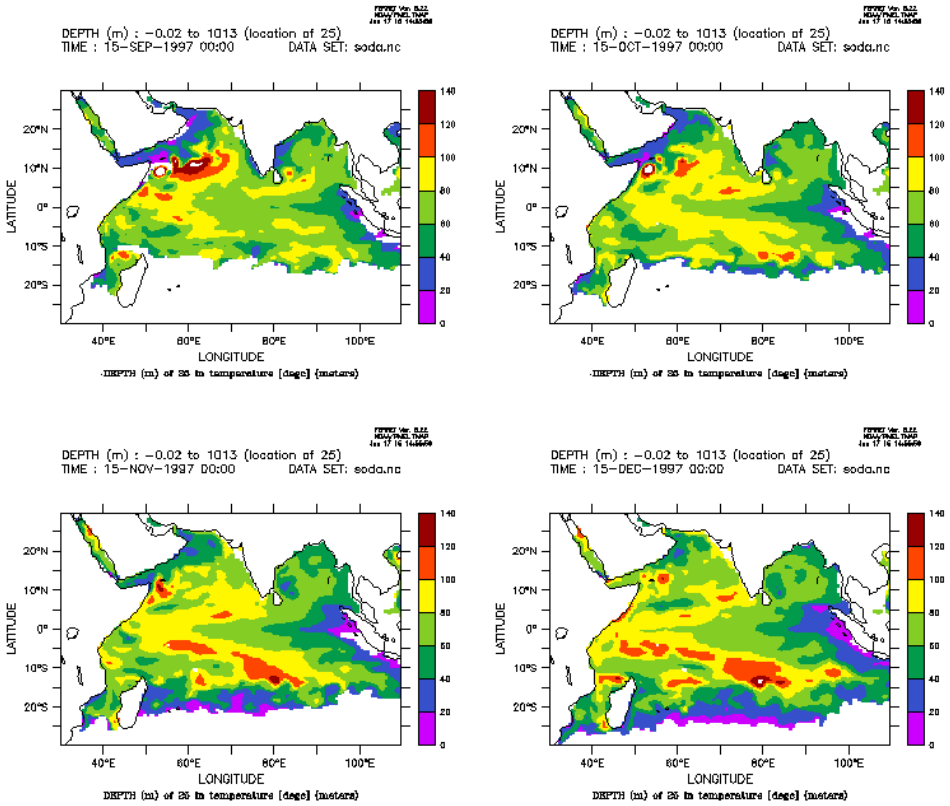

Figure 5.17 Depth of 25^{o}C isotherm using SODA data for the period September – December 1997

5.9 Relationship of SST with Heat flux and MLD

The prediction of SST has been an important task for researchers in climate studies. SST is primarily forced by solar heating. Vertical radiation at the low latitudes make the SST warmer as compared to that at higher latitudes where the inclination of solar rays makes lesser heat input to the ocean. Concurrently the ocean loses heat in the form of long wave back radiation, latent heat flux and sensible heat flux. The net radiation thus gained or lost will determine the SST locally. However, various processes in the ocean can

further modify ocean temperatures. The molecular and turbulent diffusion downwards transport heat to deeper ocean. Ocean currents can transport heat laterally to great distances. Vertical motions resulting from various dynamical processes can also make a significant contribution to the SST variability. Hence, the combined Eulerian and Lagrangian processes decide the ultimate state of SST and subsurface ocean temperature. The rate of change of SST can be expressed as

$$\frac{\partial T}{\partial t} = -\left(u\frac{\partial T}{\partial x} + v\frac{\partial T}{\partial y} + w\frac{\partial T}{\partial z}\right) + \frac{Q_{net}}{\rho C_p h} + D$$

where 'T' is temperature (SST), u, v, and w are velocity components, Qnet is the net heat flux (NHF) , 'ρ' is density of sea water, Cp is specific heat capacity of water, 'h' is the mixed layer depth (MLD) and D is diffusion. This equation predicts the change in SST (dSST) with time. The terms inside the bracket on the right side of the equation represents the three-dimensional advection of temperature by currents.

This equation is simplified by neglecting advection and diffusion to isolate the role of heat fluxes on SST. Advection is neglected considering the nearly horizontal uniformity of temperature. Even otherwise also, the uniformity in heat fluxes also impacts a similar effect on neighboring grids. Hence, neglecting advection would not appear to make any significant contribution to SST variability. The temperature equation is applied to the ocean surface mixed layer as a whole. Since mixed layer has uniform temperature in the vertical, diffusion of heat in the vertical can also be ignored. The equation thus becomes

$$dSST = (Qnet/\rho\, Cp\, h)\, dt$$

The value of dt is one month and is given in seconds. Density of ocean was taken as 1025 Kg/m^3 and *Cp* was 4000 Joules/(kg ^oC).

Earlier Suryachandra et al. (2012) have applied the temperature equation to understand the long term trend in SST. They have used a constant MLD and found a negative relationship between SST and NHF. The observed SST trend could not be reproduced with the equation. In this study, this bulk SST equation is used to predict the SST on annual and inter-annual time scales.

This study was carried out using gridded data sets on SST, Net Heat Flux (NHF) and Mixed Layer Depth (MLD) from tropical Indian Ocean. Monthly SST and NHF data of OAFlux for the period 1984 to 2000 were downloaded from APDRC web site. Both data sets were climatologically averaged to get their monthly mean. MLD was estimated using World Ocean Atlas 2005 (WOA 2005) ocean temperature climatology. Temperature profile at each grid was interpolated at 1m interval using cubic spline method. MLD was then estimated from the interpolated data using the temperature criterion with a difference of 0.8^{o}C.

The relationship between SST and NHF on the climatological time scale was obtained by applying the simplified temperature equation mentioned above. Changes in SST (called as dSST) for a given month was estimated from the previous month NHF and MLD data. Hence, the analysis was performed for each month from February onwards. The predicted new SST (SSTP) for a month was then computed by adding the estimated dSST with the previous SST value.

This method of analysis was applied to six locations in Indian Ocean. The geographic position of the locations is shown in Figure 5.18. The locations are from Arabian Sea (65E, 15N), Bay of Bengal (90E, 15N), western equatorial area (65E, 5N), eastern equatorial area (90E, 5N), south west Indian Ocean (65E, 20S) and south east Indian Ocean (90E, 20S). The analysis was then extended to the entire Indian Ocean and estimated SSTP at each grid point for each month. A correlation was obtained between SST and SSTP to understand

the role of heat fluxes (and MLD) on SST variability in Indian Ocean.

Annual Scale

Figure 5.19 shows the time series of climatological SST, SSTP and NHF at all the six locations. Heat fluxes undergo semi-annual variability in the north and equatorial Indian Ocean locations (Arabian Sea, Bay of Bengal and equatorial) and a single annual cycle at south. The impact of summer with a positive net heat flux is greatly reduced by the south west monsoon. The reduced shortwave radiation and increase in latent heat flux might be responsible for the reduced NHF during this northern summer peak. Maximum heat gain was found during the pre-monsoon (April-May) and post monsoon (September-October) seasons. It is also noted that NHF is always positive for the north Indian Ocean.

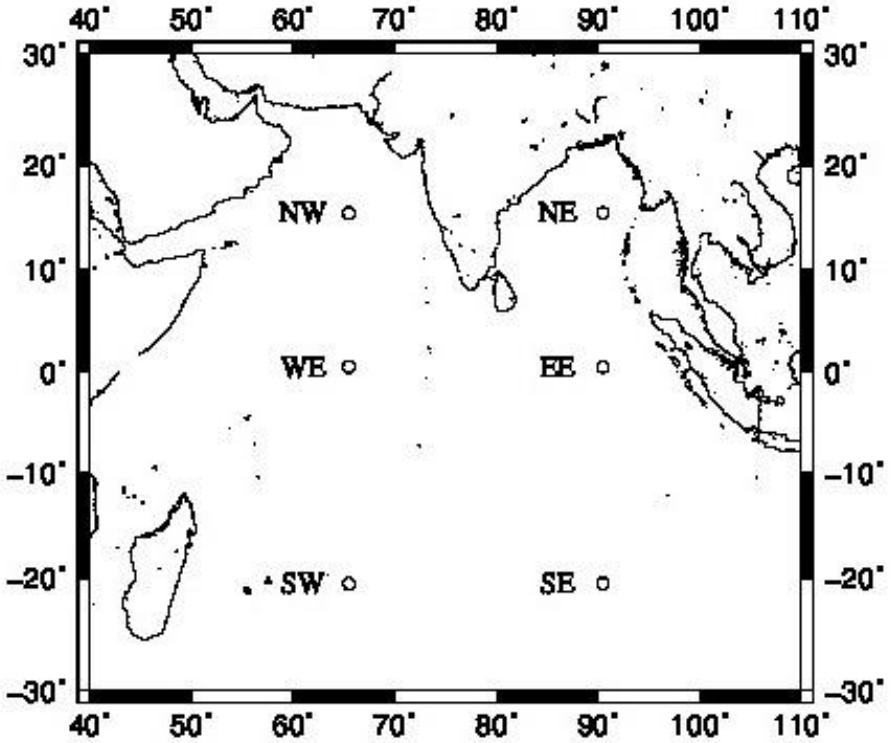

Figure 5.18 Geographic position of grids selected.

An exception is observed in Bay of Bengal during the winter months where NHF becomes negative. The amplitude of NHF is lesser at equatorial region as compared to that at north. The NHF at southern area undergoes a smooth annual cycle. The close marching of NHF with the hemispheric and warming indicates that NHF is mainly dominated by the solar heating. Maximum heat gain was observed during the southern summer months (December, January, and February) and a strong cooling in winter (May, June, and July).

The SST climatology also had a similar variation to that of NHF having semi-annual variation at northern Indian Ocean and annual variation at south. This can mislead to the conclusion that SST is controlled to a high degree by NHF alone.

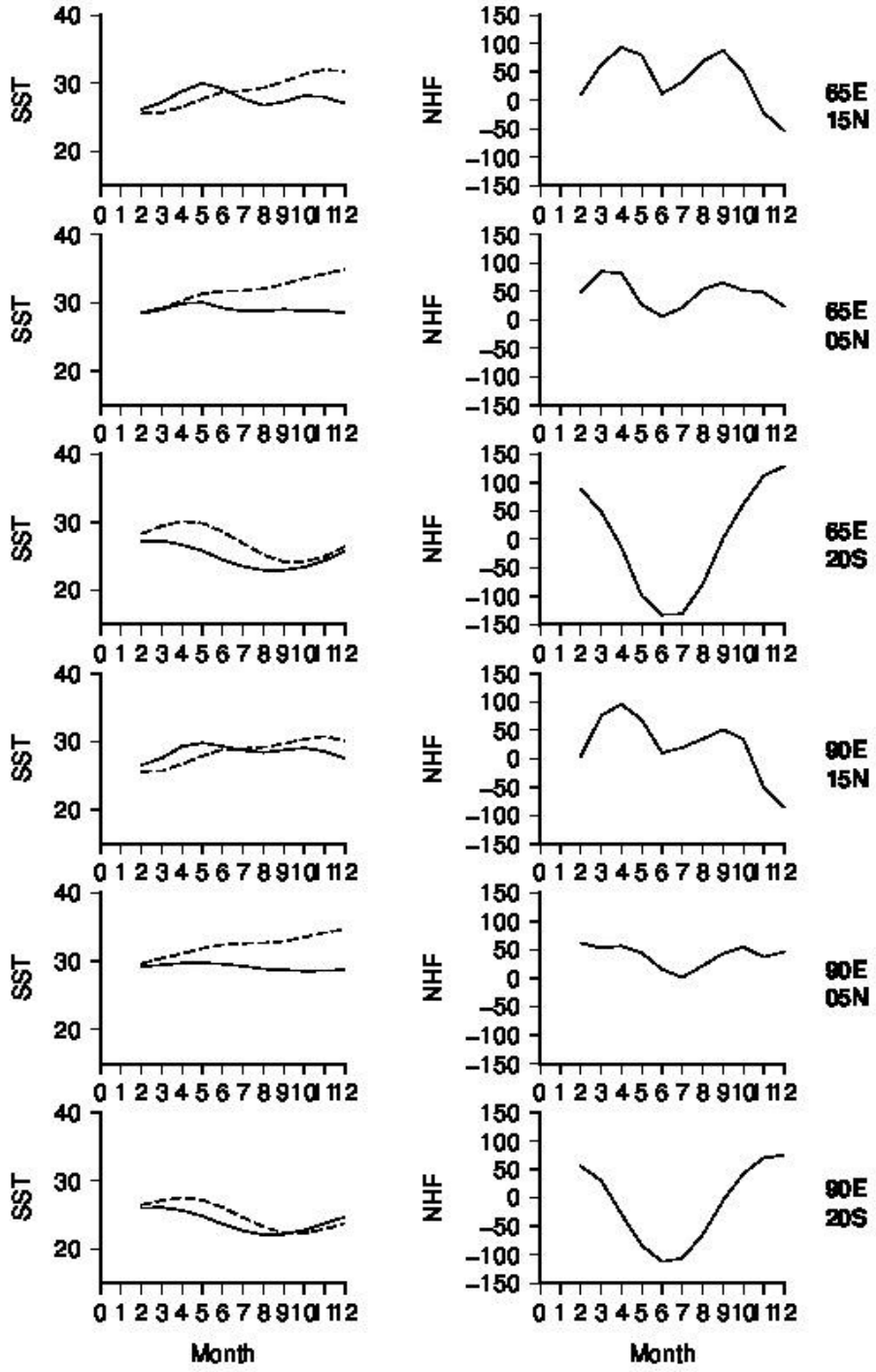

Figure 5.19 Observed (solid line) and predicted (dashed line) SST and Net Heat Flux (NHF) for the annual period.

But using the SST-NHF equation, a better understanding of the role heat fluxes can be obtained. It can be seen that there is a large difference between SST and SSTP especially in the northern areas.

The relationship is better at southern latitudes where SSTP nearly matches with the SST. As mentioned earlier, NHF at north is positive throughout the year. This positive heat input should increase SST and is represented by SSTP. SST will continue to increase as long as NHF is positive. A reduction in SST is possible only with a negative NHF. Hence, the SSTP in the north Indian Ocean will have an increasing trend throughout the year. In reality, SST does not follow such a trend but undergo a semi-annual variation. SST weakens during the summer monsoon season even though NHF is positive. Hence, it can be concluded that the observed annual variability of SST in the north Indian Ocean is not atmospherically forced though both have a similar pattern. The decrease in SST during the southwest monsoon season; hence should be driven by other processes such as advection.

Another source of error can be from the inaccurate estimate of MLD. MLD is usually higher during summer monsoon with a maximum of about 100m, but was not enough to make a cooling on SSTP as that was observed. SSTP was then computed with MLD with a higher SST difference ($2^{o}C$ and more). It resulted in a higher MLD, but still was unable to make the SSTP equivalent to that of the observed SST. It was also noticed that such a higher MLD would weaken the SSTP during the pre-monsoon season. Hence, from the analysis of MLD it was found that MLD should be lesser during the warming phase and be higher during the period of low SST.

The relative roles of NHF and MLD on SST were obtained by experimenting with reasonable values. The typical variation of NHF is from -150 to 150 W/m^2 and that of MLD is from 30 to 120m. With a NHF of 150

W/m^2 and MLD 30m, the dSST obtained was 2.1^oC. However, with the same NHF and with a MLD of 130m, the dSST was 0.48. Hence, the role of MLD on SST is found to be much lesser than that of heat fluxes.

At southern latitudes, SSTP was produced much similar to that of the real SST. This is due to the negative values of NHF. Negative NHF produces negative dSST from the equation which will cause a reduction in SSTP. SSTP in both locations of the southern latitude behaved equally to the NHF.

From this analysis it is observed that in the absence of strong advection, the local relationship of SST cannot be produced by the SST tendency equation. The better relationship at south cannot be considered as the quality of the equation but was produced by the negative NHF values. Hence, SSTP can be reduced only with a negative NHF. In other words, the equation works better for the NHF. The improvement is required in incorporating MLD into the equation. Increased MLD cannot currently reduce SST which is unrealistic.

The temperature equation was applied to each grid in Indian Ocean and correlation was obtained from the monthly values of SST and SSTP (Figure 5.20). High positive correlation between the two is found at southern areas south of 20S. Weak positive relationship is observed at the northern latitudes in Arabian Sea and Bay of Bengal. A slightly higher correlation is found in the northeastern Bay. It is very interesting to note that the correlation is very poor and even negative in the equatorial areas (10^oS to 10^oN). This is a result of the increase in SSTP and decrease of SST during the summer season.

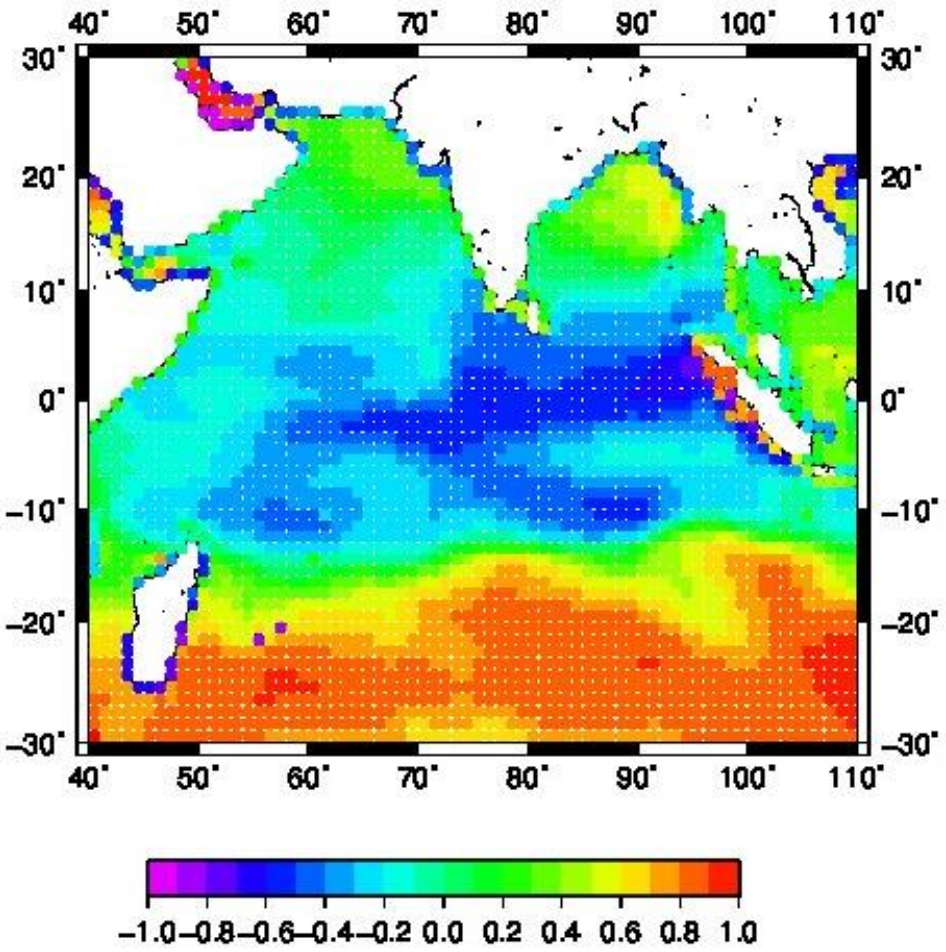

Figure 5.20 Correlation coefficient between observed and predicted SST for the annual period

Inter-annual Scale

The temperature tendency equation was then applied to the inter-annual data. SST and NHF data for a period 5 years (1984 to 1989) was used. The analysis was performed at all the six grids mentioned above. The time series of SST, SSTP and NHF is shown in Figure 5.21.

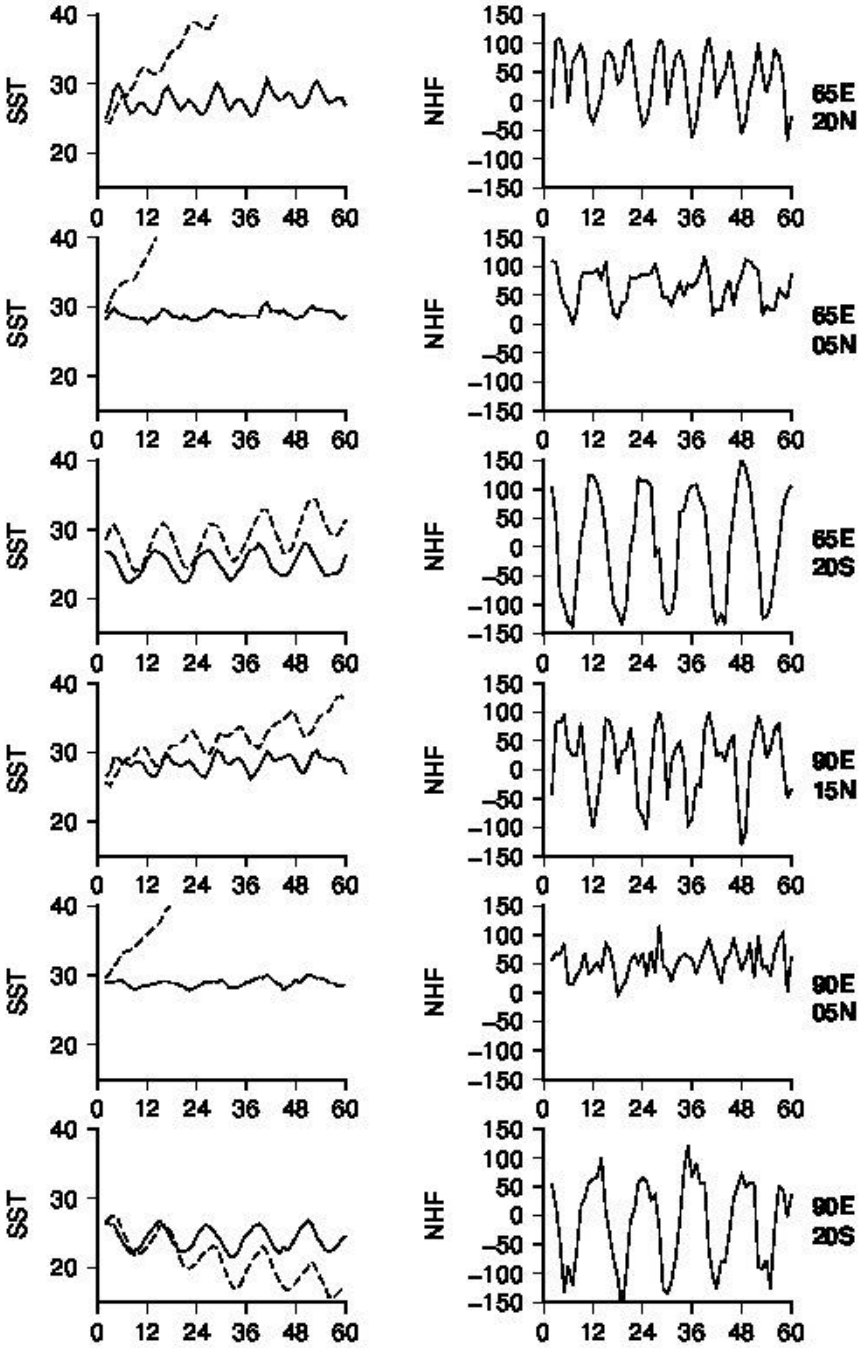

Figure 5.21 Observed (solid line) and predicted (dash line) SST and Net heat flux for the period 1984 to 1989

The semi-annual variation of NHF in the northern areas and annual variation at south are evident throughout the period. The magnitude of NHF was reduced over the equatorial area and did not show any cyclic behaviour. NHF is positive throughout the period at north and undergoes changes in sign almost equally at the southern latitudes.

The predicted SST (SSTP) showed unrealistic patterns for the northern area. Like the climatological analysis made above, SST was successfully predicted for the southern area. The positive NHF in the north results in positive dSST and hence leads to an increasing trend in SST. Hence, it is found that the bulk temperature tendency equation provides poor estimates of SST at the north Indian Ocean at both annual and inter-annual time scales.

Validity of the Equation

According to the equation, positive (negative) NHF will cause positive (negative) dSST and hence will increase (decrease) SST. This looks to be realistic. But when NHF is zero, dSST also becomes zero and SSTP remains a constant. Any change in MLD during this situation will not be accounted by the equation. It is to be noted that an increase in MLD in this case would lead to a negative dSST and hence reduce SSTP. It is also observed that according to the equation, an increase in MLD can only reduce the magnitude of dSST and not its sign. This is an issue because an increase in MLD would cause a deeper mixing and reduce the SST if NHF is assumed constant or even slightly positive. Hence, it is found that the SST tendency equation is incapable of accounting for the impact of heat fluxes and ocean mixing on SST or the mixed layer temperature. Hence an improvement in the equation is sought.

5.10 Conclusions

Climate trend and climatic anomalies are crucial for the life on Earth of which the trend may be more important for the future existence of life. It was not sure whether there exists any relationship between them. Studies indicate climatic anomalies do vary within a climate which has a trend. In this chapter, the climatic anomalies in Indian Ocean SST and warm pool were studied due to ENSO events. The dominant variabilities in each parameter were first obtained by performing the spectral analysis. The results of this analysis showed the dominance of annual and semi-annual cycles in each data. The objective of the analysis was to identify oscillations with periods higher than one year caused by inter-annual climatic events. SST only showed a peak at this period which was found to be consistent with the ENSO events.

The magnitudes of inter-annual anomalies were compared with the annual variability. It was found that inter-annual anomalies had lesser magnitude than the other and their geographical occurrence has some similarity.

The overall response of the tropical Indian Ocean to the ENSO was positive. A warming of the Indian Ocean was found in accordance with the warming in the Pacific. However, a temporal lag of 3-4 months was found in Indian Ocean SST to that of Pacific. This would mean that there may be some mechanism through which the Pacific Ocean controls Indian Ocean SST at least on inter-annual time scales. The positive relationship between Indian and Pacific SSTs even at non-El Nino years indicates that the cause of inter-annual variabilities is similar for both oceans.

Evolution of SST was studied during El Nino events. Warming anomalies begin to form by June in the western Indian Ocean during an El Nino. Warming

extends to eastern regions as El Nino strengthens. In some years, when El Nino co-occurred with IOD, the distribution of SST alters especially at the eastern Indian Ocean.

The role of heat fluxes on SST variability on inter-annual time scale was not strong. Presence of positive shortwave anomaly or negative latent heat flux anomaly was clearly absent in areas of high SST anomaly. This may indicate a weak role of heat fluxes on inter-annual SST variations. A better relationship was found with wind. In areas of high SST anomalies, wind was found weaker. Weaker wind causes less mixing in the ocean and may support for the excess warming. The temperature tendency equation was applied to examine the role of heat fluxes on determining SST. It was found that SST at southern latitudes responds better to heat fluxes. Correlation between the observed and predicted SST was high at these areas. However, the equation performs weaker in the equatorial ocean. This would indicate the role of other processes on the variability of SST in the equatorial areas.

Chapter 6

Climatic Trends in IOWP

6.1 Introduction

Planet Earth is undergoing a warming climate change that is unfortunately caused by human activities during the past few decades. Warming trend is found over land and ocean, at equator and at higher latitudes. Warming of the oceans has further implications on the planet as it can adversely affect the life in the ocean, the weather systems and also the climate.

Ocean warming trend in SST is likely to affect the natural modes of variability like Indian Ocean Dipole, monsoon, cyclone etc. Hence, studies on the ocean warming trends become an active area of climate research. The accelerated warming since 1970s supports the role of human activities from automobiles and industries as the cause of this change. The CO_2 gas, a bi-product of these activities, gets released into the atmosphere. Being a greenhouse gas, it traps the emitted long wave radiation from the Earth and thus increases the planet's mean temperature.

Ocean climate studies report warming trends in the world oceans. Role of anthropogenic activities on the current climate change is now well established [*Levitus et al*., 2001; *Barnett et al*., 2005; *Levitus et al.*, 2005; *Yan and Xie,* 2008; *Suryachandra et al*., 2012]. Warming trends has been found not only at the ocean surface but at subsurface too [*Levitus et al*., 2000; *Gille*, 2002].

Long term data set shows an increasing trend in warming since 1900. The accelerated warming in the 1960s and 70s shows the role human on the climate as a consequence of his developmental activities. The study indicates that ocean surface has warmed by 0.31°C during the past half century [*Levitus et al*., 2000]. To make it more curious, warming trend did not began [begin]

simultaneously all over the world oceans. Warming began in 1950s in Pacific and Atlantic, and began to form after a decade in Indian Ocean [*Levitus et al*., 2000]. This requires further analysis and needs to be proved that why Indian Ocean has responded differently to a global warming situation which is believed to be homogeneous.

Studies show that Indian Ocean was also been warming steadily over the past several decades [*Alory et al.*, 2007; *Suryachandra et al*., 2012]. However, there were contradicting evidences for the warming trend in the oceans. Increase in greenhouse gases should lead to an increase in the net heat gain that can increase the ocean temperature. *Levitus et al*. (2005) have reported higher heat storage in the southern Indian Ocean than at the tropics. *Alory and Meyers* (2009) were in favor of heat fluxes as the cause of ocean warming. They found an excess heat input to the Indian Ocean which explains the warming. But other studies opposed the role of heat fluxes [*Alory et al*., 2007; *Suryachandra et al*., 2012]. They observed that the excess heat fluxes alone are inadequate to explain the current warming trend and proposed the role of ocean dynamics as alternative mechanism. *Suryachandra et al*. (2012) have proposed a coupled ocean-atmosphere feedback mechanism through Rossby waves for the warming trend in Indian Ocean.

Climatic trend of warm pools was also reported in few studies. As the ocean temperature increases, a corresponding increase in the warm pool area also happens. The attention was drawn on the trend in the expansion and temperature of warm pools. Studies on the warm pool trend in the Indian Ocean is scarce. *Zhang et al*. (2009) have studied the inter-annual variability of IOWP. Along with large inter-annual variation, they have noticed that IOWP undergoes a long term expansion as a response to global warming. Expansion of the warm pool mainly occurred towards south. *Suryachandra et al*. (2012) have reported a high warming rate of 0.2^{o}C per decade in the central Indian

Ocean. They have also found an increase in the area of warm pool since 1950.

More studies are required to understand the warming trend in Indian Ocean, especially the delayed warming response and its future climatic influences. The main objectives of this chapter are formulated as follows:

- Estimate the rate of warming and its regional variations
- Long term trends in warm pool characteristics
- Role of heat fluxes on long term warming trend

Long term SST data from different sources (OAFlux, HadISST, ERSST, ECMWF) have been used in this analysis to investigate the long term trends in SST and warm pool parameters. Trend was estimated by applying the linear regression. The heat flux data from OAFlux was used to obtain long term trends in heat fluxes. Trend in wind speed was also estimated to recognize the role of wind to the observed warming.

6.2 IOWP Area

Monthly warm pool area was estimated from the total area covered by warm pool SST. The long term trend of warm pool area using various SST data sets, is shown in the Figure 6.1. Linear trend is also shown for the period 1960-2009.

Both HadISST and ERSST had longer time records. They have almost similar magnitudes for the period prior to 1960. The warming trend in that period was insignificant. Hence, the SST data for the period from 1960 onwards only was used in this study to estimate the long term trends.

Monthly warm pool area for the period 1960 to 2009 and the estimated long term trend are shown in Figure 6.1. An increasing trend in the warm pool area is evident in all the four data sets for the period chosen (1960-2010). Apart from few low values in 1970s, IOWP had undergone a steady

expansion till 2009. The magnitude of rate was, however, different among the data sets. OAFlux SST showed the largest trend (1.66 x 10^6 km^2 per decade). ECMWF showed a lesser magnitude of 1.45 x 10^6 km^2 per decade. The ERSST had the lowest value of 0.95 × 10^6 km^2 per decade. The mean warm pool area was increased from about 12 × 10^6 km^2 in 1960 to 20 × 10^6 km^2 in 2009.

To confirm this result, a comparison of the spatial distribution of the annual mean warm pool during 1960 and 2010 was prepared (Figure 6.2). From the figure it is clear that the warm pool area was much less in 1960 and was considerably increased in 2010. The temperature of the warm pool was well below 29^{o}C in 1960.

Highest temperature was seen at the eastern equatorial areas. In 2010, warm pool intensified and expanded towards west north and south. The temperature at the eastern side of the warm pool was increased by 1^{o}C by reaching the 29.5 - 30.0^{o}C range. The 29 - 29.5^{o}C temperature band occupied a large area during this period.

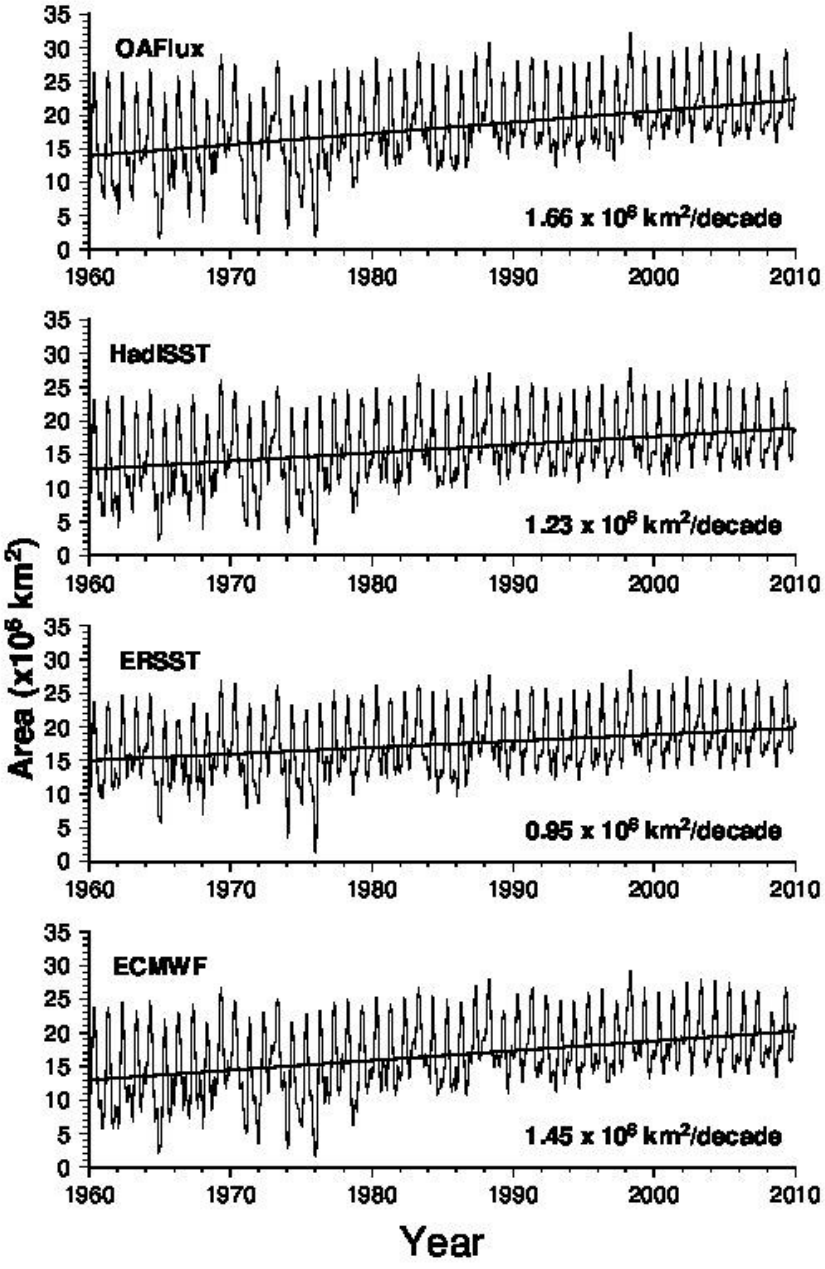

Figure 6.1 Time series of monthly IOWP area using different SST data products. The solid straight line represents the linear trend. The magnitude of the trend (per decade) is displayed.

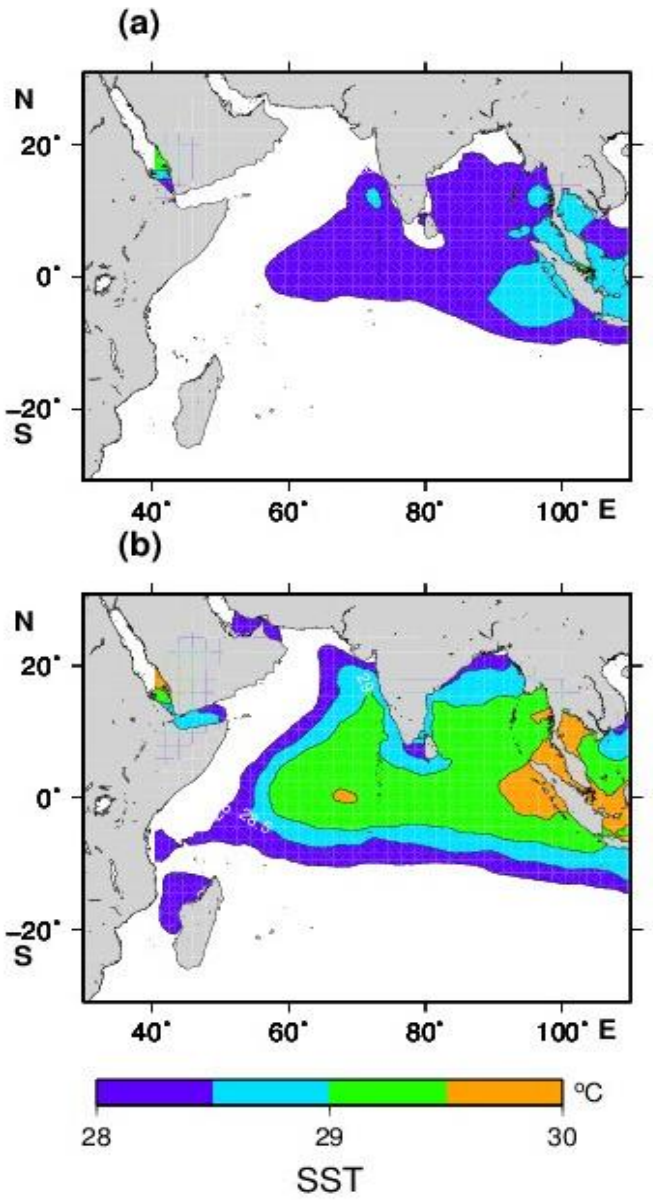

Figure 6.2 Annual mean warm pool SST distribution during (a) 1960 and (b) 2010

6.3 IOWP Temperature

A climatic trend in the mean warm pool temperature was also estimated using the same data sets. Monthly mean temperature of warm pool was estimated by averaging warm pool SST and the linear trend was estimated by linear regression. Figure 6.3 shows the time series of the mean

warm pool temperature. Similar to its area, warm pool temperature also displayed a long term trend. Both HadISST and ERSST showed similar pattern during the first half of 20^{th} century with less magnitude. The mean temperature trend for the second half of the century was more significant. Both OAFlux and ECMWF SSTs showed similar magnitude of trend (0.1^{o}C per decade) and was the highest among other data sets. HadISST showed the lowest trend. The mean temperature of IOWP was about 28.6^{o}C in 1960 and was raised to over 29.1^{o}C by 2009. A correlation of 0.9 was found between warm pool area and temperature.

6.4 Temperature Bands

To further understand the relative magnitude of temperatures on the total warm pool variability, trends in the warm pool area corresponding to each one-degree temperature band (28-29^{o}C, 29-30^{o}C and 30-31^{o}C) was obtained (Figure 6.4). The area corresponding to 28-29^{o}C temperature band showed only weak trend (0.01×10^{6} km^{2} per decade). Highest trend was found for the 29-30^{o}C band (1.34×10^{6} km^{2} per decade). The highest temperature band (30-31^{o}C) also had a significant contribution to the overall warming of the warm pool. It also had large inter-annual variabilities.

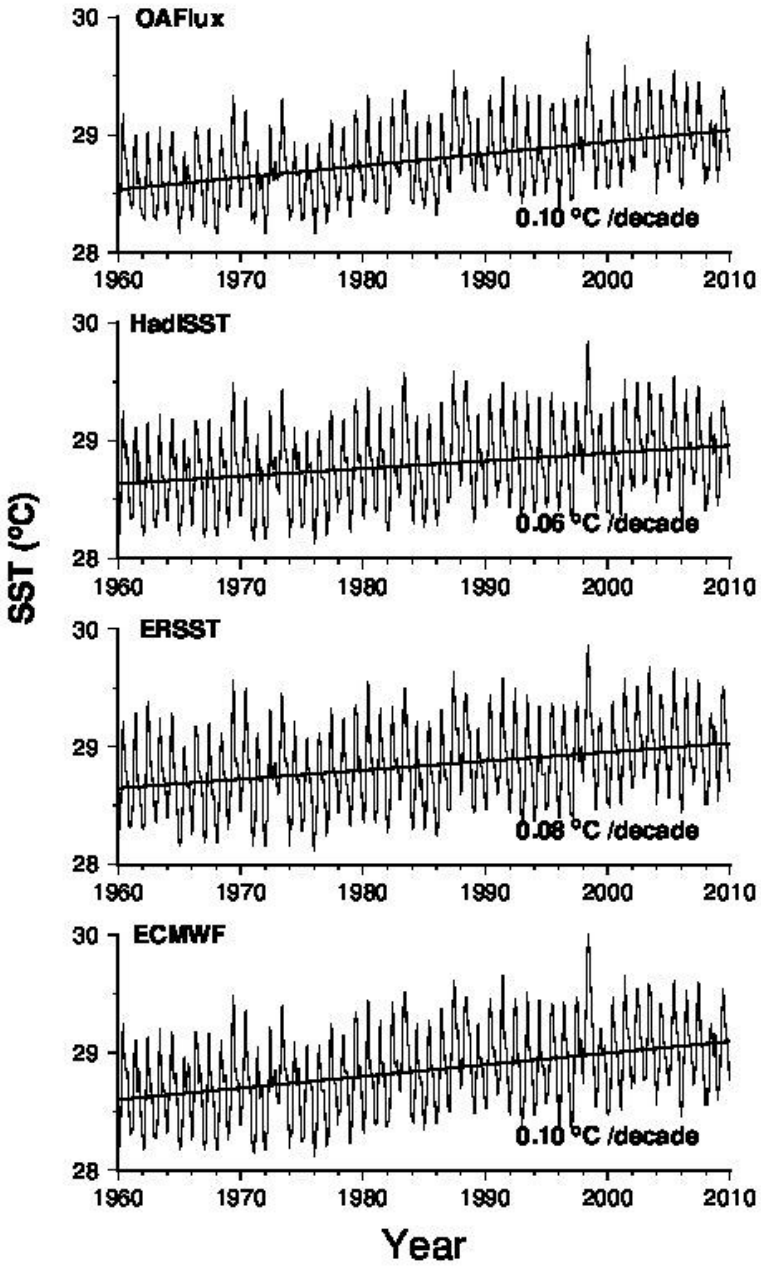

Figure 6.3 Time series of monthly IOWP mean temperature from different SST data products. The solid straight line represents the linear trend. The magnitude of rate of increase in temperature (in ^{o}C per decade) is displayed.

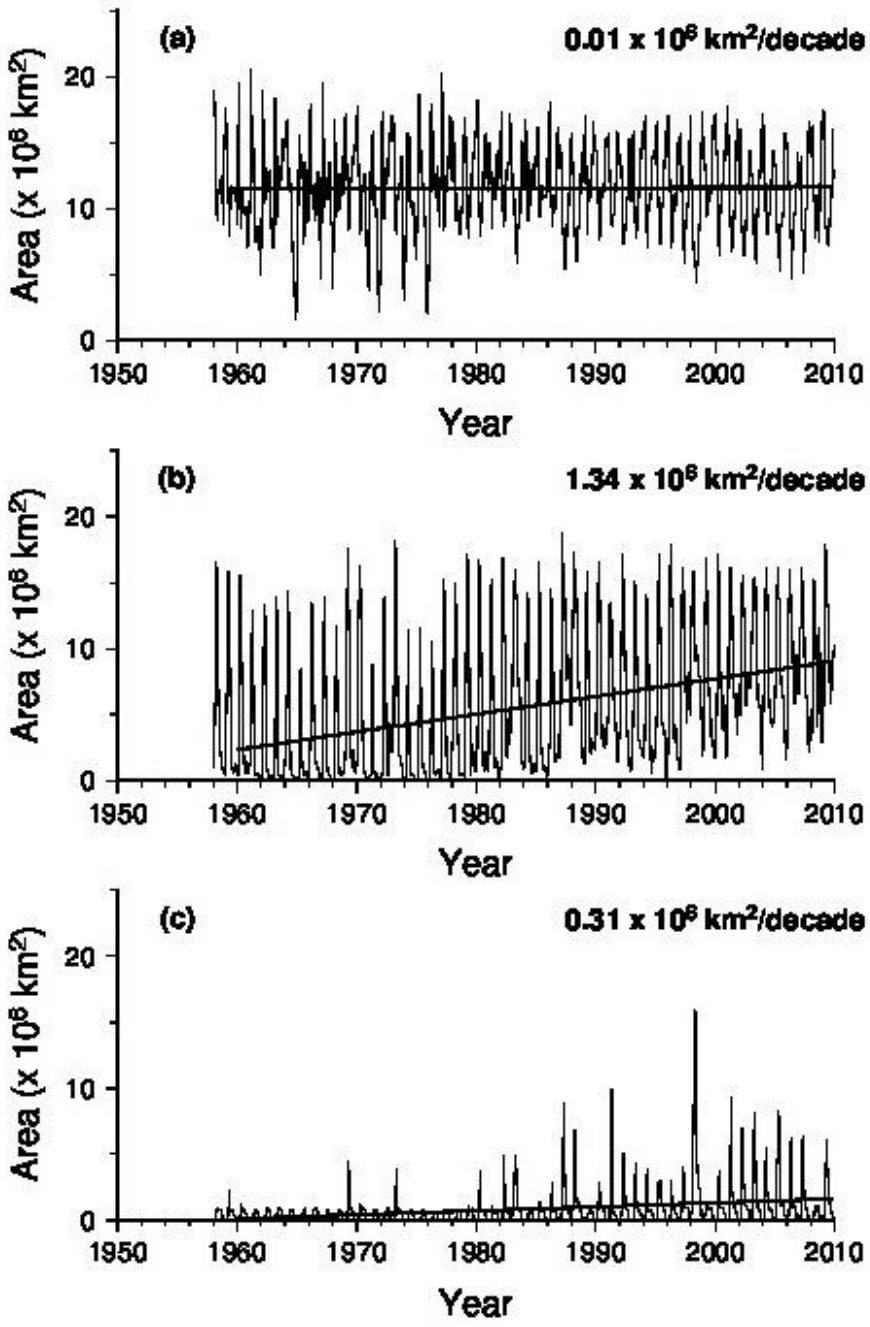

Figure 6.4 IOWP area trend for each temperature band of (a) 28-29^{o}C, (b) 29-30^{o}C and (c) higher than 30^{o}C

6.5 Spatial Distribution of Warming Trend

To understand the spatial variation in the warming trend, the regression was done using data extracted from each grid. SST data from OAFlux, HadISST, and ERSST were used for this analysis and to see the differences among them. Linear regression was applied to monthly time series of SST at each grid. *Suryachandra et al*. (2012) produced an estimate of the warming trend in the Indian Ocean. They have observed a warming trend all over the tropical Indian Ocean having the highest magnitude (~0.2^{o}C per decade) at the central Indian Ocean.

Estimates of warming trend were obtained using SST data from OAFlux, HadISST, ERSST and ECMWF (Figure 6.5). Trend was obtained for a common period 1960 to 2009 to have inter-comparison among the data sets. Among the data sets, OAFlux SST displayed the maximum warming rate (0.24^{o}C/decade). Lowest magnitude was observed in the ERSST data. In general, all data except ERSST showed the highest warming trend at the central equatorial region though there is a difference in their magnitudes. This was in general agreement with *Suryachandra et al*. (2012).

Another important outcome of the study is that the higher warming rate at the equatorial areas. This feature is very clear in all the data sets except the ERSST data. The deviation in the distribution for this data from others could be due to the difference in spatial resolution. There are large differences in the values of decadal trend for other areas in Indian Ocean. The trend values were lower at the northern Arabian Sea and Bay of Bengal for HadISST. ECMWF SST showed the lowest trend at the northern Bay of Bengal compared to others.

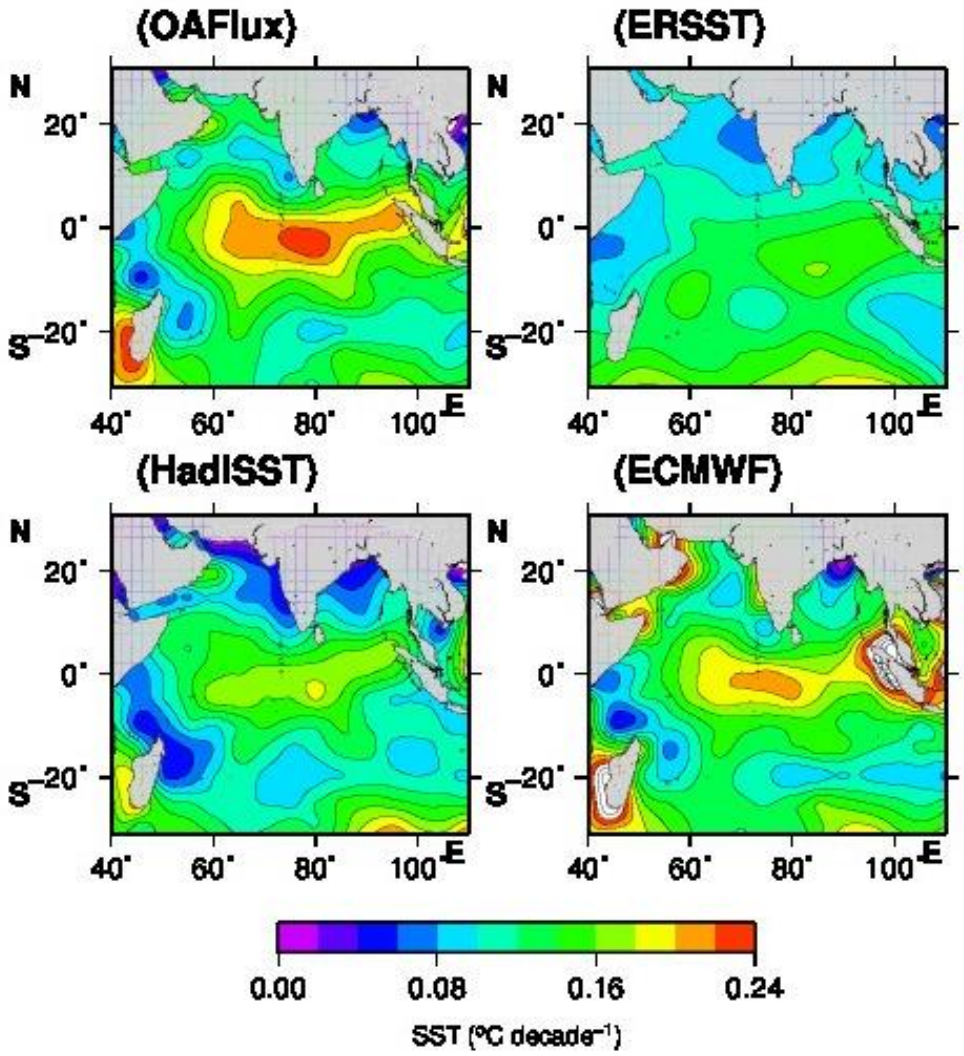

Figure 6.5 Geographical distribution of warming trend using (a) OAFlux (b) HadISST (c) ERSST and (d) ECMWF SST products. Trend was estimated for the period 1960 to 2009.

In OAFlux and ECMWF data sets, a very high warming rate was found off Madagascar. It was lesser for HadISST and was absent in the ERSST. A high warming rate was found at the eastern equatorial Indian Ocean only in ECMWF data.

6.6 Trends in Heat Flux and Wind

To understand the cause of spatial variation in the long warming trend, trend analysis was performed on heat flux data. Heat flux on shortwave radiation, longwave radiation, latent heat flux and sensible heat flux from OAFlux was used. The data covers a period of 1984 to 2009 only which is lesser than that applied for SST data. However, since the trend from 1960 onwards was nearly linear, the trend obtained on heat flux can be used to explain the variability of SST.

Figure 6.6 shows the time series of spatially mean monthly heat fluxes for the tropical Indian Ocean. Linear trend was estimated for shortwave, longwave, latent heat and net heat fluxes. The figure explains the overall trend in heat fluxes of tropical Indian Ocean. Their regional dependencies are estimated in the following section.

Shortwave radiation did not show any appreciable long term trend. The very low (negative) value indicates a steady heating from solar radiation. Since the data convers a period of 26 years, longer variabilities in solar radiation may be missing.

However, the long wave radiation had a positive trend during this period. It was increasing at a rate of about 2 Watts/m^2 per decade. Positive rate indicates an increasing heat loss from long wave radiation from the oceans. This is against the current concept on global warming. It is now established that the increase in carbon dioxide in the atmosphere causes the global warming by trapping the long wave radiation emitted from land and ocean. If this is true, then there must a reduction in the loss of long wave radiation from the earth (and oceans). However, this study indicates an opposing role of long wave radiation on the observed warming trend.

Latent heat flux also showed positive trend, indicating an increase in heat loss from the ocean. The magnitudes of the trend for LHF and LWR are comparable. Latent heat flux was considered positive for upward (ocean to atmosphere) fluxes. Hence, positive trend indicates an increase in the heat loss. The magnitude of trend was 1.84 Watts/m^2 per decade that was lesser than that of long wave. Increasing trend in the LHF is due to an increasing trend in the wind speed.

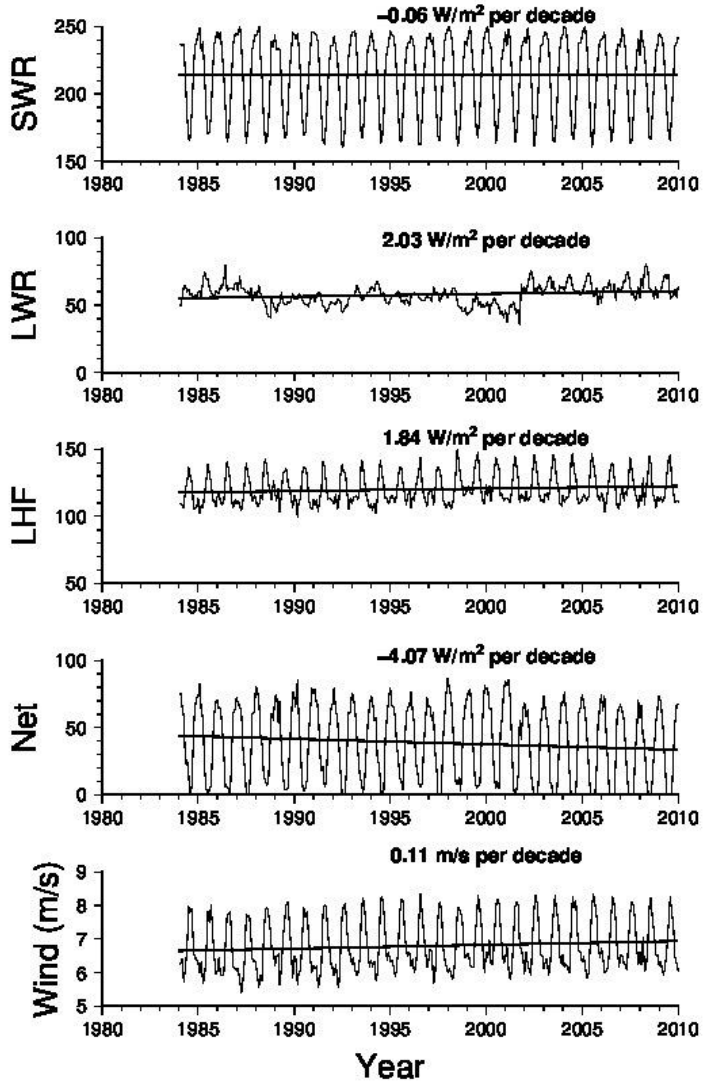

Figure 6.6 Time series of monthly mean heat fluxes (shortwave radiation, longwave radiation, latent heat and net heat flux) and wind speed averaged over the tropical Indian Ocean. The linear trend estimated for the period 1984 to 2009 is also shown.

Wind speed had an increasing trend of 0.11 m/s per decade. The trend in sensible heat flux was much less and is not shown. However, it was considered in estimating the trend in the net heat flux. Net heat flux showed a decreasing trend of 4.07 W/m^2 per decade. It is to be noted that the monthly net heat flux was positive throughout the year for the tropical Indian Ocean indicating a net heat input. The sign convention of net heat flux is that heat gain is considered as positive. The negative trend of net heat flux indicates a decrease in the net heat gain by the ocean that should cause long term cooling of the ocean. This cooling effect was mainly contributed by the long wave and latent heat. The increasing trend in the latent heat flux agrees with the increasing trend of wind speed.

Figure 6.7 shows the spatial distribution of linear trend for each heat flux data for the tropical Indian Ocean. Shortwave radiation had only a weak trend. The zone of high SST trend at the equator nearly coincides with that in the shortwave radiation. However, the correlation between the two was very poor in other areas especially at the western Indian Ocean and at the southeast Indian Ocean. SST did not show any appreciable positive trend in those areas. Hence, the shortwave radiation in general had only a little contribution to SST trend.

Figure 6.7b shows the long term trend in long wave radiation. It is to be noted that these terms are the heat loss terms for the ocean but have [are] taken as positive. The magnitude of trend in long wave was much higher than the shortwave radiation. It had high values (above 10 $Watts/m^2$ per decade) at the northern Arabian Sea. There was a decrease in the long wave heat loss at the southeast Indian Ocean.

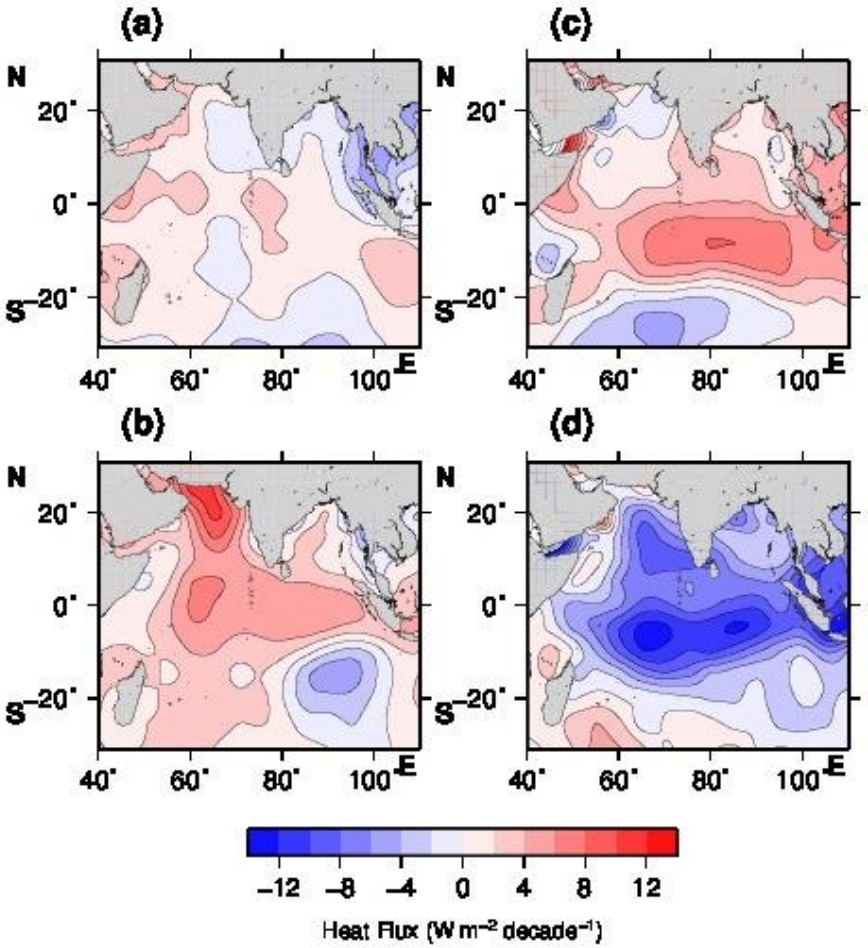

Figure 6.7 Spatial distribution in the long term trend of (a) shortwave radiation (b) longwave radiation (c) latent heat and (d) net heat flux

Latent heat flux showed positive trend (increasing heat loss) at south of equator but was negative (decreasing heat loss) further south and also at the northern Arabian Sea (Figure 6.7c). The increasing and decreasing trend in the latent heat flux should be due corresponding variations in wind speed.

Net heat flux had negative trend throughout the tropical Indian Ocean except for a positive value at the southwest Indian Ocean (figure 6.7d). This suggests that fluxes in total contribute to a cooling effect on the north Indian Ocean. Largest cooling trend was found at few degrees south of equator. It is

to be noted that SST had an increasing trend at the equatorial areas. Hence, heat fluxes do not support for the warming trends in the tropical Indian Ocean.

6.7 Conclusions

This study was envisioned to understand the warming trend in the tropical Indian Ocean and the Indian Ocean Warm Pool. Long term data sets on SST, heat fluxes and wind speed, with a time span of 50 year were used in the analysis.

Warm pool had expanded and intensified during this period. Long term trend in increasing warm pool size is evident in all the climate data sets analyzed. There were large differences in the rate of warming in the Indian Ocean. Highest warming trend was noticed at the equatorial areas. To find the cause for this warming trend, air-sea heat flux data were also subjected to long term trend analysis. Shortwave radiation did not have any significant long term trend. Both long wave radiation and latent heat flux together contributed a cooling trend. The net heat flux had a negative trend throughout the north Indian Ocean which implies a cooling impact on the ocean. If the global warming was contributed by the increased quantity of atmospheric carbon dioxide, then there must be a reduction in the long wave heat loss. This analysis, however, showed an opposite effect of long wave radiation. Hence, the increased carbon dioxide as reasoning to global warming may need further confirmation.

Chapter 7

Modelling SST In a One-Dimensional Mixed Layer Model

7.1. Introduction

The surface layer of the ocean continuously interacts with the atmosphere and undergoes changes. A number of processes are in action in this layer such as solar heating, radiative heat loss, mass exchange through evaporation, precipitation and sea spray, currents, generation of waves and wave breaking and air-sea gas exchange. The water in the surface layer is turbulent due to the action of wind, buoyancy, wave breaking and current shear and is therefore called as Ocean Mixed Layer (OML). The variability in the depth of this layer, called as mixed layer depth (MLD), has an important role in the surface layer temperatures of the ocean and is therefore crucial to the state of the ocean-atmosphere system.

OML is important to biological productivity of the ocean. Since sunlight is essential for primary production, oceanic productivity is restricted to the euphotic layer of the ocean that usually falls well within the mixed layer [*Polovina et al.*, 1995; *Fasham*, 1995]. Heat budget of the mixed layer is important in the case of climate conditioning. Acoustic properties of OML are important for defense application [*Sutton et al*., 1993]. The fate of SST is also controlled by processes within the mixed layer. Hence, an understanding of the processes in the mixed layer and its variability becomes an active area of research.

SST and hence the warm pool is primarily controlled by the local heat flux through air-sea interface. The absorbed heat at the surface of the ocean is diffused downwards through turbulent eddies. Higher mixing will deepen the mixed layer and reduce the mixed layer temperature and hence SST. It can also be influenced by the three-dimensional advective processes and remotely by the propagation of planetary waves. To quantify the role of individual processes observations alone would be insufficient. Modeling is an alternative

and dynamical approach the may help to understand complex systems like ocean. Experiments with the model help us to understand the role of each forcing terms separately.

Models of the ocean range from very simple to highly complex ones. Simple models have limited dynamics and usually lesser in dimensions. A one-dimensional model is the simplest possible one and a complex model will include realistic dynamics in all the three dimensions. Here, a one-dimensional model was used to understand the local response of the ocean in terms of SST to atmospheric forcing from heat flux and wind stress.

The structure of the surface layer of the ocean is shown in Figure 7.1. OML is typically few tens of meters deep. The energy for mixing comes from various sources such as wind forcing, wave breaking, current shear and buoyancy. As a result of mixing, the physical properties such as temperature, salinity and density become uniform within the mixed layer.

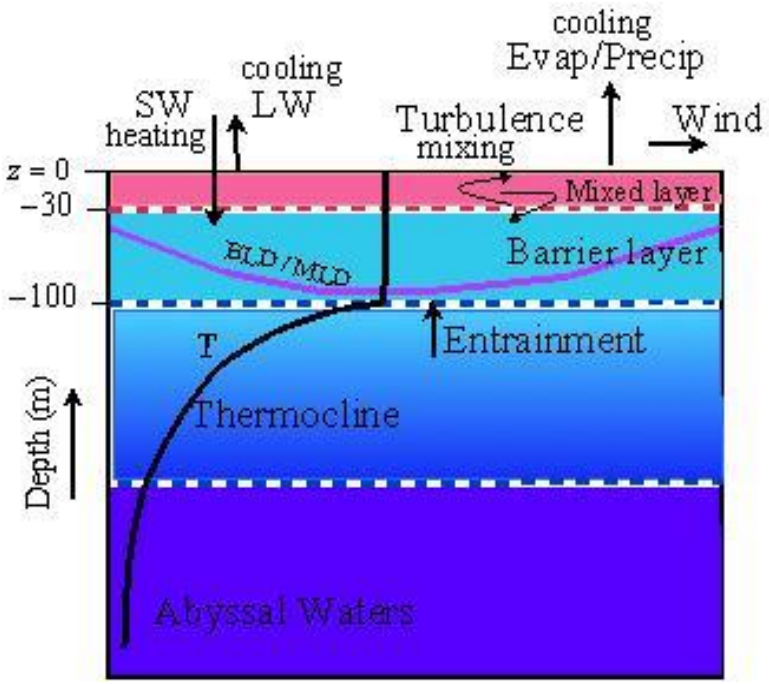

Figure 7.1 Vertical divisions of the ocean
[source: http://www.nptel.ac.in]

In the tropical and subtropical areas, OML is bounded below by a strongly stratified layer where the temperature decreases rapidly with depth, called as thermocline. Since density is mostly controlled by temperature than salinity, thermocline usually coincides with the density gradient which is called as pycnocline. In areas where salinity variations are high such as that in the Bay of Bengal, the structure of the surface layer will be modified and additional layer such as barrier layer can also form.

OML is a layer where the mixing is high. To estimate the mixed layer depth (MLD), it is necessary to measure the turbulent intensity. However, measuring turbulence is a difficult task at ocean and is not practical in routine observations at the sea. Due to this reason, mixed layer is defined based on physical properties such as temperature, salinity and density that are influenced by turbulent mixing. As a result of mixing, the properties become nearly homogeneous within the surface layer.

In its simplest form, MLD is defined as the depth up to which the temperature or density is homogeneous.Density method is often preferred over temperature as it includes the effect of both temperature and salinity. Since the upper ocean is not completely homogeneous, this definition is slightly relaxed and defined as the depth where the absolute difference of a property from that of its surface exceeds certain threshold value. However, there is no consensus on the value of this threshold and is usually decided by the researcher. For example, in the case of temperature, different threshold values such as 1.0, 0.8, and 0.5^{o}C are used [*Obata et al*., 1996]. The threshold for density is about 0.125 Kg/m^3, but can also vary. Table 3 and 4 show relevant literatures on the temperature and density criteria used to compute mixed layer depth.

Ocean surface is heated by solar radiation. Shortwave part of the

spectrum penetrates few meters deep into the ocean, thus heating the layer below the air-sea interface. On the other hand, the longwave part of radiation gets absorbed within few centimeters at the surface. The cooling of the OML comes from both radiative (long wave) and turbulent (latent and sensible) heat fluxes. The heat absorbed from net heat is then transported deeper into the ocean by turbulence mixing. If the net heat is negative, the convection occurs due to instability and can cause deeper mixing.

Author	Δt
Thompson (1976)	0.2
Lamb (1984)	1.0
Price et al. (1986)	0.5
Kelly and Qiu (1995)	0.5
Martin (1985)	0.1
Wagner (1996)	1.0
Obata et al., (1996)	0.5
Monterey and Levitus (1997)	0.5

Table 3 Temperature-based criteria used to estimate MLD

Author	$\Delta\sigma_t$
Miller (1976)	0.125
Levitus (1982)	0.125
Lewis et al., (1990)	0.130
Spall (1991)	0.125
Huang and Russell (1994)	0.125

Table 4 Density-based criteria used to estimate MLD

The deepening of mixed layer can occur only through an entrainment process at the base of the mixed layer. Entrainment occurs when there is sufficient turbulent energy to deepen the mixed layer and can result in the overall cooling of mixed layer. The water at the deepest part of the mixed-layer need not be re-entrained within a seasonal cycle and hence subducted. Large subduction rates are found in regions of where horizontal gradients in the mixed layer are large. Thus variation in mixed-layer depth is important to the ocean thermal structure.

7.2 Mixed Layer Variability

Unlike atmospheric boundary layer, OML variability is lesser known. This is mostly due to the limited observations in the oceans and partly due to the lack of clarity in defining the mixed layer. By using different criteria and different threshold values, MLD can have different values even for a single profile data. Because of these reasons, the accuracy in the MLD is of little importance.

Diurnal Variability

On diurnal scale, OML is heated by the shortwave radiation and makes the OML shallow during day time. At night, heat is lost from surface and the water column becomes unstable and induces convective mixing which leads to

an increase in the OML depth [*Spigel et al*., 1986].

Seasonal Variability

Seasonal variability of the OML is a prime factor that modulates air-sea interaction at mid and low latitudes. The spring and summer warming makes the surface water more stratified and makes the OML shallow. Stronger wind and surface cooling deepens OML during autumn and winter. At higher latitudes, convection further deepens OML depth.

Mixed layer has been studied for specific regions and also on global scales. *Schott et al*. (2002) have studied the seasonal variation of MLD in the north Indian Ocean. A fairly good information about the MLD in Arabian Sea now become available from observational data [*Rao et al.,* 1989; *Rao and Sivakumar,* 2003; *Sreenivas et al*., 2008] and modeling [*Prasad,* 2004; *de Boyer et al*., 2007; *McCreary and Kundu,* 1989]. MLD undergoes seasonal variabilities in the north Indian Ocean. Ekman dynamics dominate MLD during summer whereas convective process during winter. During the intra seasonal periods MLD become shallow due to high heat input and weak wind.

Marked difference was found in the MLD distribution in Bay of Bengal as compared to that in Arabian Sea [*Gopalakrishna et al*., 1988; *Rao et al*., 1989; *Shenoi et al.,* 2002; *Prasad,* 2004; *Narvekar and Kumar,* 2006]. This was mostly due to the higher stratifiaction and weak winds. MLD at the equatorial Indian Ocean is driven by Wyrtki Jet (*Wyrtki*, 1973). Regional MLD studies were also carried out at the eastern equatorial Indian Ocean [*Masson et al*., 2002; *Qu and Meyers,* 2005; *Du et al*., 2005]. *Kara et al.* (2003) have obtained the climatological MLD distribution over the global oceans.

Inter-annual Variability

Only few attempts were made on the inter-annual variability of OML especially that driven by ENSO and IOD [*Carton et al.*, 2008; *Keerthi et al*.,

2012]. It was well established that the Indian Ocean experiences a basinwide increase in SST during an El Nino event [*Klein et al*., 1999]. Using a general circulation model, *Keerthi et al*. (2012) found that the magnitude of inter-annual variability of MLD is higher for IOD than ENSO. However, the impacts of such climatic events are not spatially uniform but have a strong regional dependency. It will be interesting to find the regional impact climatic events on SST and MLD.

7.3 Mixed Layer Model

There are two approaches to model the ocean mixed layer; bulk (or slab) models and turbulent diffusion models. Bulk models treat the mixed layer as a slab of water in which the governing equations are vertically integrated. The variability of mixed layer then depends on the parameterized value of entrainment rate at the base of the OML. Entrainment is parameterized in terms of surface fluxes of heat and buoyancy. The mixed layer depth is the prognostic variable in such models.

On the other hand, diffusion models consider the turbulence within the mixed layer. Mixed layer is related to the changes in turbulence kinetic energy budget. There are first and second turbulence closure schemes. In second-moment closure models, the turbulence equations are closed at the second moment level. The governing equations consist of conservation equation for Turbulent Kinetic Energy (TKE) and a set of algebraic equations for turbulence.

A one dimensional mixed layer model, developed at the Naval Post-Graduate School (NPS), was used to understand the SST dynamics in respect to high frequency atmospheric forcings [*Garwood*, 1977]. This model was based on the previous model formulated by *Kraus and Turner* (1967). The model incorporates the production, alteration and destruction of turbulent kinetic energy within the mixed layer. However, the model ignores the

dissipation effect on turbulent kinetic energy budget. Later, various parameterizations were put forwarded for the modeling dissipation. The advantage of Garwood's model is the application of better parameterization schemes.

The objective here is to simulate SST and temperature profile in the ocean with surface forcings from wind stress and heat fluxes. The model is initialized with temperature and salinity profiles. The time step of the model is 3600 seconds. The model is forced with heat and momentum fluxes at hourly intervals. Experiments with the model were made to understand the role of heat flux and wind stresses on mixed layer variability and SST. Role of wind stress was studied by running the model with different wind stress scenarios while keeping the heat fluxes constant. Similarly, the model was forced with different heat fluxes to understand the response of the ocean to changes in heat exchanges alone. The model was then run with real initial conditions and forcings to simulate the real MLD variability.

7.4 Role of Wind Stress

The model was run with idealized conditions to understand the roles of each forcing terms. Model was initialized with standard temperature and salinity profiles up top 200m. For this, temperature was taken constant (28^{o}C) from surface to 100m and allowed to decrease linearly with depth up to 200m. Since salinity variations are smaller in the ocean, a constant salinity profile was used. Therefore, experiments with the model were not performed with freshwater fluxes. Standard forcing of the model was then generated. As the objective here is to experiment the model with different wind stress, heat flux was kept constant. Different cases of wind stress such as constant and varying were considered.

Constant Wind Stress

To understand the role of wind stress on the ocean surface layer variability and SST, the model was run with different wind forcing conditions keeping constant heat fluxes. In the first run, the model was forced with a wind stress of 0.3 dynes/cm^2 and is shown in Figure 7.2. A typical temperature profile of the tropical ocean was used as initial conditions for all the cases. The temperature is taken constant up to 100m and then allowed to decrease linearly further with depth. The maximum depth was 200m with a resolution of 1m. Since salinity does not have a typical profile in the ocean, a constant salinity was assumed. Thermal forcing was done in terms of heat gain and total heat loss. Here both terms were kept zero and hence the net heat flux also was zero. Model was run for 20 days with a time step of 3600 seconds.

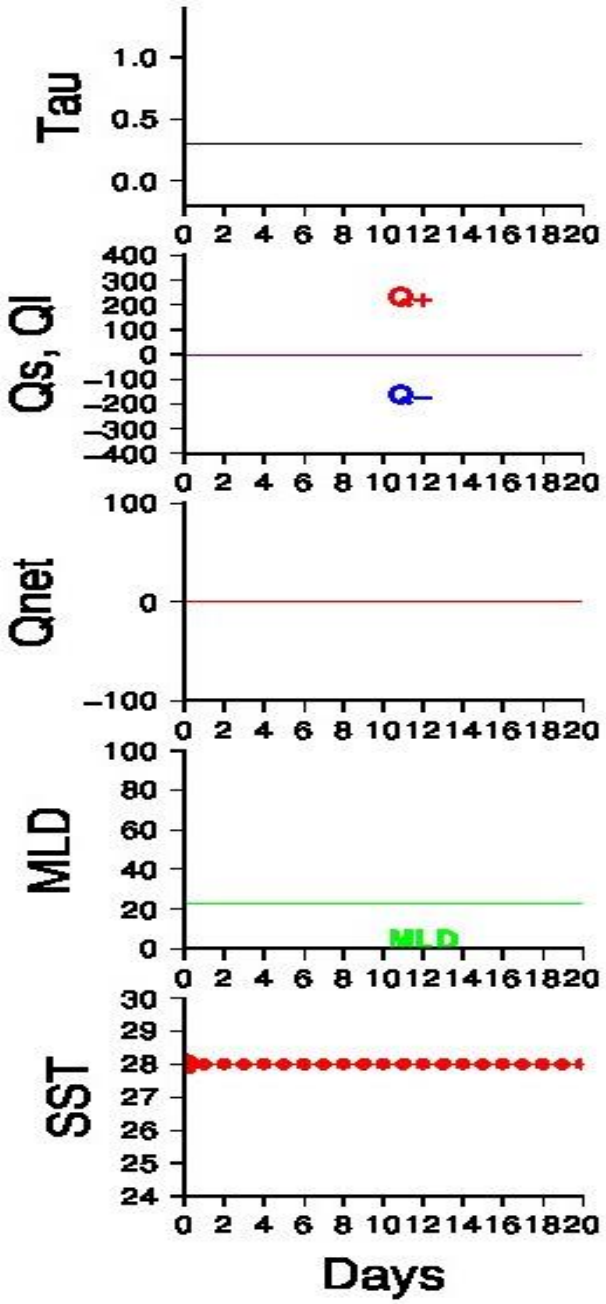

Figure 7.2 Model run forced with a constant wind stress (Tau = 0.3 dynes/cm^2). No forcing from heat flux was included where heat gain, heat losses and hence net heat fluxes were zero. MLD and SST are the model outputs.

Model output shows a constant MLD (~25m) during the entire period of the model run. The wind stress used was low and hence resulted in a shallow mixed layer. The temperature profile remained unchanged (not shown). This is reasonable as there was no heat exchange, the temperature profile should

remain the same and so SST.

Higher wind stress

The objective here was to observe the ocean response to a higher wind forcing. a higher wind stress of 0.6 dynes/cm^2 forcing was applied to the same condition as the first model run. Figure 7.3 shows the result of this model run. In this case, MLD was increased in response to the higher wind stress. There was no change in the temperature profile and SST.

Increasing Wind Stress

In this run (Figure 7.4), the model was forced with linearly increasing wind stress. From this model run it was observed that the mixed layer responded positively to the wind forcing with an increase. This is a good result from the model where the mixed layer depth has changed from enhancing turbulent mixing. SST and temperature profiles were, however, remained the same.

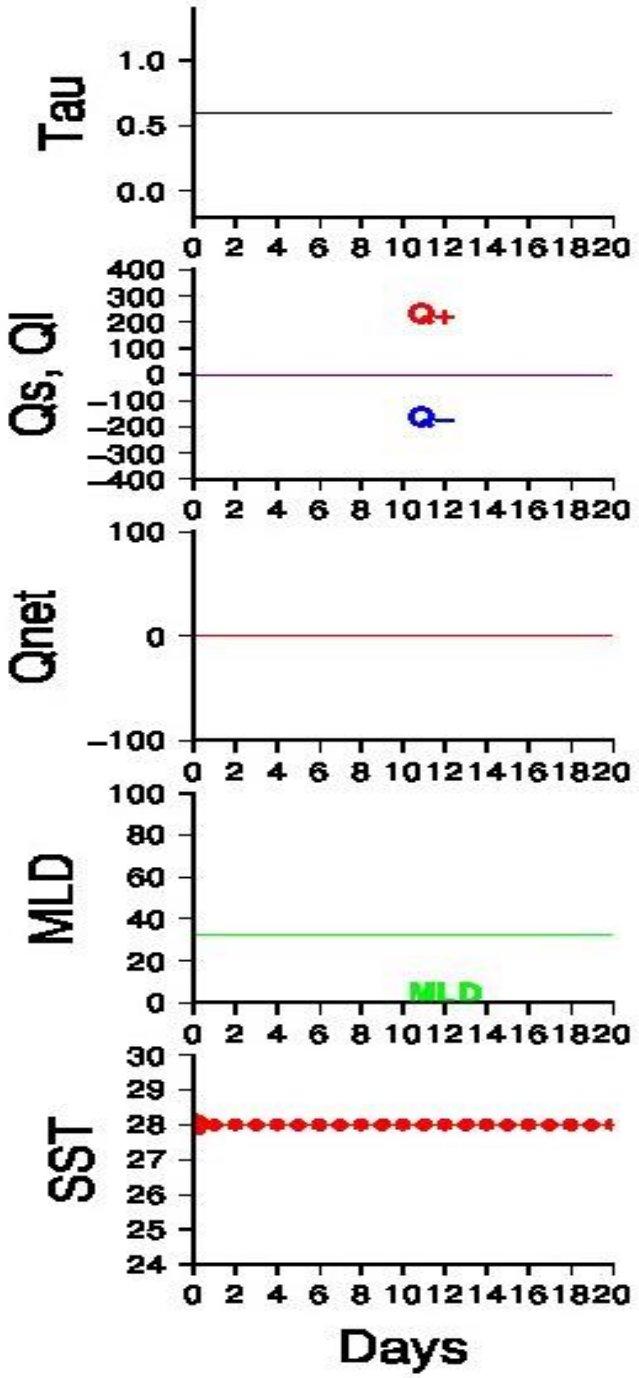

Figure 7.3 Model output with higher wind stress

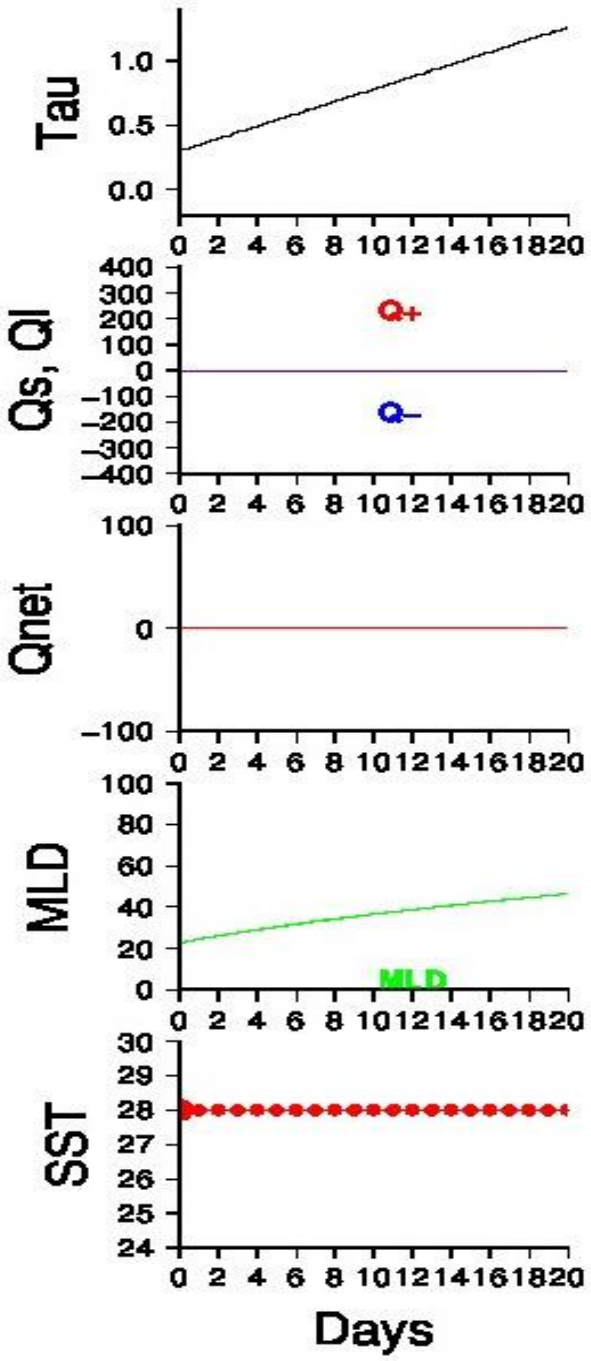

Figure 7.4 Model output with linearly increasing wind stress

7.5 Role of Heat fluxes

The objective here was to understand the response of ocean to varying heat flux conditions. Different heat flux forcings scenarios were applied while keeping the wind stress constant.

Constant Heat Fluxes and Zero Net Flux

Figure 7.5 shows the conditions for this model run. In this run, the model was forced with a constant wind stress. Same profiles were used as in the previous runs. A heat gain of about 330 W/m^2 was applied and was taken constant throughout the period and also during day and night. This is a hypothetical condition because in reality there is no solar input during night. An equal amount of heat loss was also applied to have a zero net heat flux between ocean and atmosphere.

The model result showed a small increase in the MLD during the period of model run. The increase was nonlinear suggesting some dependency of MLD on heat fluxes even though net heat flux is zero. SST remained constant as the net heat flux was zero.

Positive Net Heat Flux

The model was initialized as before and forced with a positive net heat flux to see the ocean's response to a positive net heat input (Figure 7.6). As before, the heat fluxes were constant during the diurnal period and also throughout the model run. The heat loss was taken 80% of heat gain so that net heat flux is positive. Model produced an increase in the temperature of the surface layer and hence SST. MLD was found almost steady during this run. There is a good response from the model; with an excess heat input, ocean surface turns warmer.

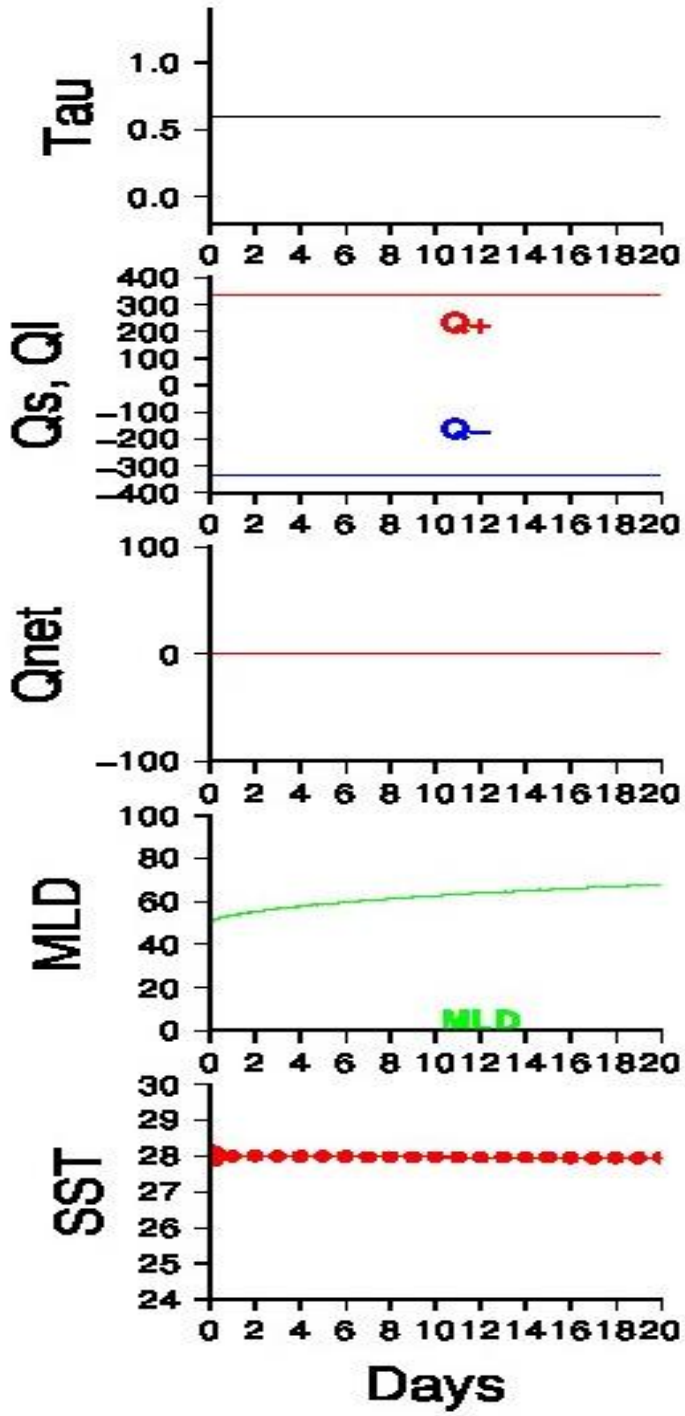

Figure 7.5 Constant heat flux with zero net heat flux

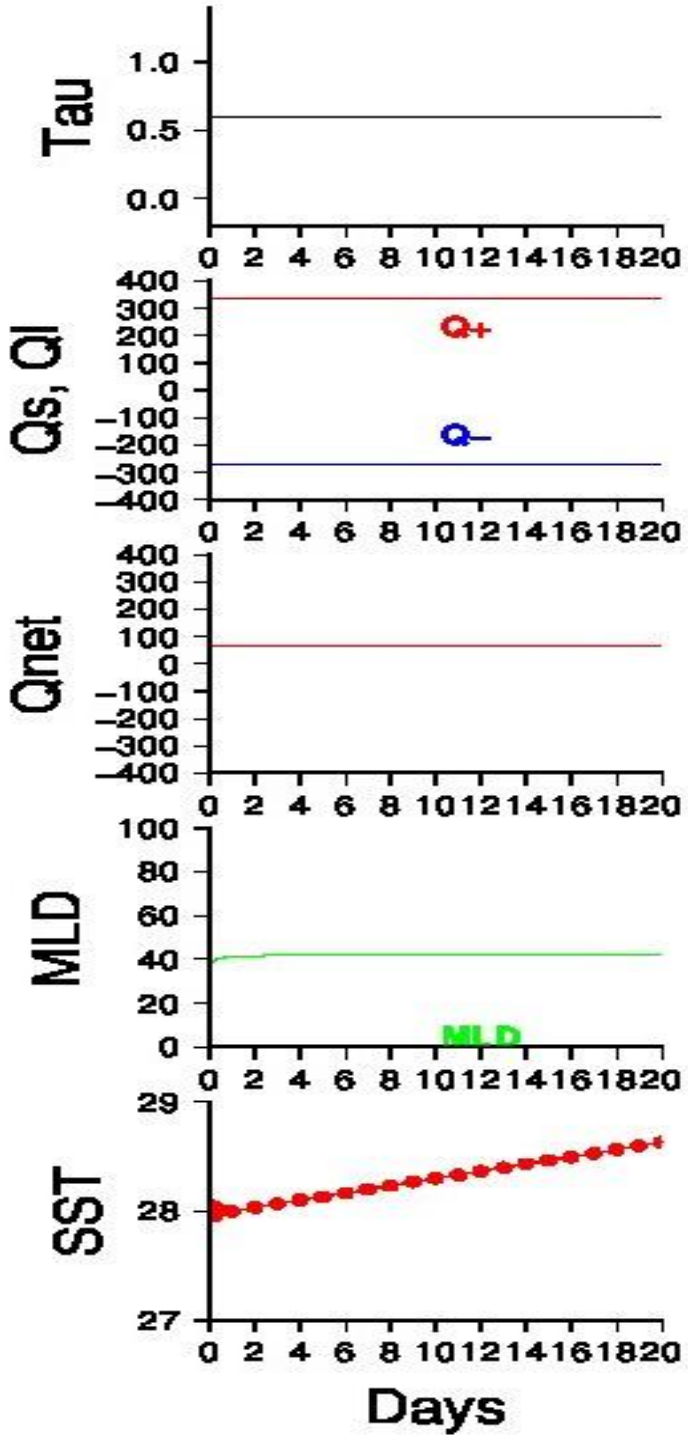

Figure 7.6 Constant heat fluxes with positive net heat flux

Negative Net Heat Flux

In this run, heat fluxes were adjusted to have a negative net heat flux (Figure 7.7). Heat loss was taken higher than the heat gain so that net heat is negative. The diurnal variation in the heat flux was again not taken into account and was rather made independent of day and night.

The model showed a different result in this case. MLD was found increasing with time though the wind stress remained constant. The deepening of MLD should be due to the negative buoyancy created with the net heat loss at the surface. Due to heat loss, convective processes develop that can increase MLD through convective mixing.

To understand the role of entrainment at the bottom of the mixed layer, the model was run with and without entrainment (Figure 7.8). Without entrainment, the part of the temperature profile at the bottom of mixed layer showed an unrealistic behavior. For example, the layer below mixed layer was totally unaffected by the changes occurring in the mixed layer. In other words, the surface mixed layer is isolated from the layer below. This shows that entrainment is necessary to keep the profile more realistic.

Diurnal Heat Flux with Zero Net Flux

The model was run with more realistic heat flux forcing having diurnal variability (Figure 7.9). Shortwave radiation was assigned zero values during night and allowed to vary during the day time. Heat gain was highest around noon time. An equal but negative flux was assigned for the heat loss so that net heat flux is zero at each time of the day.

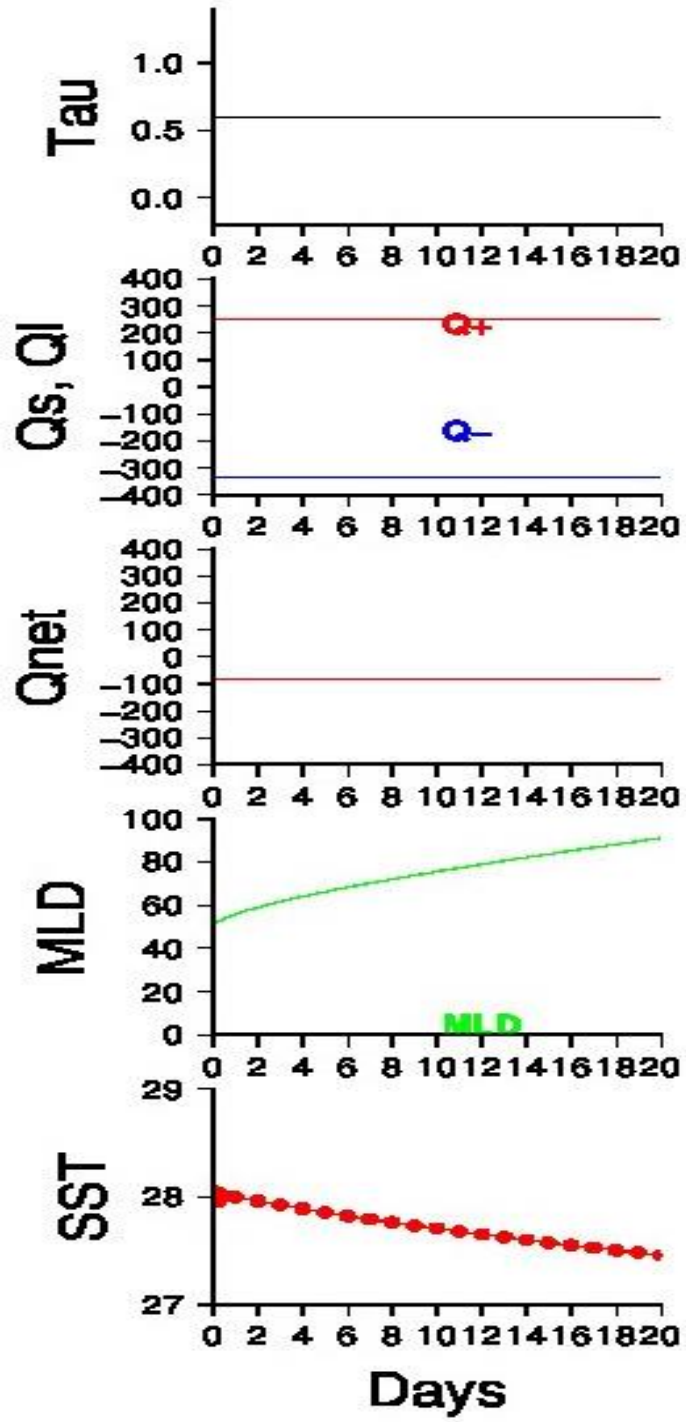

Figure 7.7 Constant heat flux with negative net heat flux

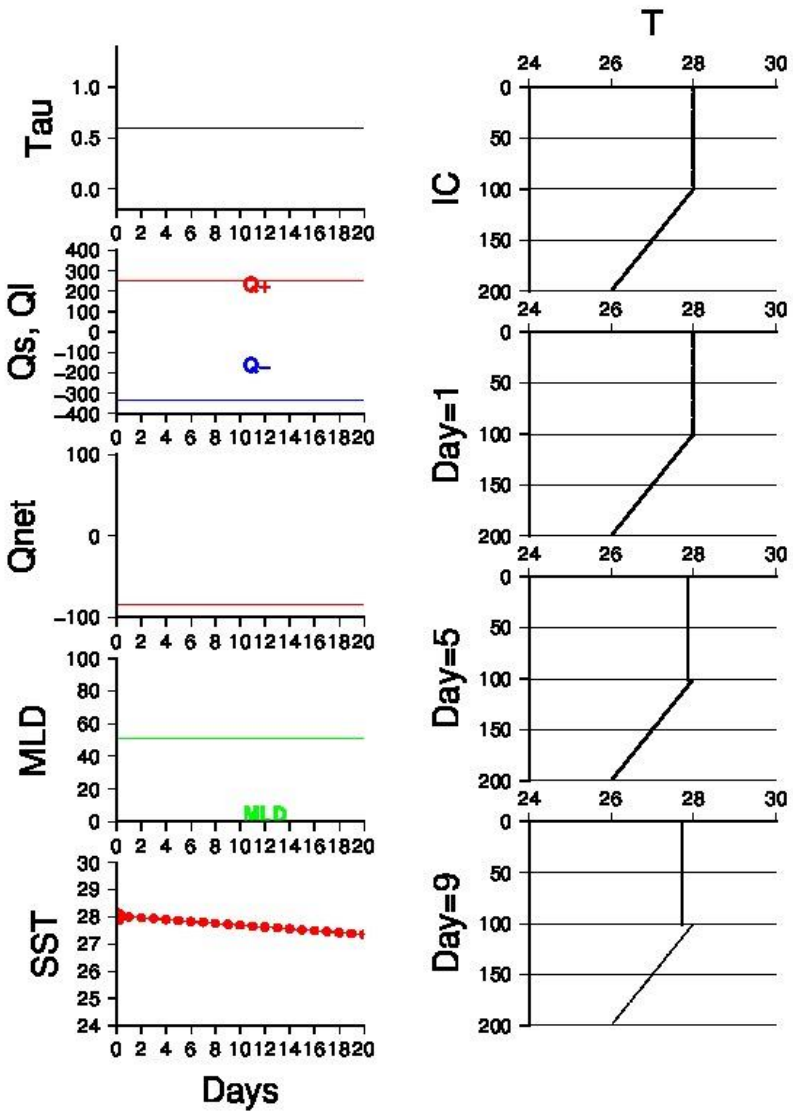

Figure 7.8 Model run without mixed layer entrainment

The response of the ocean to this hypothetical forcing was interesting. A diurnal variability of the mixed layer was found during the period of model run. Since wind stress was constant, the response of the mixed layer should be due to the diurnally varying heat fluxes alone. The amplitude of oscillation was found to increase with time.

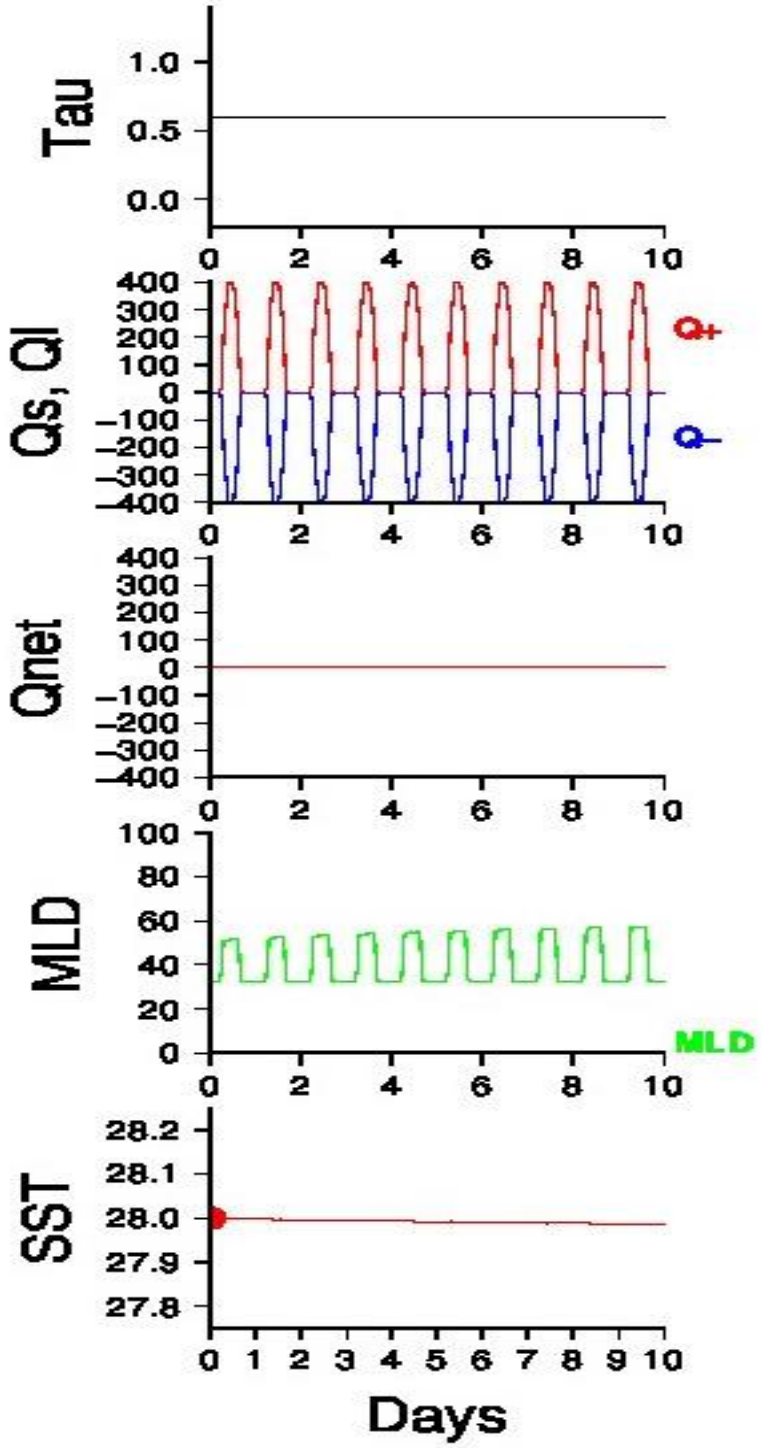

Figure 7.9 Diurnal heat fluxes with zero net heat flux

Diurnal Heat Flux with Positive Net Flux

In this case, a net positive heat flux was introduced in the diurnal heat flux forcing (Figure 7.10). Heat gain was taken higher than the heat loss so that ocean gains heat during each time of the day time. Heat loss was taken 0.6 times that of the heat gain. At night, however, both heat gain and loss terms were set zero. This is also different from the real situation that oceans do have a heat loss during night time mainly from the long wave radiation.

Model MLD output showed a different behavior in this case. It had smaller values (~20m) as compared to the previous case where net heat flux was zero. The diurnal variation of the MLD was also greatly damped. With the positive heat input, the upper layer of the ocean responded with an unusual increase in the temperature. The temperature up to a depth of about 70m only was responded to this heating. This is also evident in the SST which showed a continuous increase.

Diurnal Heat Flux with Negative Net Flux

Here, the heat loss was higher than heat gain so that net heat is negative (Figure 7.11). Heat loss was taken 1.4 times that of heat gain. The diurnal cycle of heat flux was retained. Model result showed an MLD that had diurnal oscillations.

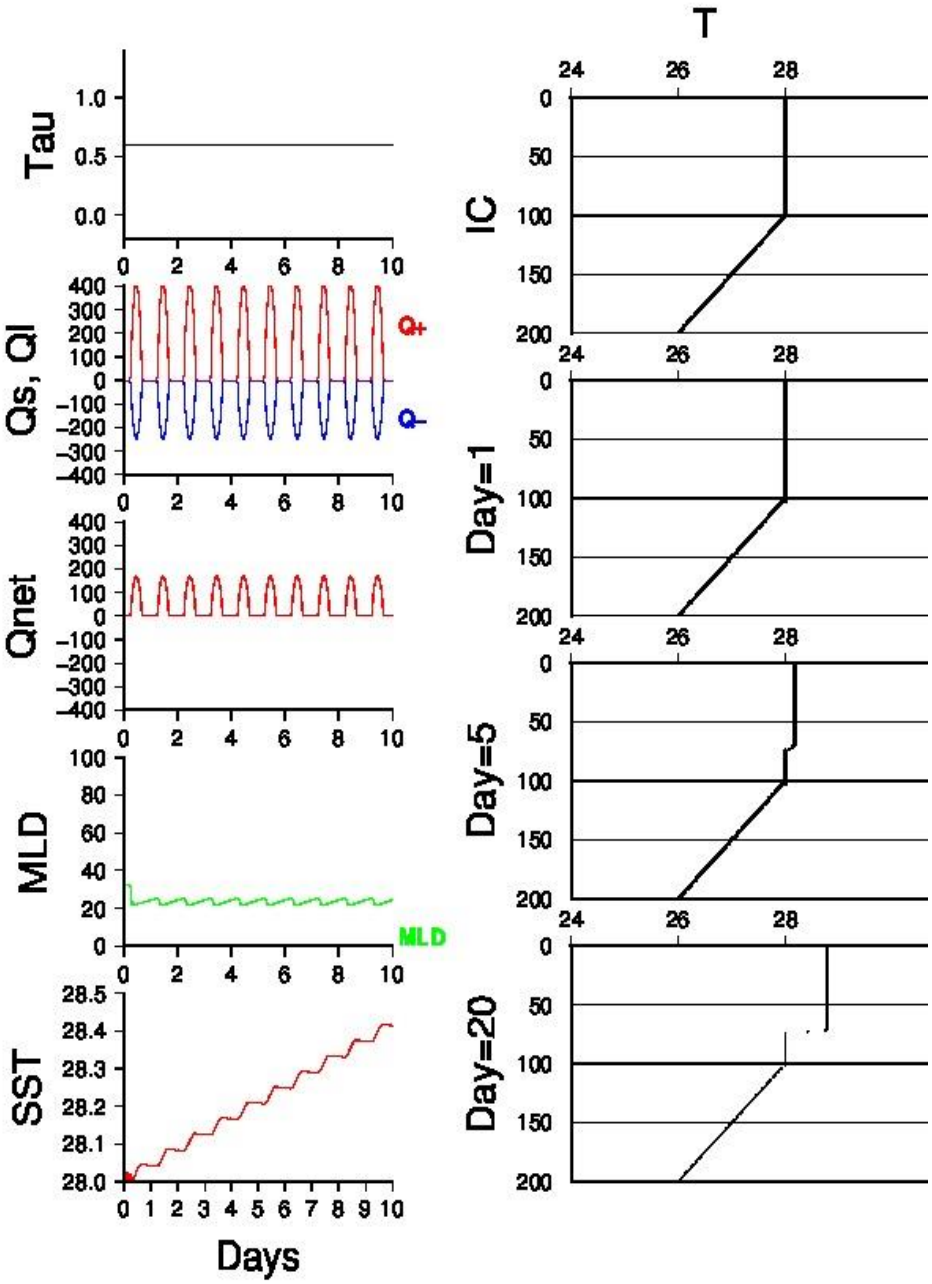

Figure 7.10 Diurnal heat fluxes with positive net heat flux
Right panel shows the evolution of temperature profile

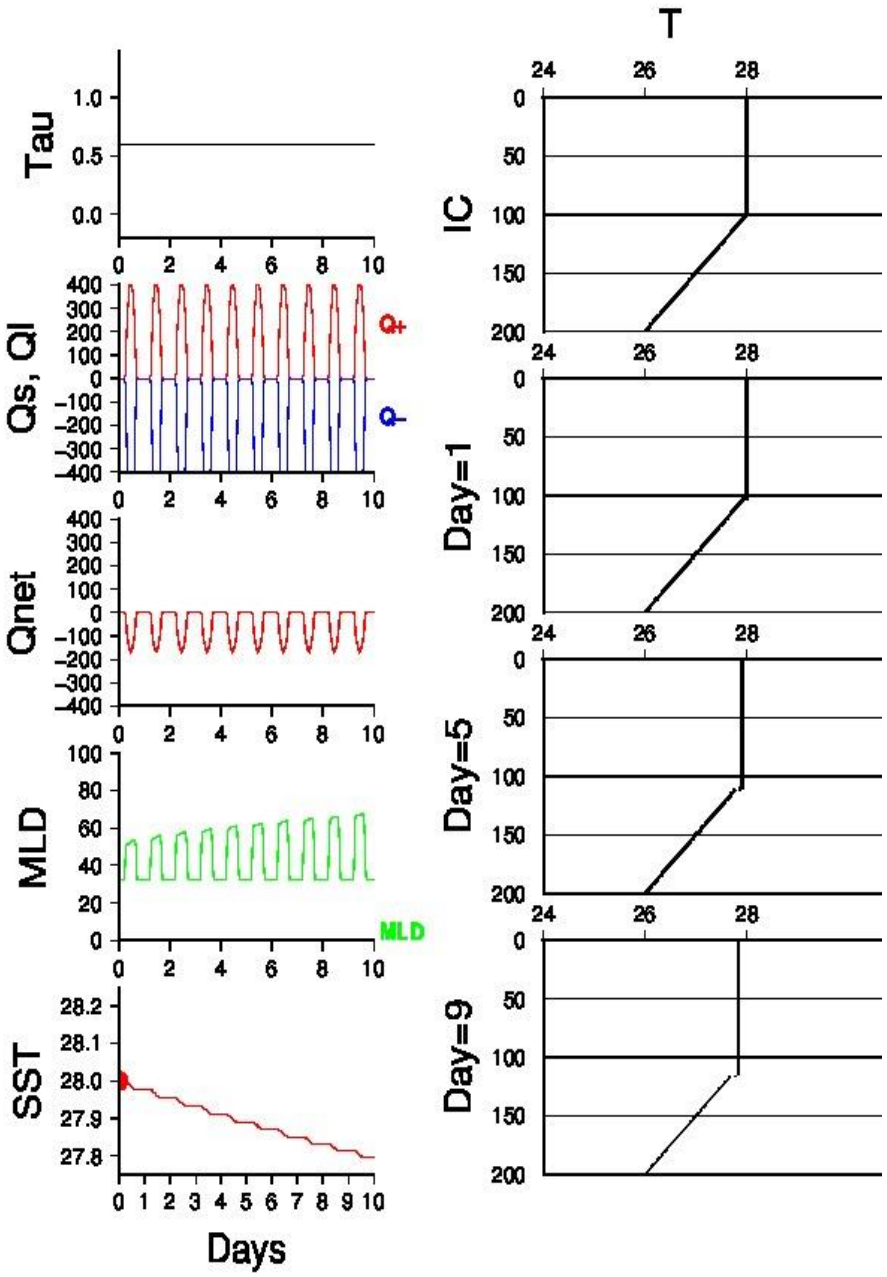

Figure 7.11 Diurnal heat fluxes with negative net heat flux.
Right panel shows the evolution of temperature profile

7.6. Simulation

Here the model was run with realistic ocean and atmospheric data to simulate SST. The model was applied to the geographic location of 8^{O}S, 67^{O}E. The model was initialized with temperature profile of 16-08-2008. The temperature data was obtained from RAMA (Research Moored Array for African-Asian-Australian Monsoon Analysis and Prediction) buoys. RAMA buoys are the buoy systems in Indian Ocean as part of the Global Tropical Moored Buoy Array. The temperature profile was interpolated linearly at each one meter depth. It was found that the interpolation by cubic spline method was not suitable as it introduced subsurface temperature inversion that appeared unrealistic. A constant salinity profile was used as in the previous test runs. This was because of two reasons. One is that RAMA data had salinity readings only up to 100m which was not sufficient for model run. Another reason is that the RAMA salinity data up to 100m was found nearly constant with depth.

The forcing data was obtained from OAFlux project (*Yu and Weller*, 2007). The daily averaged OAFlux data on Wind and heat fluxes (shortwave radiation, longwave radiation, latent heat and sensible heat) were downloaded from the Asia-Pacific Data Research Center (APDRC) website. The total heat loss was computed as the sum of longwave radiation, latent heat and sensible heat fluxes. It is to note that the model had to be forced with hourly wind and heat fluxes. Since hourly data was not available, the daily mean was used after interpolating at hourly intervals. This forcing does not contain a diurnal variability and may not truly represent the real ocean. The wind stress forcing was made using daily wind speed data of OAFlux downloaded from APDRC website. Wind stress was computed using the bulk formula for wind stress and was also interpolated at hourly interval. The

model was forced for 15 days.

The result of the model run is shown in Figure 7.12. The initial temperature profile was similar to that of the typical profile used in the test runs. The discontinuity below the isothermal layer is a result of linear interpolation. Wind stress had showed a variation of about 0.2 to 0.3 dynes/cm^2. Shortwave radiation had a variation from 200 to 300 W/m^2. Total heat loss also had a similar magnitude. The net heat flux varied between ± 100 W/m^2.

MLD estimated by the model had a lower magnitude (~20m) and was almost steady during the period. However, there was an increase in the isothermal layer with time. The model was validated with daily SST obtained from OAFlux. The SST output from the model (red color) was compared with the daily mean SST obtained during the same period from OAFlux (blue color). From the comparison it was found that the model performance was satisfactory, though not excellent. The absence of a close match could be due to several reasons especially from the one-dimensional restriction that ignores the three dimensional processes that contribute to SST variability and also from the lack of hourly forcing data.

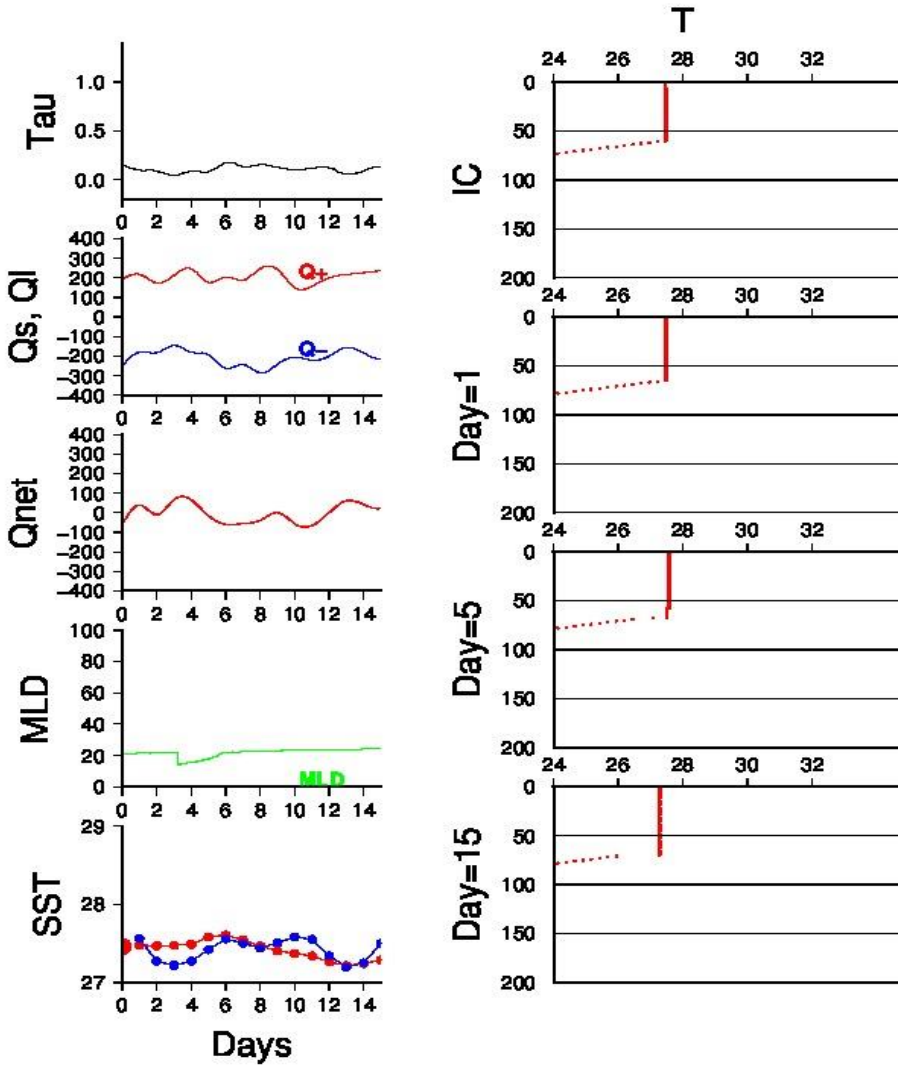

Figure 7.12 Simulation of SST and temperature profile. Model SST is shown in red color and observed SST is in blue color

7.7 Conclusions

A one-dimensional numerical ocean model [*Garwood et al.*, 1977] was used to study the mechanism for the evolution of SST. The model employs a second order turbulence scheme and is forced with hourly wind stress and heat fluxes. Hence, the model can be used to simulate the diurnal cycle of mixed layer and SST.

The model was forced with test forcings as controlled experiments to

understand the role of each forcing on MLD variability. Running time of the model was up to 20 days. Role of wind stress was studied by keeping the heat fluxes constant (zero net heat flux in this case) and applying different wind stresses. Three cases of wind stresses were considered. In the first case, wind stress was constant for the entire period of model run. In the second run, a higher constant wind stress was used. Then an increasing wind stress was used. The result showed a positive response of MLD to wind stress. As the wind stress increased, a corresponding MLD was obtained. Since the net heat flux was zero, there was no change in the mixed layer temperature and hence SST.

In the second test case, role of heat fluxes were studied. Here, a constant wind stress was used and allowed the model to respond to varying heat fluxes. Two cases of heat flux conditions were used such as constant heat flux throughout the period and a diurnally varying heat fluxes. In each case, sub cases of zero, positive and negative net heat fluxes were considered. In the constant heat flux cases, SST responded well with the net heat fluxes. As the net heat flux was set to zero, SST remained unchanged. With positive (negative) net heat fluxes, SST showed a continuous increase (decrease) with time. In the diurnal forcing cases, SST behaved in the similar fashion responding positively to heat fluxes. The MLD also had a diurnal response to heat fluxes. As the net heat flux was positive, MLD did not show much variation whereas when net heat flux was negative, MLD had large (> 20m) variation in a day. This could be due to the convective mixing at night caused by the net heat loss which the model correctly simulated.

In the real case, the model was run with daily mean forcing data as hourly data was unavailable. Obviously, the model was not expected to simulate the exact magnitudes of MLD and SST, but was intended to follow only the trend. The model output of SST was compared with observation. It

was found that the model SST pattern had a closer resemblance with that of observation, even though the forcing was not fully realistic. Hourly forcing is expected to give a better response from the model.

Chapter 8

Summary and Conclusions

Ocean temperature change is a major concern for the climate system. The impact of the current global warming is reflected in atmosphere, ocean and over land. Oceanic warming is now identified in all the oceans both at surface and subsurface. The warmest waters of the ocean have further consequences on the weather through anomalies in atmospheric convection, cyclones and monsoons. Hence, such warm oceanic areas were studied with special interest and are often called as 'warm pools'. The thesis targets the variabilities in the SST and warm pool of the Indian Ocean (IOWP) for the past several decades.

A climatological variability of the warm pool was obtained to understand the seasonal and annual variabilities of warm pool. It was found that warm pools attain maximum intensity during the spring season rather than at the peak summer season. The cause of this was found to be due to strong advection in the ocean and also due to a reduction in solar radiation by increase in clouds. A variation in the geographical position of the warm pool also was identified. Wind tends to converge at core of the warm pool. Hence, a seasonal oscillation in the wind does occur as the warm pool undergoes seasonal variabilities in its orientation. Warm pools are zones of strong air-sea interaction. Strong vertical movements in the air associated with deep atmospheric convection control the weather system. Low outgoing long wave radiation was found over IOWP that indicates strong convection. Annual heat budget estimate was done for the Indian Ocean to understand the role of heat fluxes on SST on annual scale. The correlation between them was found weak over many areas.

The seasonality is a strong cycle of variability in the ocean and atmosphere. Though it repeats each year, there can be small variations in their magnitude from year to year, called as inter-annual variation. Even though small in magnitude, they can have significant changes to the

seasonality of that year. The inter-annual variability of IOWP and SST in general was studied. A major shift in the seasonality in Indian Ocean is associated with ENSO. ENSO is an inter-annual changes occurring in the SST of tropical Pacific Ocean. Though geographically constrained, all the oceans are connected to each other through atmospheric processes. Hence, anomalous signals in one ocean can affect other oceans. It was found that inter-annual variabilities in Indian Ocean are mostly associated with ENSO in the Pacific. In this context, the changes to Indian Ocean SST and warm pool were studied on inter-annual scale.

The spectral analysis showed the major variabilities in the SST data at annual and semi-annual time scales. Weak signals of inter-annual variability were also observed at ENSO time scale. This has confirmed the role of ENSO on Indian Ocean SST as both had variabilities at nearly the same period. The magnitude of inter-annual anomalies in SST was comparable to that of seasonal. Weaker inter-annual changes occurred at the equatorial areas. The Indian Ocean SST as a whole responded positively to developments in the Pacific. A lag of 3-4 months between them is interesting and needs more research to identify the mechanism that links both the oceans. Excess warming was observed in Indian Ocean associated with each El Nino. Initial signals of warming were found at the western Indian Ocean which spreads to other areas as an El Nino intensifies. There had been different opinions about the cause of anomalous warming in Indian Ocean during El Nino periods. A heat budget analysis was performed to see the role of heat fluxes on the anomalous warming. However, a positive relationship between them was lacking. Role of oceans through mixing and planetary waves were found to be as major factors for the inter-annual variations in SST.

The long term trend of warming was studied using data over 100 years. Warming trend until 1950s was not significant but enhanced since 1960s.

Study showed that IOWP was expanded considerably during the past 50 years. A substantial increase (67%) in warm pool area was observed during the period 1960 to 2010. Rate of warming was, however, found to be varying among the data sets. The spatial bias in the warming trend was estimated. The analysis showed a higher warming rate at the equatorial Indian Ocean. This result is in agreement with earlier reports [*Suryachandra et al*., 2012]. Again, variations in magnitude were found among the data sets. The trends in heat fluxes and wind speed were estimated to find their role in the long term warming trend in the ocean. The result showed very interesting and contradicting evidence on the present concept of global warming. Due to excess carbon dioxide in the atmosphere, a decrease in the net heat loss from long wave back radiation was expected. However, the trend in long wave radiation was against this concept. A higher heat loss was found in both long wave back radiation and latent heat flux, both contributed to an increasing heat loss from the ocean. Hence, the role of heat fluxes on the long term trend of SST is absent and was in fact found opposing.

The role of heat fluxes was quantified using the temperature tendency equation. The equation was simplified by neglecting advective and diffusive effects. This is reasonable for variations over shorter time periods. The changes in SST were considered only due to net heat fluxes and ocean mixing. With constant mixed layer depth, the SST was reproduced well but failed when realistic MLD was used. This may point to the importance of the terms neglected or to a better formulation of the relationship.

A modeling study was attempted to understand the ocean's responds to short-term forcings. A one-dimensional mixed layer model of the ocean with hourly forcing of wind stress and heat fluxes was used to simulate the response of ocean to individual and combined forcings. The model was forced with a variety of combinations of forcings. Model Ocean's response to varying

wind stress was satisfactory. Higher mixing occurred with increased wind stress. Forcing from heat flux was found to influence the SST to some extent. As the net heat flux was zero, SST remained unchanged. With positive (negative) net heat fluxes, SST showed a continuous increase (decrease) with time. This response of the model was encouraging and helps in explaining the warming trend in the Indian Ocean. Diurnal oscillation in mixed layer is also interesting and needs further study. Due to the non-availability of realistic forcing data at hourly basis, the model was simulated with daily mean wind stress and heat fluxes. Though the result from this model run is not fully convincing, it inspires for a deeper study in the future.

References

Ajayamohan R. S. and A. S. Rao (2008) Indian Ocean dipole modulates the number of extreme rainfall events over India in a warming environment. *J. of the Meteorological Society of Japan*. Ser. II, 86(1), 245-252.

Alexander M. A., I. Bladé, M. Newman, J. R. Lanzante, N. C. Lau and J. D. Scott (2002) The atmospheric bridge: The influence of ENSO teleconnections on air-sea interaction over the global oceans. *J. of Climate*, *15*(16), 2205-2231.

Allan R., J. Lindesay and D. E. Parker (1996) El Nino Southern Oscillation and Climatic Variability , 416 pp., CSIRO, Collingwood, Victoria, Australia.

Alory G. and G. Meyers (2009) Warming of the upper Equatorial Indian Ocean and changes in the heat budget (1960-99). *J. of Climate*, *22*(1), 93-113.

Alory G., S. Wijffels and G. Meyers (2007) Observed temperature trends in the Indian Ocean over 1960–1999 and associated mechanisms. *Geophysical Research Letters*, 34(2). doi:10.1029/2006GL028044.

Annamalai H., S. P. Xie, J. P. McCreary and R. Murtugudde (2005) Impact of Indian Ocean sea surface temperature on developing El Nino. *J. of Climate*, 18, 302–319.

Ardanuy P., P. Cuddapah and H. L. Kyle (1987) Remote sensing of water vapor convergence, deep convection and precipitation over the tropical Pacific Ocean during 1982-83 El Nino. *J. of Geophysical Research*, 92, 14204-14216.

Barnett T. P., J. C. Adam and D. P. Lettenmaier (2005) Potential impacts of a warming climate on water availability in snow-dominated regions. *Nature*, *438*(7066), 303-309.

Boyer T. P., S. Levitus, J. I. Antonov, R. A. Locarnini and H. E. Garcia (2005) Linear trends in salinity for the World Ocean, 1955–1998. *Geophysical Research Letters*, 32:L01604. doi:10.1029/2004GL021791.

Brunke M. A., X. Zeng, V. Misra and A. Beljaars (2008) Integration of a prognostic skin sea surface temperature scheme into climate and weather models. *J. of Geophysical Research*, **113**, D21117, doi:10.1029/2008JD010607.

Cadet D. L. (1985) The southern oscillation over the Indian Ocean. *J. of Climatology*, *5*(2), 189-212.

Cadet D. L. and B. C. Diehl (1984) Interannual variability of surface fields over the Indian Ocean during recent decades. *Monthly Weather Review*, *112*(10), 1921-1935.

Cai W., M. Lengaigne, S. Borlace, M. Collins, T. Cowan, M. J. McPhaden, A. Timmermann, S. Power, J. Brown, C. Menkes, A. Ngari, E. M. Vincent and M. J. Widlansky (2012) More extreme swings of the South Pacific convergence zone due to greenhouse warming. *Nature*, *488*(7411), 365-369.

Cai W., S. Borlace, M. Lengaigne, P. Van Rensch, M. Collins, G. Vecchi, A. Timmermann, A. Santoso, M. J. McPhaden, L. Wu, M. H. England, G. Wang, E. Guilyardi and F. F. Jin (2014) Increasing frequency of extreme El Niño events due to greenhouse warming. *Nature Climate Change*, *4*(2), 111-116.

Cai W., G. Wang, A. Santoso, M. J. McPhaden, L. Wu, F. F. Jin, A. Timmermann, M. Collins, G. Vecchi, M. Lengaigne, M. H. England, D. Dommenget, Ken Takahashi and E. Guilyardi (2015) Increased frequency of extreme La Nina events under greenhouse warming. *Nature Climate Change*, *5*(2), 132-137.

Carton J. A., G. A. Chepurin, X. Cao and B. Giese (2000) A Simple Ocean Data Assimilation retrospective analysis of the global ocean 1950-1995. Part I: Methodology. *J. of Physical Oceanography*, 30, 294-309.

Carton J. A., B. S. Giese and S. A. Grodsky (2005) Sea level rise and the warming of the oceans in the SODA ocean reanalysis. *J. of Geophysical Research*, 110, doi 10.1029/2004JC002817.

Carton J. A. and B. S. Giese (2008) A reanalysis of ocean climate using Simple Ocean Data Assimilation (SODA). *Monthly Weather Review*, 136(8): 2999–3017. doi:10.1175/2007MWR1978.1.

Carton J. A., S. A. Grodsky and H. Liu (2008) Variability of the oceanic mixed layer, 1960-2004. *J. of Climate*, *21*(5), 1029-1047.

Chacko K. V., P. V. Hareesh Kumar, M. R. Ramesh Kumar, B. Mathew and V. M. Bannur (2012) A note on Arabian sea warm pool and its possible relation with monsoon onset over Kerala. *International Journal of Scientific and Research Publications*, 2, 1-4.

Chen G., C. Fang, C. Zhang and Y. Chen (2004) Observing the coupling effect between warm pool and "rain pool" in the Pacific Ocean. *Remote Sens. Env.*., 91, 153–159. doi:10.1016/j.rse.2004.02.010.

Clement A. C., R. Seager and R. Murtugudde (2005) Why Are There Tropical Warm Pools? *J. of Climate*, 18, 5294-5311.

da Silva A. M., C. C. Young and S. Levitus (1994) Anomalies of Directly Observed Quantities. Vol. 2, Atlas of Surface Marine Data 1994, NOAA Atlas NESDIS 7, pp 416.

de Boyer M. C., J. Mignot, A. Lazar and S. Cravatte (2007) Control of salinity on the mixed layer depth in the world ocean: 1. General description. *J. of Geophysical Research, Oceans (1978–2012)*, *112*(C6).

Del Genio A. D. and W. Kovari (2002) Climatic properties of tropical precipitating convection under varying environmental conditions. *J. of Climate*, 15(18), 2597-2615.

Delcroix T. (1998) Observed surface oceanic and atmospheric variability in the tropical Pacific at seasonal and ENSO timescales: a tentative overview. *J. of Geophysical Research: Oceans* 103(9), 18611-18633.doi:10.1029/ 98JC00814

Delcroix T., B. Dewitte, Y. du Penhoat, F. Masia and J. Picau (2000) Equatorial waves and warm pool displacements during the 1992-1998 El Nino Southern Oscillation events: Observation and modeling. *J. of Geophysical Research: Oceans*, 105, 26045 – 26062.

Du Y., T. Qu, G. Meyers, Y. Masumoto and H. Sasaki (2005) Seasonal heat budget in the mixed layer of the southeastern tropical Indian Ocean in a high-resolution ocean general circulation model. *J. of Geophysical Research: Oceans, (1978–2012)*, *110*(C4).

Du Y., S. -P Xie, G. Huang and K. Hu (2009) Role of Air-Sea Interaction in the Long Persistence of El Nino–Induced North Indian Ocean Warming. *J. of Climate*, 22, 2023-2038.

Emanuel K., R. Sundararajan and J. William (2008) Tropical cyclones and global warming: Results from downscaling IPCC AR4 simulations. *Bull. Am. Meterol. Soc*., 89, 347–367.

Esbensen S. K. and V. Kushnir (1981) The heat budget of the global oceans: An atlas based on estimates from marine surface observations. *Oregon State University Climate Research Institute Rep*. 29, pp 27.

Fairall C. W., E. F. Bradley, D. P. Rogers, J. B. Edson and G. S. Young (1996a) Bulk parameterization of air–sea fluxes for Tropical Ocean-Global Atmosphere Coupled–Ocean Atmosphere Response Experiment. *J. of Geophysical Research*, 101, (C2) 3747–3764.

Fairall C. W., E. F. Bradley, J. S. Godfrey, G. A. Wick and J. B. Edson (1996b) Cool-skin and warm-layer effects on sea surface temperature. *J. of Geophysical Research*, **101**, 1295-1308.

Fasham M. J. R. (1995) Variations in the seasonal cycle of biological production in subarctic oceans: A model sensitivity analysis. *Deep Sea Research Part I: Oceanographic Research Papers*, *42*(7), 1111-1149.

Fasullo J. and P. J. Webster (1999) Warm Pool SST Variability in Relation to the Surface Energy Balance. *J. of Climate*, 12, 5, 1292–1305.

Fu R., A. D. Del Genio, W. B. Rossow and W. T. Liu (1992) Cirrus-cloud thermostat for tropical sea surface temperatures tested using satellite data. *Nature*, 358, 394-397.

Gadgil S., N. V. Joshi and P. V. Joseph (1984) Ocean-atmosphere coupling over monsoon regimes. *Nature*, 312, 141-143.

Garwood R. W., Jr. (1977) An oceanic mixed layer model capable of simulating cyclic states. *J. of Physical Oceanography*, 7, 455-468.

Gill A. E. and E. M. Rasmusson (1983) The 1982-83 climatic anomaly in the equatorial Pacific. *Nature*, 306, 229-234.

Gille S. T. (2002) Warming of the Southern Ocean since the 1950s. *Science*, *295*(5558), 1275-1277.

Godfrey J. S. and E. Lindstrom (1989) On the heat budget of the equatorial West Pacific surface mixed layer. *J. of Geophysical Research*, 94, 8007-8017.

Gopalakrishna V. V., Y. Sadhuram, V. Ramesh Babu and M. V. Rao (1988) Variability of wind stress and currents at selected locations over the north Indian Ocean during 1977 and 1979 summer monsoon seasons. *Mausam*, *39*, 159-166.

Gopinathan C. K. and J. S. Sastry (1990) Relationship between Indian summer monsoon rainfall and position of Pacific Ocean warm pool. *Indian J. of Marine Sciences*, 19, 246-250.

Graham N. E. and T. P. Barnet (1987) Sea surface temperature, surface wind divergence and convection over tropical oceans. *Science*, 238, 657-659.

Hartmann D. L., M. E. Ockert-Bell, and M. L. Michelsen (1992) The effect of cloud type on Earth's energy balance: Global analysis. *J. of Climate*, 5(11), 1281-1304.

Hartmann D. L. and M. L. Michelsen (1993) Large-Scale Effects on the Regulation of Tropical Sea Surface Temperature. *J. of Climate*, 6, 2049-2062.

Hastenrath S. and P. J. Lamb (1979) The Oceanic Heat Budget. Part 2, Climatic Atlas of the Indian Ocean, University of Wisconsin Press, pp 110.

Hastenrath S., A. Nicklis and L. Greischar (1993) Atmospheric-hydrospheric mechanisms of climate anomalies in the western equatorial Indian Ocean. *J. of Geophysical Research: Oceans (1978–2012)*, *98*(C11), 20219-20235.

Hendon H. H. (2003) Indonesian rainfall variability: Impacts of ENSO and local air-sea interaction. *J. of Climate*,*16*(11), 1775-1790.

Ho Chung-Ru, X. -H. Yan and Q. Zheng (1995) Satellite-observations of upper layer variabilities in the Western Pacific Warm Pool. *Bull. Am. Meteorol. Soc*., 76(5), 669-679.

Hsiung J. (1985) Estimates of global oceanic meridional heat transport. *J. of Physical Oceanography*, 15, 1405–1413.

Huang B. and J. L. Kinter (2002) Interannual variability in the tropical Indian Ocean. *J. of Geophysical Research: Oceans (1978–2012)*,*107*(C11), 20-1.

Huang B. and V. M. Mehta (2004) Response of the Indo-Pacific warm pool to interannual variations in net atmospheric freshwater. *J. of Geophysical Research*, 109, C06022, doi: 10.1029/2003JC002114.

Huang R. X. and S. Russell (1994) Ventilation of the subtropical North Pacific. *J. of Physical Oceanography*. 24, 2589-2605.

Huang W. G and L. S. Robinson (1995) Size estimates of the factors controlling sea surface temperature with AVHRR data. *Int. J. of Remote Sensing*, 16, 597-612.

IPCC **(**2014) *Climate Change 2014: Impacts, Adaptation, and Vulnerability. Part A: Global and Sectoral Aspects. Contribution of Working Group II to the Fifth Assessment Report of the Intergovernmental Panel on Climate Change* [Field, C.B., V.R. Barros, D.J. Dokken, K.J. Mach, M.D. Mastrandrea, T.E. Bilir, M. Chatterjee, K.L. Ebi, Y.O. Estrada, R.C. Genova, B. Girma, E.S. Kissel, A.N. Levy, S. MacCracken, P.R. Mastrandrea, and L.L. White (eds.)]. Cambridge University Press, Cambridge, United Kingdom and New York, NY, USA, pp1132.

Josey S. A., E. C. Kent and P. K. Taylor (1999) New insights into the ocean heat budget closure problem from analysis of the SOC air-sea flux climatology. *J. of Climate*, *12*(9), 2856-2880.

Kara A. B., P. A. Rochford and H. E. Hurlburt (2003) Mixed layer depth variability over the global ocean. *J. of Geophysical Research: Oceans (1978–2012)*, *108*(C3).

Karnauskas K. B. and A. J. Busalacchi (2009) The role of SST in the east Pacific warm pool in the interannual variability of Central American rainfall. *J. of Climate*, *22*(10), 2605-2623.

Keerthi M. G., M. Lengaigne, J. Vialard, C. de Boyer Montégut and P. M. Muraleedharan (2012) Interannual variability of the Tropical Indian Ocean mixed layer depth. *Climate Dynamics*, *40*(3-4), 743-759.

Kelly K. A. and B. Qiu (1995) Heat flux estimates for the western North Atlantic, I, Assimilation of satellite data into a mixed layer model. *J. of Physical Oceanography*, 25, 2344-2360.

Kiladis G. N. and H. F. Diaz (1989) Global climatic anomalies associated with extremes in the Southern Oscillation. *J. of Climate*, *2*(9), 1069-1090.

Kim T. K., J. -Y. Yu and M. -M. Lu (2012) The distinct behaviours of Pacific and Indian Ocean warm pool properties on seasonal and interannual time scales., *J. of Geophysical Research*, 117, D05128 doi:10.1029/2011JD016557

Klein S. A., B. J. Soden and N. -C. Lau (1999) Remote sea surface temperature variations during ENSO: Evidence for a tropical atmospheric bridge. *J. of Climate*, 12, 917–932.

Kraus E. B. and J. S. Turner (1967) A one-dimensional model of the seasonal thermocline II. The general theory and its consequences. *Tellus A*, *19*(1).

Krishnamurthy V. and B. P. Kirtman (2003) Variability of the Indian Ocean: Relation to monsoon and ENSO. *Quarterly Journal of the Royal Meteorological Society*, *129*(590), 1623-1646.

Krishnamurti T. N., P. Ardanuy, Y. Ramanathan and R. Pasch (1981) On the Onset Vortex of the Summer Monsoon. *Monthly Weather Review*, 109, 344–363.

Kumar P. K. D., Y. S. Paul, K. R. Muraleedharan, V. S. N. Murty and P. N. Preenu (2015) Comparison of long-term variability of Sea Surface Temperature in the Arabian Sea and Bay of Bengal. *Regional Studies in Marine Science*. Available online 21 May 2015, ISSN 2352-4855.

Kumar S. P., A. Ishida, K. Yoneyama, M. R. Kumar, Y. Kashino and H. Mitsudera (2005) Dynamics and thermodynamics of the Indian Ocean warm pool in a high-resolution global general circulation model. *Deep Sea Research* Part II: Topical Studies in Oceanography, 52(14), 2031-2047.

Lamb P. J. (1984) On the mixed layer climatology of the north and tropical Atlantic, *Tellus*, *Set. A,* 36, 292-305.

Landsea C. W., B. A. Harper, K. Hoarau and J. A. Knaff (2006) Can we detect trends in extreme tropical cyclones? *Science*, 313, 452–454.

Lau N. C. and M. J. Nath (2000) Impact of ENSO on the variability of the Asian-Australian monsoons as simulated in GCM experiments. *J. of Climate*,*13*(24), 4287-4309.

Lau N. C. and M. J. Nath (2003) Atmosphere-ocean variations in the Indo-Pacific sector during ENSO episodes. *J. of Climate*,*16*(1), 3-20.

Levitus S. (1982) Climatological atlas of the world ocean, NOAA Prof. Pap. 13173 pp., U.S. Govt. Print. Off., Washing- ton, D.C.

Levitus S. and T.P. Boyer (1994) World Ocean Atlas 1994, Volume 4: Temperature, number 4.

Levitus S., J. I. Antonov, T. P. Boyer and C. Stephens (2000) Warming of the world ocean. *Science,* 287(5461), 2225–2229.

Levitus S., J. I. Antonov, J. Wang, T. L. Delworth, K. W. Dixon and A. J. Broccoli (2001) Anthropogenic warming of Earth's climate system. *Science*, *292*(5515), 267-270.

Levitus S., J. Antonov and T. Boyer (2005) Warming of the world ocean, 1955-2003. *Geophysical Research Letters*, 32, L02604, doi:10.1029/2004GL0215923.

Lewis M. R., M. Cart, G. Feldman, W. Esaias and C. Mc- Clain (1990) Influence of penetrating solar radiation on the heat budget of the equatorial Pacific Ocean. *Nature*, 347, 543- 544.

Liebmann B. and C. A. Smith (1996) Description of a Complete (Interpolated) Outgoing Longwave Radiation Dataset. *Bull. Am. Meterol. Soc*., 77, 1275-1277.

Lindstrom E., R. Lukas, R. Fine, E. Firing, S. Godfrey, G. Meyers and M. Tsuchiya (1987) The western equatorial Pacific Ocean circulation study. *Nature*, 330, 533-537.

Liu H., C. Wang, S. K. Lee and D. Enfield (2013) Atlantic warm pool variability in the CMIP5 simulations. *J. of Climate*, *26*(15), 5315-5336.

Liu N., W. D. Yu, H. X. Chen, F. Hua and O. H. Zhang (2005) Interannual variation of the Indo-Pacific warm pool and the atmospheric response to the variations. *Advances in Marine Science*, 23(3), 249-255. (in Chinese with English abstract)

Liu W. T., K. B. Katsaros and J. A. Businger (1979) Bulk parameterization of air–sea exchanges of heat and water vapor including the molecular constraints at the interface. *J. of Atmospheric Sciences*, 36, 1722–1735.

Lukas R. and P. Webster (1989) TOGA-COARE: A coupled ocean - atmospheric response experiment for the warm pool regions of the western Pacific. Scientific plan compiled by R Lukas and P Webster.

Lukas R. and E. Lindstrom (1991) The mixed layer of the western equatorial Pacific Ocean. *J. of Geophysical Research*, 96, 3343–3358. doi:10.1029/91JC00062.

Martin P. J. (1985) Simulation of the mixed layer at OWS November and Papa with several models. *J. of Geophysical Research*, 90, 903-916.

Masson S., P. Delecluse, J. P. Boulanger and C. Menkes (2002) A model study of the seasonal variability and formation mechanisms of the barrier layer in the eastern equatorial Indian Ocean. *J. of Geophysical Research: Oceans (1978–2012)*, *107*(C12), SRF-18.

McCreary J. P. and P. K. Kundu (1989) A numerical investigation of sea surface temperature variability in the Arabian Sea. *J. of Geophysical Research: Oceans*, (1978–2012), 94(C11), 16097-16114.

McPhaden M. J. and J. Picaut (1990) Eastern tropical ocean response to changing wind systems: with application to El Nino. *J. of Physical Oceanography*, 6, 632–645.

McPhaden M. J., G. Meyers, K. Ando, Y. Masumoto, V. S. N. Murty, M. Ravichandran, F. Syamsudin, J. Vialard, L. Yu and W. Yu (2009) RAMA: The Research Moored Array for African–Asian–Australian Monsoon Analysis and Prediction. *Bull. Am. Meterol. Soc.*, 90, 459–480.

Meehl G. A. (1987) The annual cycle and interannual variability in the tropical Pacific and Indian Ocean regions. *Monthly Weather Review*, *115*(1), 27-50.

Meinen C. and M. J. McPhaden (2000) Observations of warm water volume changes in the equatorial Pacific and their relationship to El Nino and La Nina. *J. of Climate*, 13, 3551–3559.

Mignot J., C. de Boyer Montégut, A. Lazar and S. Cravatte (2007) Control of salinity on the mixed layer depth in the world ocean: 2. Tropical areas, *J. Geophysical Research*, 112, C10010, doi:10.1029/2006JC003954.

Miller J. R. (1976) The salinity effect in a mixed layer ocean model. *J. of Physical Oceanography*. 6, 29-35.

Monterey G. and S. Levitus (1997) Seasonal Variability of Mixed Layer Depth for the World Ocean, NOAA Atlas NESDIS 1,i, 100 pp., U.S. Govt. Print. Off., Washington, D.C.

Murtugudde R. G., J. P. McCreary and A. J. Busalacchi (2000) Oceanic processes associated with anomalous events in the Indian Ocean with relevance to 1997–1998. *J. Geophysical Research*, 105, 3295–3306.

Narvekar J. and S. P. Kumar (2006) Seasonal variability of the mixed layer in the central Bay of Bengal and associated changes in nutrients and chlorophyll. *Deep Sea Research Part I: Oceanographic Research Papers*, *53*(5), 820-835.

Newell R. E. (1979) Climate and the ocean: Measurements of changes in sea-surface temperature should permit us to forecast certain climatic changes several months ahead. *American Scientist*, 67, 405-416.

Nicholls N. (1984) The Southern Oscillation and Indonesian sea surface temperature. *Monthly Weather Review*, *112*(3), 424-432.

Obata A., J. Ishizaka and M. Endoh (1996) Global verification of critical depth theory for phytoplankton bloom with climatological in situ temperature and satellite ocean color data. *J. of Geophysical Research*, 101, 20657 – 20667.

Oberhuber J. M. (1988) An atlas based on the COADS data set: The budget of heat, buoyancy and turbulent kinetic energy at the surface of the Global Ocean. MPI Rep. 15, pp198.

Picaut J. and T. Delcroix (1995) Equatorial wave sequence associated with warm pool displacements during the 1986–1989 El Nino-La Nina. *J. of Geophysical Research*, 100(C9), 18393–18408. doi:10.1029/95JC01358.

Picaut J., M. Ioualalen, C. Menkes, T. Delcroix and M. J. McPhaden (1996) Mechanism of the zonal displacements of the Pacific warm pool: implications for ENSO. *Science*, 274(5292), 1486–1489. doi:10.1126/ science.274.5292.1486.

Polovina J. J., G. T. Mitchum and G. T. Evans (1995) Decadal and basin-scale variation in mixed layer depth and the impact on biological production in the Central and North Pacific, 1960-88. *Deep Sea Research Part I: Oceanographic Research Papers*, *42*(10), 1701-1716.

Prasad T. G. (2004) A comparison of mixed-layer dynamics between the Arabian Sea and Bay of Bengal: One-dimensional model results. *J. of Geophysical Research: Oceans (1978–2012)*, *109*(C3).

Price J. F., R. A. Weller and R. Pinkel (1986) Diurnal cycling: Observations and models of the upper ocean response diurnal heating, cooling, and wind mixing, *J. of Geophysical Research*., 91, 8411-8427.

Qi Q. H., Q. L. Zhang and Y. J. Hou (2008) Zonal displacement of the western Pacific Warm Pool and its effects on ENSO. *Oceanologia et Limnologia Sinica*, 39(1): 66-73.

Qu T. and G. Meyers (2005) Seasonal variation of barrier layer in the southeastern tropical Indian Ocean. *J. of Geophysical Research: Oceans (1978–2012)*, *110*(C11).

Ramanathan V. and W. Collins (1991) Thermodynamic regulation of ocean warming by cirrus clouds deduced from observations of the 1987 E1 Nino. *Nature*, 351, 27-32.

Rao R. R. and R. Sivakumar (1999) On the possible mechanisms of the evolution of a mini-warm pool during the pre-summer monsoon season and the genesis of onset vortex in the South-Eastern Arabian Sea. *Quarterly Journal of the Royal Meteorological Society*, 125: 787–809. doi: 10.1002/qj.49712555503

Rao R. R. and R. Sivakumar (2003) Seasonal variability of sea surface salinity and salt budget of the mixed layer of the north Indian Ocean. *J. of Geophysical Research: Oceans (1978–2012)*, *108*(C1), 9-1.

Rao R. R., R. L. Molinari and J. F. Festa (1989) Evolution of the climatological near-surface thermal structure of the tropical Indian Ocean: 1. Description of mean monthly mixed layer depth, and sea surface temperature, surface current, and surface meteorological fields. *J. of Geophysical Research: Oceans (1978–2012)*, *94*(C8), 10801-10815.

Rao R. R., V. Jitendra, M. S. GirishKumar, M. Ravichandran and S. S. V. S. Ramakrishna (2015) Interannual variability of the Arabian Sea Warm Pool: observations and governing mechanisms. *Climate Dynamics*, *44*(7-8), 2119-2136.

Rasmusson E. M. and T. H. Carpenter (1982) Variations in tropical sea surface temperature and surface wind fields associated with the Southern Oscillation/El Nino. *Monthly Weather Review*, 110, 354-384.

Rasmusson E. M. and J. M. Wallace (1983) Meteorological Aspects of the E1 Nino/Southern Oscillation. *Science*, 222, 1195-1202.

Rayner N. A., D. E. Parker, E. B. Horton, C. K. Folland, L. V. Alexander, D. P. Rowell, E. C. Kent and A. Kaplan (2003) Global analyses of sea surface temperature, sea ice, and night marine air temperature since the late nineteenth century *J. of Geophysical Research,* 108, D14, 4407 10.1029/2002JD002670.

Reynolds R. W. and T. M. Smith (1995) A high-resolution global sea surface temperature climatology. *J. of Climate*, *8*(6), 1571-1583.

Reynolds R.W., N. A. Rayner, T. M. Smith, D. C. Stokes and W. Wang (2002) An improved in situ and satellite SST analysis for climate. *J. Climate*, 15, 1609-1625.

Reynolds R.W., T. M. Smith, C. Liu, D. B. Chelton, K. S. Casey and M. G. Schlax (2007) Daily High-Resolution-Blended Analyses for Sea Surface Temperature. *J. of Climate*, 20, 5473–5496.

Robert M. K., S. Emanuel, S. Chonabayashi and L. Bakkensen (2012) The impact of climate change on global tropical cyclone damage., *Nature Climate Change,* 2, 205–209.

Roxy M. K., K. Ritika, P. Terray, R. Murtugudde, K. Ashok and B. N. Goswami (2015) Drying of Indian subcontinent by rapid Indian Ocean warming and a weakening land-sea thermal gradient. *Nature communications*, 6, DOI: 10.1038/ncomms8423.

Sadhuram Y., D. P. Rao and B. P. Rao (1999) Mean surface fields of heat budget components over the warm pool in the Bay of Bengal during post-monsoon season. *Advanced Technologies in Meteorology Symposium Proceedings* (TROPMET 1995), 285-289.

Saji N. H., B. N. Goswami, P. N. Vinayachandran and T. Yamagata (1999) A dipole mode in the tropical Indian Ocean. *Nature*, 401(6751), 360-363.

Saji N. H. and T. Yamagata (2003) Possible impacts of Indian Ocean dipole mode events on global climate. *Climate Research*, 25(2), 151-169.

Sanilkumar K. V., P. H. Kumar, J. Joseph and J. K. Panigrahi (2004) Arabian Sea mini warm pool during May 2000. *Current Science*, *86*(1), 180-184.

Schiffer R. A. and W. B. Rossow (1985) ISCCP Global Radiance Data Set: A New Resource for Climate Research. *Bull. Am. Meterol. Soc*., 66, 1498-1505.

Schluessel P., H.-Y. Shin, W. J. Emery and H. Grassl (1987) Comparison of satellite-derived sea surface temperatures with in situ skin measurements. *J. of Geophysical Research*, **92**, 2859-2874.

Schneider N., T. Barnet, M. Latif and T. Stockdale (1996) Warm pool physics in a coupled GCM. *J. of Climate*, 9, 219-239.

Schott F. and J. P. McCreary (2001) The monsoon circulation of the Indian Ocean. *Progress in Oceanography*, 51, 1–124.

Schott F. A., M. Dengler and R. Schoenefeldt (2002) The shallow overturning circulation of the Indian Ocean. *Progress in Oceanography*, *53*(1), 57-103.

Shea D. J., K. E. Trenberth and R. W. Reynolds (1992) A global monthly sea surface temperature climatology. *J. of Climate*, *5*(9), 987-1001.

Shenoi S. S. C., D. Shankar and S. R. Shetye (2002) Differences in heat budgets of the near-surface Arabian Sea and Bay of Bengal: Implications for the summer monsoon. *J. of Geophysical Research: Oceans (1978–2012)*,*107*(C6), 5-1.

Shenoi S. S. C., D. Shankar and S. R. Shetye (2004) Why is Bay of Bengal warmer than Arabian Sea during the summer monsoon?. *Proceedings of the National Symposium METOC-2004 on Emerging trands in the field of Oceanography and Meteorology*, 87-93.

Shetye S. R. (1986) A model study of the seasonal cycle of the Arabian Sea surface temperature. *J. of Marine Research*, 44, 521-542.

Shinoda T., H. H. Hendon and M. A. Alexander (2004) Surface and subsurface dipole variability in the Indian Ocean and its relation with ENSO. *Deep Sea Research Part I: Oceanographic Research Papers*,*51*(5), 619-635.

Smith T. M. and R. W. Reynolds (2004) Improved extended reconstruction of SST (1854-1997). *J. of Climate*, 17(12), 2466-2477.

Sophie C., T. Delcroix, D. Zhang, M. McPhaden and J. Leloup (2009) Observed freshening and warming of the western Pacific Warm pool. *Climate Dynamics*, 33, 565-589 doi 10.1007/s00382-009-0526-7.

Spall M. A. (1991) A diagnostic study of the wind and buoyancy driven North Atlantic circulation. *J. of Geophysical Research*, 96, 18509-18518.

Spigel R. H., J. Imberger and K. N. Rayner (1986) Modeling the diurnal mixed layer. *Limnology and oceanography*, *31*(3), 533-556.

Sreenivas P., K. V. K. R. K. Patnaik and K. V. S. R. Prasad (2008) Monthly variability of mixed layer over Arabian Sea using ARGO data. *Marine Geodesy*, *31*(1), 17-38.

Stuecker M. F., A. Timmermann, F. F. Jin, S. McGregor and H. L. Ren (2013) A combination mode of the annual cycle and the El Niño/Southern Oscillation. *Nature Geoscience*, *6*(7), 540-544.

Sun D-Z (2003) A possible effect of an increase in the warm pool SST on the magnitude of El Nino warming. *J. of Climate* 16(2), 185-205. doi: 10.1175/ 1520-0442(2003)016 \0185: PEOAI[2.0.CO;2.

Suryachandra A. R., A. R. Dhakate, S. K. Saha, S. Mahapatra, H. S. Chaudhari, S. Pokhrel and S. K. Sahu (2012) Why is Indian Ocean warming consistently? *Climatic Change*, 110:709-719 DOI 10.1007/s10584-011-0121-x.

Sutton P. J., P. F. Worcester, G. Masters, B. D. Cornuelle and J. F. Lynch (1993) Ocean mixed layers and acoustic pulse propagation in the Greenland Sea. *The Journal of the Acoustical Society of America*, *94*(3), 1517-1526.

Thompson R. O. R. Y. (1976) Climatological models of the surface mixed layer of the ocean. *J. of Physical Oceanography*, 6, 496-503.

Trenberth K. E. (1997) The definition of el nino. *Bull. Am. Meterol. Soc.*, *78*(12), 2771-2777.

Venzke S., M. Latif and A. Villwock (2000) The coupled GCM ECHO-2. Part II: Indian ocean response to ENSO. *J. of Climate*, *13*(8), 1371-1383.

Vinayachandran P. N. and S. R. Shetye (1991) The warm pool in the Indian Ocean. *Proc. Indian Acad. Sci*., 100, 165–175.

Vinayachandran P. N., D. Shankar, J. Kurian, F. Durand and S. S. C. Shenoi (2007) Arabian Sea mini warm pool and the monsoon onset vortex. *Current Science*., 93, 203-214.

Wagner R. G. (1996) Decadal scale trends in mechanisms controlling meridional sea surface temperature gradients in the tropical Atlantic. *J. of Geophysical Research*, 101, 16683-16694.

Wallace J. (1992) Effect of deep convection on the regulation of tropical sea surface temperature. *Nature*, 357, 230-231.

Wang B. I. N., R. Wu and T. I. M. Li (2003) Atmosphere-Warm Ocean Interaction and Its Impacts on Asian-Australian Monsoon Variation. *J. of Climate*, *16*(8), 1195-1211.

Wang H. and V. M. Mehta (2008) Decadal Variability of the Indo-Pacific Warm Pool and Its Association with Atmospheric and Oceanic Variability in the NCEP–NCAR and SODA Reanalyses. *J. of Climate*, 21, 5545-5565.

Webster P. J. and R. Lukas (1992) TOGA-COARE: The Coupled Ocean-Atmosphere Response Experiment. *Bull. Am. Meterol. Soc*., 73, 1377-1416.

Webster P. J., G. J. Holland, J. A. Curry and H. R. Chang (2005) Changes in tropical cyclone number, duration, and intensity in a warming environment. *Science*, 309, 1844–1846.

Webster P. J., J. Gulledge and J. Curry (2006) Expanding tropical warm pool: increased tropical cyclone season length and storm duration. In: American Geophysical Union, Fall meeting, U51C-055

Webster P. T., A. M. Moore, J. P. Loschning and R. L. Robert (1999) Couple ocean-atmosphere dynamics in the Indian Ocean during 1997-1998. *Nature*, 401, 356-360.

Wick G. A., W. J. Emery, L. H. Kantha and P. Schluessel (1996) The behavior of the bulk-skin sea surface temperature difference under varying wind speed and heat flux. *J. of Physical Oceanography*, **26**, 1969-1988.

Williams A. P. and C. Funk (2011) A westward extension of the warm pool leads to a westward extension of the Walker circulation, drying eastern Africa. *Climate Dynamics*, *37*(11-12), 2417-2435.

Willis J. K., D. Roemmich and B. Cornuelle (2004) Interannual variability in upper ocean heat content, temperature, and thermosteric expansion on global scales. *J. of Geophysical Research*, 109, C12036, doi:10.1029/2003JC002260.

Wittenberg A. T., A. Rosati, T. L. Delworth, G. A. Vecchi and F. Zeng (2014) ENSO modulation: Is it decadally predictable?. *J. of Climate*, *27*(7), 2667-2681.

Wyrtki K. (1971) Oceanographic Atlas of the International Indian Ocean Expedition. National Science Foundation Publ. OCE/NSF 86-00-001, pp 531.

Wyrtki K. (1973) Physical oceanography of the Indian Ocean. In *The biology of the Indian Ocean,* 18-36, Springer Berlin Heidelberg.

Wyrtki K. (1985) Water displacements in the Pacific and the genesis of El Nino cycles. *J. of Geophysical Research*, 90, 7129-7132.

Wyrtki K. (1989) Some thoughts about the West Pacific Warm Pool. Proc. Western Pacific Int. Meeting and Workshop on TOGA/COARE, Noumea, New Caledonia, 99–109. [Available from Centre ORSTOM de Noumea, B.P. A5 98848, Noumea Cedex, New Caledonia.]

Xie S. -P., H. Annamalai, F. Schott and J. P. McCreary Jr. (2002) Origin and predictability of South Indian Ocean climate variability. *J. of Climate*, 15, 864–878.

Xie S.-P., K. Hu, J. Hafner, Y. Du, G. Huang and H. Tokinaga (2009) Indian Ocean capacitor effect on Indo-western Pacific climate during the summer following El Nino. *J. of Climate*, 22, 730-747.

Yan D. and S. Xie (2008) Role of atmospheric adjustments in the tropical Indian Ocean warming during the 20th century in climate models. *Geophysical Research Letters*, 35, L08712, doi:10.1029/2008GL033631.

Yan X. H., R. H. Chung, Q. A. Zheng and V. Klemas (1992) Temperature and size variabilities of the Western Pacific Warm Pool. *Science*, 258, 1643-1645.

Yang J., Q. Liu, S.-P. Xie, Z. Liu and L. Wu (2007) Impact of the Indian Ocean SST basin mode on the Asian summer monsoon. *Geophysical Research Letters*, 34, L02708, doi: 10.1029/2006GL028571.

Yu L and R. A. Weller (2007) Objectively analyzed air–sea heat fluxes for the global ice-free oceans (1981–2005). *Bull. Am. Meteorol. Soc*., 88, 527–539. doi:10.1175/BAMS-88-4-527.

Yu L. and M. M. Rienecker (1999) Mechanisms for the Indian Ocean warming during the 1997-98 El Nino. *Geophysical Research Letters*, 26, 6, 735-738.

Yu L. and M. M. Rienecker (2000) Indian Ocean warming of 1997–1998. *J. Geophysical Research*, 105(C7),16923–16939, doi: 10.1029/2000JC900068.

Yu L., X. J. Xiangze and R. A. Weller (2007) Annual, seasonal, and interannual variability of air–sea heat fluxes in the Indian Ocean. *J. of Climate*, 20, 3190-3209.

Zeng X. and A. Beljaars (2005) A prognostic scheme of sea surface skin temperature for modeling and data assimilation. *Geophysical Research Letters*, **32**, doi:10.1029/2005GL023030.

Zhang Q., Z. Qinghua, H. Yijun, X. Jianping, W. Xuechuan and C. Minghua (2007) Zonal displacement of western Pacific warm pool and zonal wind anomaly over the Pacific Ocean. *Chinese Journal of Oceanology and Limnology*, 25(3), 277-285, DOI: 10.1007/s00343-007-0277-4.

Zhang Q., H. Yijun, Q. Qinghua and B. Xuezhi (2009) Variations in the eastern Indian Ocean warm pool and its relation to the dipole in the tropical Indian Ocean. *Chinese J. of Oceanology and Limnology*, 27(3), 640-649, DOI: 10.1007/s00343-009-9148-5.

Zhang Q. L., X. C. Weng and Y. J. Hou (2004) Zonal movement of surface warm water in the western Pacific warm pool. *Acta Oceanologica Sinica*, 26(1), 33-39.

Zhong A., H. H. Hendon and O. Alves (2005) Indian Ocean Variability and Its Association with ENSO in a Global Coupled Model. *J. of Climate*, 18, 3634-3649.

Appendix

List of Publications

1. Saji P. K., A. N. Balchand and R. Sajeev (2014) Seasonal warming trend in Indian Ocean. *Proceedings of National Seminar on Climate Change and Marine Ecosystems (CCME 2014), CUSAT, Kochi, 20-21, March 2014.*

2. Saji P. K. and A. N. Balchand (2014) Investigation on the warming trends of Indian Ocean Warm Pool, *Proceedings of 28th Kerala Science Congress*, Wayanad: 28-31 Jan 2014, 1781-1787 (in absentia).

3. Saji P. K., A. N. Balchand and M. R. Ramesh Kumar (2015) On some aspects of Indian Ocean warm pool, *Indian J. of Geo-Marine Sciences*, Vol 44(4), 475-479.

4. Maya L. Pai, P. K. Saji, K. V. Pramod and A. N. Balchand (2015) Trend analysis of Sea Surface Temperature of Indian Ocean during the period 1960-2012. *International J. of Oceans and Oceanography*, Vol. 9 (2), 229-242.

5. Nisa Anil, M. R. Ramesh Kumar, R. Sajeev and P. K. Saji (2016) Role of distinct flavaours of IOD events on Indian summer monsoon. *Natural Hazards*, 82(2), 1317-1326.

Seasonal Warming Trend in Indian Ocean

Saji P. K., Sajeev, R. and Balchand, A.N.
Department of Physical Oceanography, School of Marine Sciences, Cochin University of Science and Technology, Cochin-682016, India
Email: sajipk1975@gmail.com

Abstract

Recent studies have indicated that the tropical Indian Ocean is warming consistently with varying spatial magnitudes. Higher warming trend (0.2°C per decade) was observed at central equatorial areas and a relatively lesser warming rate in the northern Indian Ocean. Though the warming trend has been identified, it is not clear whether the trend is uniformly distributed for each month or it is seasonally biased. This paper investigates the warming trend on monthly and seasonal basis to further understand its seasonality. The results are reviewed in light of global warming and analyzed in relation to known variability in climatic parameters.

Introduction

Climatic variability studies have shown warming trends in tropical oceans during the past several decades (Levitus *et al.* 2000, 2005; Willis *et al.* 2004; Webster *et al.*, 2006; Alory *et al.*, 2007; Du and Xie, 2008; Zhang *et al.*, 2009; Rao *et al.* 2012). The warming trend has been identified in all types of climatic data sets.

Levitus *et al.* (2000, 2005) observed an increase in the heat content of about $2x10^{23}$ Joules for the upper 3000m of oceans during a period of 50 years. This increase in heat content was due to an increase in the warming of the water volume. It is also interesting to note that the timing of warming trend is different for each ocean. Warming trend in Indian Ocean began after a gap of about 10 years of that in the Pacific and Atlantic. Willis *et al.* (2004) also found an increase in the heat content of world oceans for a shorter data period of 10 years and estimated the rate as 0.86 watts per square meter. Due to warming, the sea level also increased during the period and that confirms warming. They found that the major part of this mean global warming trend was contributed by the southern mid latitudes where the rate of warming is higher.

Webster *et al.* (2006) detected expansion of warm pools in a 150 year long data. Warm pool is defined as oceanic surface waters with SST higher than 28°C (Wyrtki, 1989). Zhang *et al.* (2009) studied the trend of warm pool in Indian Ocean.Warm pools have been found to have increased by 80% in a time span of 50 years. Using historical temperature data, Alory *et al.* (2007) found a linear trend in the warming of upper waters. Cause of this warming was believed to be an increase in the

05-15

Investigation on the warming trends of Indian Ocean warm pool

Saji P. K. and A. N. Balchand

Department of Physical Oceanography,

Cochin University of Science and Technology, Kochi, India

sajipk1975@gmail.com, balchand@rediffmail.com

INTRODUCTION

Oceanic surface waters, having temperatures higher than 28°C are often called 'warm pools'. Warm pools are found in all tropical oceans and are important indices to climate and climate changes. Higher Sea Surface Temperatures (SST) in warm pool makes it as areas of active air-sea interaction and favor atmospheric convection [Gadgil, (1986); Graham and Barnet, (1987)].

It has been observed recently that the Indian Ocean Warm Pool (IOWP) varies seasonally [Vinayachandran and Shetye, (1991); Saji et al., (2013)] and expanding year by year on a consistent manner [Alory et al., (2007); Suryachandra et al., (2012)]. The expansion has accelerated since 1970 which supports the human contribution to the warming phenomenon. The increase in the area of IOWP was also confirmed with the southward and westward displacement of southern and western edges of the warm pool respectively on interannual time scale [Zhang et al., (2009)].

The increase in SST, as part of global warming, is considered as a consequence of human induced climate change as suggested by Yan and Xie (2008). As reasoning to the warming, the authors hypothesize that the increase in greenhouse gas emissions enhances the net downward longwave radiation which further leads to a weakening in wind speed and thereby suppress the turbulent heat loss from the ocean.

The objective of this study is to recognize the longterm trends (per decade) in IOWP surface area and its mean temperature. Though it was revealed that IOWP, as a whole, was expanding over the last few decades, longterm trend in its subdivision of temperatures have not been analyzed yet. Hence we present the trend analysis in temperature within subdivisions of the warm pool to identify their contributions to the total warm pool behavior. Spatial distribution too of warming trend was obtained to identify the regional differences. SST trend was compared with that of net heat flux to find the role of heat fluxes on SST.

MATERIALS AND AND METHODS

In this study, we use the monthly, 1 x 1° gridded data sets of SST, heat fluxes (shortwave, longwave, latent heat and sensible heat) of Objectively Analyzed air-sea Fluxes (OAFlux)

Indian Journal of Geo-Marine Sciences
Vol. 44(4), April 2015, pp. 475-479

On some aspects of Indian Ocean Warm Pool

Saji P. K.*, A. N. Balchand & M. R. Ramesh Kumar[1]
Department of Physical Oceanography, Cochin University of Science and Technology, Cochin-682016, India
Physical Oceanography Division, National Institute of Oceanography, Goa-403004, India[1]
*[E.mail : sajipk1975@gmail.com]

Received 5 September 2013; revised 6 November 2013

Annual and interannual variation of Indian Ocean Warm Pool (IOWP) was studied using satellite and *in situ* ocean temperature data. IOWP surface area undergoes a strong annual cycle attaining a maximum of 24 x $10^6 km^2$ during April and minimum of 10 x $10^6 km^2$ in August. Unlike surface area, warm pool was deeper (90m) during August than in April. Higher vertical extent was found both at eastern equatorial Indian Ocean and south-eastern Arabian Sea. Frequency distribution of temperatures at one degree interval (28-29, 29-30, 30-31) exhibited independent seasonal variations. The interannual variation of IOWP was found to be associated with ENSO events.

[**Keywords**: Warm Pool; Sea Surface Temperature; Indian Ocean; IOWP]

Introduction

Warm oceanic waters are often called as warm pools[1]. Researchers have used different criteria to define warm pool based on the lower limit of temperature. For example, Wyrtki[1] had used 28°C as the lower limit whereas Chacko et al[2] used 30°C. The selection of lower temperature limit depends on the spatial scale of the warm pool of interest. For the study of warm pools on a larger scale, 28°C was considered as a better choice whereas for small scale warm pools ('mini warm pool'), higher cut off values can be adopted. Since the focus of our study is on a basin scale warm pool of Indian Ocean, we follow Wyrtki's criteria of 28°C to define the warm pool.

Warm pools are features of tropical oceans and are an important entity for the climate[3-8]. Warm pools are identified as areas of strong atmospheric convection, convergence of surface wind, and high precipitation[9-16]. Among the warm pools, Pacific warm pool has been studied extensively over the last two decades due to its close association with the formation of El Nino. Recent studies on IOWP now confirm its role on the climate of Indian Ocean and Indian monsoon rainfall. Vinayachandran and Shetye[17] studied the climatological aspect of IOWP. Joseph[18] found that the monsoon vortex which is essential for the onset of summer monsoon rainfall over India, forms over the warmest part of IOWP in Arabian Sea. Zhang et al[19] identified the role of Indian Ocean Dipole on IOWP variability.

Present study consists the evolution and features of IOWP on seasonal and interannual time scales. Climatological evolution of IOWP studied earlier used Levitus data which had a spatial resolution of 1° x 1°. In this study, we also use satellite data which had a better resolution and accuracy than Levitus data.

Material and Methods

The data used in this study consist of Sea Surface Temperature (SST) data (monthly and climatology) from Tropical Rainfall Measuring Mission (TRMM) Microwave Imager (TMI) and Levitus World Ocean Atlas subsurface temperature data[20]. TMI SST has a spatial resolution of 0.25°×0.25°. Climatological version of this data was used to study the annual evolution of IOWP. IOWP surface area for a month was obtained by computing the number of grids having SST greater than 28°C and then multiplying it with unit grid area (27.5 x 27.5 km^2). Levitus climatology was used to estimate the depth of warm pool by locating the 28°C isotherm (D28) in the vertical. Monthly TMI SST data for the period 1998 to 2009 was used to study the interannual variations in IOWP surface area.

Result and Discussions

Climatological variability

Figure 1 shows the climatological variation of IOWP surface area. It showed a simple annual cycle with one minimum and one maximum.

International Journal of Oceans and Oceanography
ISSN 0973-2667 Volume 9, Number 2 (2015), pp. 229-242

http://www.ripublication.com

Trend Analysis of Sea Surface Temperature of Indian Ocean during the Period 1960-2012

Maya L. Pai[1], P. K. Saji[2], K. V. Pramod[3], A. N. Balchand[2*]

[1]Department of Mathematics, Amrita Vishwa Vidyapeetham, Cochin 682024.
[2]Department of Physical Oceanography, CUSAT, Cochin 682016.
[3]Department of Computer Applications, CUSAT, Cochin 682022.
*Corresponding author: *balchand57@gmail. com*

Abstract

Oceans are currently undergoing a warming phase in response to global climate change. Rate of warming is however not uniform within a particular ocean and also between the oceans. Utilizing Sea Surface Temperature (SST) data of 53 years (1960-2012), we studied the warming trend(s) in Indian Ocean (IO) on a monthly, seasonal and annual scale applying statistical regression tools. Higher warming rate [0. 30^0C/decade] has been identified in the equatorial IO. Over the tropical Indian Ocean, rate of warming had varied from 0. 05 to 0. 30^0C/decade. We also find that ICOADS data has limitations in producing the basin wide estimate of long term warming trend due to the limited data coverage.

Keywords: Globalwarming, SST, Indian Ocean, Trend analysis

Introduction

The two key environmental issues among climate researchers in the last two decades are global warming and climate change. Both are related in such a way that the reason for ongoing climate changes is the impact of global warming. There is a steady increase in the greenhouse gases since the industrial revolution and 70% increase was noticed between 1970 and 2004 [1]. Many studies have confirmed that Indian Ocean (IO) is warming consistently [2-6]. It is observed that the changes in net air-sea heat flux induced by green house gases are responsible for this warming [2-5, 7]. From the study of the linear trend over the last 100 years (1906-2005), thefourth assessment report of the Intergovernmental Panel on Climate Change (IPCC 2007) have observed that the global mean surface temperature have risen by 0. $74^0 \pm 0.$ 18^0C. This means that the rate of warming over the recent 50 years is almost double of that over the past

DOI 10.1007/s11069-016-2245-9

ORIGINAL PAPER

Role of distinct flavours of IOD events on Indian summer monsoon

Nisa Anil[1] · M. R. Ramesh Kumar[2] · R. Sajeev[1] · P. K. Saji[1]

Received: 6 May 2015 / Accepted: 11 February 2016

Abstract The summer monsoon contributes to about 75 % of mean annual rainfall over the various meteorological subdivisions of India. The role of ocean–atmosphere phenomena such as Indian Ocean Dipole (IOD) and El Nino–Southern Oscillation (ENSO) on the Indian monsoon activity is intriguing. The impacts of ENSO, IOD and Equatorial Indian Ocean Oscillation on monsoon are distinct. The ENSO (IOD) in general affects the monsoon negatively (positively). The present study aims to understand the role of different types of IOD such as early IOD (EIOD), normal IOD and prolonged IOD (PIOD) on Indian Summer Monsoon Rainfall (ISMR). We find that an EIOD, which peaks in the mid-monsoon months (July and August), plays a significant role like PIOD in enhancing ISMR even though it has a medium Dipole Mode Index amplitude value compared to other IODs. During an EIOD, the combined effect of excess evaporation from Arabian Sea and the stronger cross-equatorial flow leads to the enhanced monsoon activity. In addition, there is a substantial decrease in the number of break spells during EIOD years.

Keywords Monsoon · Break · Indian Ocean Dipole · Indian Ocean

1 Introduction

The IOD is a coupled ocean and atmosphere phenomenon in the Indian Ocean (IO) that affects the seasonal climate of countries that surround the Indian Ocean (Saji et al. 1999). The intensity of IOD is represented by an index called Dipole Mode Index (DMI), which is

✉ Nisa Anil
nisaanil1111@gmail.com

[1] Department of Physical Oceanography, Cochin University of Science and Technology, Cochin 680216, India

[2] Physical Oceanography Divisions, National Institute of Oceanography, Dona Paula, Goa 403004, India

Published online: 26 February 2016

Natural Hazards, 82(2), 1317–1326.